FINITE ELEMENTS FOR BIOMECHANICS

Version 1.4

Theory Manual

Last Updated: October 11, 2011

Contributors

- Steve Maas (steve.maas@utah.edu)
- Dave Rawlins (rawlins@sci.utah.edu)
- Dr. Jeffrey Weiss (jeff.weiss@utah.edu)
- Dr. Gerard Ateshian (ateshian@columbia.edu)

Contact address

Musculoskeletal Research Laboratories, University of Utah
72 S. Central Campus Drive, Room 2646
Salt Lake City, Utah

Website

MRL: http://mrl.sci.utah.edu
FEBio: http://mrl.sci.utah.edu/software/febio

Forum
http://mrlforums.sci.utah.edu/forums/

Development of the FEBio project is supported in part by a grant from the U.S. National Institutes of Health (R01GM083925).

Table of Contents

Chapter 1. Introduction **5**
1.1. Overview of FEBio 5
1.2. About this document 5
Chapter 2. Continuum Mechanics **7**
2.1. Vectors and Tensors 7
2.2. The Directional Derivative 10
2.3. Deformation, Strain and Stress 11
2.3.1. The deformation gradient tensor 11
2.3.2. Strain 12
2.3.3. Stress 12
2.4. Hyperelasticity 13
2.4.1. Isotropic Hyperelasticity 14
2.4.2. Isotropic Elasticity in Principal Directions 15
2.4.3. Nearly-Incompressible Hyperelasticity 16
2.4.4. Transversely Isotropic Hyperelasticity 17
2.5. Biphasic Material 19
2.5.1. Governing Equations 19
2.6. Biphasic-Solute Material 21
2.6.1. Governing Equations 21
2.6.2. Continuous Variables 24
2.7. Mixture of Solids 25
2.8. Equilibrium Swelling 27
2.8.1. Perfect Osmometer 28
2.8.2. Cell Growth 28
2.8.3. Donnan Equilibrium Swelling 29
Chapter 3. The Nonlinear FE Method **31**
3.1. Weak formulation for solid materials 31
3.1.1. Linearization 31
3.1.2. Discretization 33
3.2. Weak formulation for biphasic materials 35
3.2.1. Linearization 35
3.2.2. Discretization 37
3.3. Weak formulation for biphasic-solute materials 39
3.3.1. Linearization of Internal Virtual Work 40
3.3.2. Linearization of External Virtual Work 44
3.3.3. Discretization 45
3.4. Newton-Raphson method 48
3.4.1. Full Newton Method 48
3.4.2. BFGS Method 48
3.4.3. Line Search Method 49
Chapter 4. Element Library **51**
4.1. Solid Elements 51
4.1.1. Hexahedral elements 51

4.1.2. Pentahedral Elements ... 52
4.1.3. Tetrahedral Elements ... 52
4.2. Shell Elements ... 53
4.2.1. Shell formulation ... 54
4.2.2. Quadrilateral shells ... 55
4.2.3. Triangular shells ... 56
Chapter 5. Constitutive Models ... 57
5.1. Linear Elasticity ... 57
5.2. Compressible Materials ... 59
5.2.1. Isotropic Elasticity ... 59
5.2.2. Neo-Hookean Hyperelasticity ... 59
5.2.3. Ogden Unconstrained ... 60
5.2.4. Holmes-Mow ... 60
5.2.5. Donnan Equilibrium Swelling ... 61
5.2.6. Perfect Osmometer Equilibrium Osmotic Pressure ... 62
5.3. Nearly-Incompressible Materials ... 62
5.3.1. Mooney-Rivlin Hyperelasticity ... 62
5.3.2. Ogden Hyperelastic ... 63
5.3.3. Veronda-Westmann Hyperelasticity ... 63
5.3.4. Arruda-Boyce Hyperelasticity ... 64
5.3.5. Transversely Isotropic Hyperelastic ... 64
5.3.6. Ellipsoidal Fiber Distribution ... 65
5.3.7. Fiber with exponential Power law ... 66
5.3.8. Fung Orthotropic ... 66
5.3.9. Tension-Compression Nonlinear Orthotropic ... 67
5.4. Viscoelasticity ... 68
5.5. Hydraulic Permeability ... 70
5.5.1. Constant Isotropic Permeability ... 70
5.5.2. Holmes-Mow ... 70
5.5.3. Referentially Isotropic Permeability ... 70
5.5.4. Referentially Orthotropic Permeability ... 70
5.5.5. Referentially Transversely Isotropic Permeability ... 71
5.6. Solute Diffusivity ... 72
5.6.1. Constant Isotropic Diffusivity ... 72
5.6.2. Constant Orthotropic Diffusivity ... 72
5.6.3. Referentially Isotropic Diffusivity ... 72
5.6.4. Referentially Orthotropic Diffusivity ... 72
5.7. Solute Solubility ... 74
5.7.1. Constant Solubility ... 74
5.8. Osmotic Coefficient ... 75
5.8.1. Constant Osmotic Coefficient ... 75
5.9. Active Contraction Model ... 76
Chapter 6. Contact and Coupling ... 77
6.1. Rigid-Deformable Coupling ... 77
6.1.1. Kinematics ... 77
6.1.2. A single rigid body ... 78

6.1.3. Multiple Rigid Bodies ... 78
6.2. Rigid Joints ... 79
6.3. Sliding Interfaces ... 80
6.3.1. Contact Kinematics ... 81
6.3.2. Weak Form of Two Body Contact ... 82
6.3.3. Linearization of the Contact Integral ... 83
6.3.4. Discretization of the Contact Integral ... 84
6.3.5. Discretization of the Contact Stiffness ... 84
6.3.6. Augmented Lagrangian Method ... 85
6.3.7. Automatic penalty calculation ... 86
6.3.8. Alternative formulations ... 87
6.4. Biphasic Contact ... 88
6.4.1. Contact Integral ... 88
6.4.2. Gap Function ... 89
6.4.3. Penalty Method ... 89
6.4.4. Discretization ... 90
6.5. Biphasic-Solute Contact ... 92
6.5.1. Contact Integral ... 92
6.5.2. Gap Function ... 93
6.5.3. Penalty Method ... 94
6.5.4. Discretization ... 95
6.6. Tied Contact ... 99
6.6.1. Gap Function ... 99
6.6.2. Tied Contact Integral ... 99
6.6.3. Linearization of the Contact Integral ... 100
6.6.4. Discretization ... 100
References ... 102

Chapter 1. Introduction

1.1. Overview of FEBio

FEBio is an implicit, nonlinear finite element solver that is specifically designed for applications in biomechanics. It offers analyses, constitutive models and boundary conditions that are relevant for this particular field. This section describes briefly the available features of FEBio. A more detailed overview of features can be found in the User's Manual.

FEBio supports two analysis types, namely *quasi-static* and *quasi-static poroelastic*. In a *quasi-static* analysis the (quasi-) static response of the system is sought; inertial terms are ignored. In a *quasi-static poroelastic* analysis a coupled solid-fluid problem is solved. The latter analysis type is useful for modeling tissues that have high water content and the explicit modeling of fluid movement relative to the solid phase is important.

Several nonlinear constitutive models are available to allow the user to model the often complicated biological tissue behavior. Several isotropic constitutive models are supported such as Neo-Hookean, Mooney-Rivlin, Veronda-Westmann, Arruda-Boyce and Ogden. These models have a nonlinear stress-strain response. In addition to the isotropic models, there are several anisotropic models available. These materials show anisotropic behavior in at least one preferred direction and are useful for modeling biological tissues such as tendons, muscles and other tissues that contain fibers. FEBio also contains a *rigid body* material model, which can be used to model rigid structures whose deformation is negligible compared to the deformable geometry.

Biological tissues can interact in very complicated ways. Therefore FEBio supports a wide range of boundary conditions to model these interactions. These include prescribed displacements, nodal forces, and pressure forces. Deformable models can also be connected to rigid bodies so that the user can model prescribed rotations and torques. Rigid bodies can be connected with rigid joints. Even more complicated interactions can be modeled using FEBio's contact interfaces. The user can choose between different types of contact interfaces, such as sliding interfaces, tied interfaces and rigid wall interfaces. A sliding interface is defined between two surfaces that are allowed to separate and slide across each other but are not allowed to penetrate. The rigid wall interface is also similar to the sliding interface, except that one of the contacting surfaces is a movable rigid wall. As of version 1.2, there is an implementation of a sliding interface that allows for fluid flow crossing the contact interface. The tied interface is similar to the sliding interface, but in this case, the surfaces are not allowed to slide or separate. In addition, the user may specify a body force which can be used to model the effects of gravity or base acceleration.

1.2. About this document

This document is a part of a set of three manuals that accompany FEBio: the *User's Manual*, describing how to use FEBio, the online code documentation for users who wish to modify or

add features to the code, and this manual, which describes the theory behind most of the FEBio algorithms.

The purpose of this manual is to provide theoretical background on many of the algorithms that are implemented in FEBio. In this way the user can develop a better understanding of how the program works and how it can be used to create well defined biomechanical simulations. The authors have tried to be as detailed as possible to make the text coherent and comprehensible, but due to the complexity of some of the topics, some descriptions only skim the surface. Many of the theoretical ideas discussed in this manual can and have filled entire bookshelves. The explanations contained herein should be sufficient to give the reader a basic understanding of the theoretical developments. References to textbooks and the primary literature are provided for further reading.

Chapter 2 starts with a brief overview of some of the important concepts in continuum mechanics. Readers who are already familiar with this field can skip this chapter, although the material may be useful to get familiar with the notation and terminology used in this manual.

Chapter 3 describes the nonlinear finite element method. It also explains the Newton-Raphson method, which is the basis for most implementations of the nonlinear finite element method. A more specialized version of this algorithm, the BFGS method, is described as well since it is used in FEBio.

In Chapter 4 the different element types that are available in FEBio are described in detail. FEBio currently supports 3D solid elements, such as the linear hexahedral, pentahedral and tetrahedral elements, as well as quadrilateral and triangular shell elements.

Chapter 5 contains a detailed description of the material models in FEBio. Most of these models are based on hyperelasticity, which is introduced in chapter 2. Several transversely isotropic materials are described as well. This also discusses the biphasic material and its implementation in FEBio.

Chapter 6 describes the basics of the theory of contact and coupling. In FEBio the user can connect the different parts of the geometry in a variety of ways. There are rigid interfaces where a deformable model is attached to a rigid model, rigid joints where two or more rigid bodies connect, and sliding interfaces where two surfaces are allowed to separate and slide across each other but are not allowed to penetrate. The various contact and coupling algorithms are discussed as well together with their implementation in FEBio.

Chapter 2. Continuum Mechanics

This chapter contains an overview of some of the important concepts from continuum mechanics and establishes some of the notation and terminology that will be used in the rest of this document. The section begins by introducing the important concepts of deformation, stress and strain. Next the concept of hyperelasticity is discussed. Finally the concept of virtual work is discussed. This concept will be used later to derive the nonlinear finite element equations. For a more thorough introduction to the mathematics needed for continuum mechanics, the user can consult [1].

2.1. Vectors and Tensors

It is assumed that the reader is familiar with the concepts of vectors and tensors. This section summarizes the notation and some useful relations that will be used throughout the manual.

Vectors are denoted by small, bold letters, e.g. **v**. Their components will be denoted by v_i, where, unless otherwise stated, Latin under scripts such as *i* or *I* will range from 1 to 3. In matrix form a vector will be represented as a column vector and its transpose as a row vector:

$$\mathbf{v} = \begin{pmatrix} v_1 \\ v_2 \\ v_3 \end{pmatrix}, \quad \mathbf{v}^T = \begin{pmatrix} v_1, & v_2, & v_3 \end{pmatrix}. \tag{2.1}$$

The following products are defined between vectors. Assume **u**, **v** are vectors. Also note that the Einstein summation convention is used throughout this manual [2].

The *dot* or *scalar product*:

$$\mathbf{u} \cdot \mathbf{v} = u_i v_i . \tag{2.2}$$

The *cross product*:

$$\mathbf{u} \times \mathbf{v} = \begin{bmatrix} u_2 v_3 - u_3 v_2 \\ u_3 v_1 - u_1 v_3 \\ u_1 v_2 - u_2 v_1 \end{bmatrix}. \tag{2.3}$$

The *vector outer product*:

$$\left(\mathbf{u} \otimes \mathbf{v}\right)_{ij} = u_i v_j . \tag{2.4}$$

Note that vectors are also known as first order tensors. Scalars are known as zero order tensors. The outer product, defined by equation (2.4), is a second order tensor.

Second order tensors are denoted by bold, capital letters, e.g. **A**. Some exceptions will be made to remain consistent with the literature. For instance, the Cauchy stress tensor is denoted by $\boldsymbol{\sigma}$. However, the nature of the objects will always be clear from the context. The following operations on tensors are defined. Assume **A** and **B** are second-order tensors.

The *double contraction* or *tensor inner product* is defined as:

$$\mathbf{A}:\mathbf{B} = A_{ij}B_{ij}\,. \tag{2.5}$$

The *trace* is defined as:

$$\operatorname{tr}\mathbf{A} = \mathbf{I}:\mathbf{A} = A_{ii}\,. \tag{2.6}$$

Here **1** is the second order identity tensor with components δ_{ij}.

In general the components of tensors will change under a change of coordinate system. Nevertheless, certain intrinsic quantities associated with them will remain invariant under such a transformation. The scalar product between two vectors is such an example. The double contraction between two second-order tensors is another example. The following set of invariants for second-order tensors is commonly used:

$$\begin{aligned} I_1 &= \operatorname{tr}\mathbf{A}, \\ I_2 &= \frac{1}{2}\left(\left(\operatorname{tr}\mathbf{A}\right)^2 - \operatorname{tr}\mathbf{A}^2\right), \\ I_3 &= \det\mathbf{A}. \end{aligned} \tag{2.7}$$

A tensor **S** is called symmetric if it is equal to its transpose:

$$\mathbf{S} = \mathbf{S}^T\,. \tag{2.8}$$

A tensor **W** is called anti-symmetric if it is equal to the negative of its transpose:

$$\mathbf{W} = -\mathbf{W}^T\,. \tag{2.9}$$

Any second order tensor **A** can be written as the sum of a symmetric tensor **S** and an anti-symmetric tensor **W**:

$$\mathbf{A} = \mathbf{S} + \mathbf{W}\,, \tag{2.10}$$

where

$$\mathbf{S} = \frac{1}{2}\left(\mathbf{A} + \mathbf{A}^T\right), \text{ and } \mathbf{W} = \frac{1}{2}\left(\mathbf{A} - \mathbf{A}^T\right). \tag{2.11}$$

Also note that for any tensor **B** the following holds:

$$\mathbf{B}:\mathbf{A} = \mathbf{B}:\mathbf{S}, \quad \mathbf{B}:\mathbf{W} = \mathbf{0}\,. \tag{2.12}$$

With any anti-symmetric tensor a vector **w** can be associated such that,

$$\hat{\mathbf{w}}\mathbf{u} = \mathbf{w}\times\mathbf{u}\,, \tag{2.13}$$

where the second order tensor $\hat{\mathbf{w}}$ is defined as,

$$\hat{\mathbf{w}} = \begin{bmatrix} 0 & -w_3 & w_2 \\ w_3 & 0 & -w_1 \\ -w_2 & w_1 & 0 \end{bmatrix}. \tag{2.14}$$

A second order **Q** tensor is called *orthogonal* if $\mathbf{Q}^{-1} = \mathbf{Q}^T$.

In the implementation of the FE method it is often convenient to write symmetric second-order tensors using *Voigt notation*. In this notation the components of a 2nd order symmetric tensor **A** are arranged as a column vector:

$$\left[\underline{\mathbf{A}}\right]=\begin{bmatrix} A_{11} \\ A_{22} \\ A_{33} \\ A_{12} \\ A_{23} \\ A_{13} \end{bmatrix}. \tag{2.15}$$

Higher order tensors will be denoted by bold, capital, script symbols, e.g. $\boldsymbol{\mathcal{A}}$. An example of a third-order tensor is the *permutation tensor* $\mathcal{E}_{ijk}$, whose components are 1 for an even permutation of $(1,2,3)$, -1 for an odd permutation of $(1,2,3)$ and zero otherwise. The permutation symbol is useful for expressing the cross-product of two vectors in index notation:

$$\left(\mathbf{u}\times\mathbf{v}\right)_i=\mathcal{E}_{ijk}u_j v_k\,. \tag{2.16}$$

An example of a fourth order tensor is the elasticity tensor $\boldsymbol{\mathcal{C}}$ which, in linear elasticity theory, relates the small strain tensor $\boldsymbol{\varepsilon}$ and the Cauchy stress tensor $\boldsymbol{\sigma}=\boldsymbol{\mathcal{C}}:\boldsymbol{\varepsilon}$.

Higher order tensors can be constructed from second order tensors in a similar way as second order tensors can be constructed from vectors. If $\mathbf{A}$ and $\mathbf{B}$ are second order tensors, then the following fourth order tensors can be defind by requiring that the following must hold for any second order tensor $\mathbf{X}$:

$$\left(\mathbf{A}\otimes\mathbf{B}\right):\mathbf{X}=\left(\mathbf{B}:\mathbf{X}\right)\mathbf{A}\,, \tag{2.17}$$

$$\left(\mathbf{A}\underline{\otimes}\mathbf{B}\right):\mathbf{X}=\mathbf{A}\cdot\mathbf{X}\cdot\mathbf{B}^T\,, \tag{2.18}$$

$$\left(\mathbf{A}\overline{\otimes}\mathbf{B}\right):\mathbf{X}=\mathbf{A}\cdot\mathbf{X}^T\cdot\mathbf{B}^T \tag{2.19}$$

$$\left(\mathbf{A}\overline{\underline{\otimes}}\mathbf{B}\right):\mathbf{X}=\frac{1}{2}\left(\mathbf{A}\cdot\mathbf{X}\cdot\mathbf{B}^T+\mathbf{A}\cdot\mathbf{X}^T\cdot\mathbf{B}^T\right). \tag{2.20}$$

The Cartesian component forms of the operators $\otimes$, $\underline{\otimes}$, $\overline{\otimes}$ and $\overline{\underline{\otimes}}$ are defined as follows:

$$\left(\mathbf{A}\otimes\mathbf{B}\right)_{ijkl}=\mathbf{A}_{ij}\mathbf{B}_{kl}\,, \tag{2.21}$$

$$\left(\mathbf{A}\underline{\otimes}\mathbf{B}\right)_{ijkl}=\mathbf{A}_{ik}\mathbf{B}_{jl}\,, \tag{2.22}$$

$$\left(\mathbf{A}\overline{\otimes}\mathbf{B}\right)_{ijkl}=A_{il}B_{jk} \tag{2.23}$$

$$\left(\mathbf{A}\overline{\underline{\otimes}}\mathbf{B}\right)_{ijkl}=\frac{1}{2}\left(\mathbf{A}_{ik}\mathbf{B}_{jl}+\mathbf{A}_{il}\mathbf{B}_{jk}\right). \tag{2.24}$$

The fourth order identity tensors are defined as:

$$\begin{aligned}\mathbf{A}&=\boldsymbol{\mathcal{I}}:\mathbf{A},\\ \mathbf{A}^T&=\overline{\boldsymbol{\mathcal{I}}}:\mathbf{A}.\end{aligned} \tag{2.25}$$

where $\boldsymbol{\mathcal{I}}=\mathbf{I}\underline{\otimes}\mathbf{I}$ and $\overline{\boldsymbol{\mathcal{I}}}=\mathbf{I}\overline{\otimes}\mathbf{I}$. The components are given by:

$$\begin{aligned} \mathcal{I}_{ijkl} &= \delta_{ik}\delta_{jl}, \\ \bar{\mathcal{I}}_{ijkl} &= \delta_{il}\delta_{jk}. \end{aligned} \tag{2.26}$$

2.2. The Directional Derivative

In later sections the nonlinear finite element method will be formulated. Anticipating an iterative solution method to solve the nonlinear equations, it will be necessary to linearize the quantities involved. This linearization process will utilize a construction called the *directional derivative* [1].

The directional derivative of a function $f(\mathbf{x})$ is defined as follows:

$$Df(\mathbf{x})[\mathbf{u}] = \left.\frac{d}{d\varepsilon}\right|_{\varepsilon=0} f(\mathbf{x}+\varepsilon\mathbf{u}). \tag{2.27}$$

The quantity **x** may be a scalar, a vector or even a vector of unknown functions. For instance, consider a scalar function $f(\mathbf{x})$, where **x** is the position vector in $\mathbb{R}^3$. In this case the directional derivative is given by:

$$\begin{aligned} Df(\mathbf{x})[\mathbf{u}] &= \left.\frac{d}{d\varepsilon}\right|_{\varepsilon=0} f(\mathbf{x}+\varepsilon\mathbf{u}) \\ &= \frac{\partial f}{\partial x_i} u_i \\ &= \nabla f \cdot \mathbf{u}. \end{aligned} \tag{2.28}$$

Here, the symbol ∇ (“del”) depicts the gradient operator.

The linearization of a function implies that it is approximated by a linear function. Using the directional derivative, a function *f* can be linearized as follows:

$$f(\mathbf{x}+\mathbf{u}) \cong f(\mathbf{x}) + Df(\mathbf{x})[\mathbf{u}]. \tag{2.29}$$

The directional derivative obeys the usual properties for derivatives.

(a) *sum rule*: If $f = f_1 + f_2$, then

$$Df(\mathbf{x})[\mathbf{u}] = Df_1(\mathbf{x})[\mathbf{u}] + Df_2(\mathbf{x})[\mathbf{u}]. \tag{2.30}$$

(b) *product rule*: If $f = f_1 \cdot f_2$, then

$$Df(\mathbf{x})[\mathbf{u}] = f_1(\mathbf{x}) \cdot Df_2(\mathbf{x})[\mathbf{u}] + f_2 \cdot Df_1(\mathbf{x})[\mathbf{u}]. \tag{2.31}$$

(c) *chain rule*: If $f = g(h(\mathbf{x}))$, then

$$Df(\mathbf{x})[\mathbf{u}] = Dg(h(\mathbf{x}))\left[Dh(\mathbf{x})[\mathbf{u}]\right]. \tag{2.32}$$

2.3. Deformation, Strain and Stress

2.3.1. The deformation gradient tensor

Consider the deformation of an object from an initial or *reference configuration* to a deformed or *current configuration*. The location of the material particles in the reference configuration are denoted by $\mathbf{X}$ and are known as the *material coordinates.* Their location in the current configuration is denoted by $\mathbf{x}$ and known as the *spatial coordinates*. The *deformation map* $\boldsymbol{\varphi}$, which is a mapping from $\mathbb{R}^3$ to $\mathbb{R}^3$, maps the coordinates of a material point to the spatial configuration:

$$\mathbf{x} = \boldsymbol{\varphi}(\mathbf{X}). \tag{2.33}$$

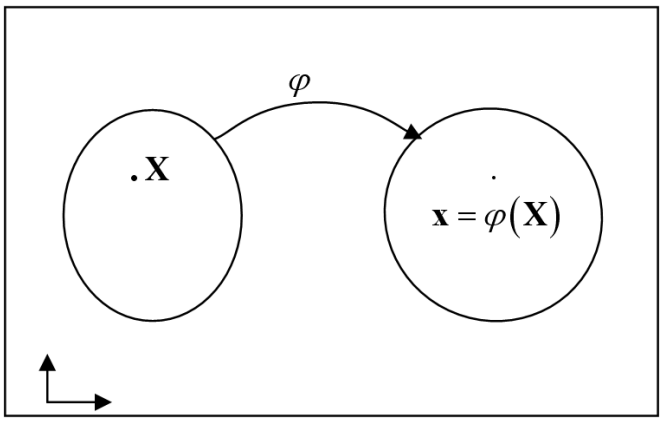

Figure 2-1. The deformation map

The displacement map $\mathbf{u}$ is defined as the difference between the spatial and material coordinates:

$$\mathbf{x} = \mathbf{X} + \mathbf{u}(\mathbf{X}). \tag{2.34}$$

The *deformation gradient* is defined as

$$\mathbf{F} = \frac{\partial \boldsymbol{\varphi}}{\partial \mathbf{X}}. \tag{2.35}$$

The deformation gradient relates an infinitesimal vector in the reference configuration $d\mathbf{X}$ to the corresponding vector in the current configuration:

$$d\mathbf{x} = \mathbf{F} \cdot d\mathbf{X}. \tag{2.36}$$

The determinant of the deformation tensor $J = \det \mathbf{F}$ gives the volume change, or equivalently the change in density:

$$\rho_0 = \rho J. \tag{2.37}$$

Here ρ_0 is the density in the reference configuration and ρ is the current density.

When dealing with incompressible and nearly incompressible materials it will prove useful to separate the volumetric and the deviatoric (distortional) components of the deformation gradient. Such a separation must ensure that the deviatoric part of the deformation gradient, namely $\tilde{\mathbf{F}}$, does not produce any change in volume. Noting that the determinant of the deformation gradient gives the volume ratio, the determinant of $\tilde{\mathbf{F}}$ must therefore satisfy,

$$\det \tilde{\mathbf{F}} = 1. \tag{2.38}$$

This condition can be achieved by choosing $\tilde{\mathbf{F}}$ as,

$$\tilde{\mathbf{F}} = J^{-1/3}\mathbf{F} . \tag{2.39}$$

Using the polar decomposition of a second order tensor, the deformation gradient can be written as a product of a positive definite symmetric tensor $\mathbf{V}$ **(or** $\mathbf{U}$ **)** and a proper orthogonal tensor **R**:

$$\mathbf{F} = \mathbf{V}\mathbf{R} = \mathbf{R}\mathbf{U} . \tag{2.40}$$

$\mathbf{V}$ is called the *left stretch tensor*, $\mathbf{U}$ is called the *right stretch tensor* and the orthogonal tensor $\mathbf{R}$ is called the *rotation*.

2.3.2. Strain

The *right Cauchy-Green deformation tensor* is defined as follows:

$$\mathbf{C} = \mathbf{F}^T\mathbf{F} . \tag{2.41}$$

This tensor is an example of a *material tensor* and is a function of the material coordinates **X**. The *left Cauchy-Green deformation tensor* is defined as follows:

$$\mathbf{b} = \mathbf{F}\mathbf{F}^T . \tag{2.42}$$

This tensor is an example of a *spatial tensor* and is a function of the spatial coordinates **x**. The implementation of the updated Lagrangian finite element method used by FEBio is described in the spatial configuration.

The left and right deformation tensors can also be split into volumetric and deviatoric components. With the use of,(2.39) the deviatoric deformation tensors are:

$$\begin{aligned} \tilde{\mathbf{C}} &= \tilde{\mathbf{F}}^T\tilde{\mathbf{F}} = J^{-2/3}\mathbf{C} \\ \tilde{\mathbf{b}} &= \tilde{\mathbf{F}}\tilde{\mathbf{F}}^T = J^{-2/3}\mathbf{b} \end{aligned} . \tag{2.43}$$

The deformation tensors defined above are not good candidates for strain measures since in the absence of strain they become the identity tensor $\mathbf{I}$. However, they can be used to define strain measures. The *Green-Lagrange strain tensor* is defined as:

$$\mathbf{E} = \frac{1}{2}\left(\mathbf{C} - \mathbf{I}\right) . \tag{2.44}$$

This tensor is a material tensor. Its spatial equivalent is known as the *Almansi strain tensor* and is defined as:

$$\mathbf{e} = \frac{1}{2}\left(\mathbf{I} - \mathbf{b}^{-1}\right) . \tag{2.45}$$

In the limit of small displacement gradients, the components of both strain tensors are identical, resulting in the *small strain tensor* or *infinitesimal strain tensor*:

$$\boldsymbol{\varepsilon} = \frac{1}{2}\left(\frac{\partial \mathbf{u}}{\partial \mathbf{x}} + \left(\frac{\partial \mathbf{u}}{\partial \mathbf{x}}\right)^T\right) . \tag{2.46}$$

Note that the small strain tensor is also the linearization of the Green Lagrange strain,

$$D\mathbf{E}\left[\mathbf{u}\right] = \mathbf{F}^T\boldsymbol{\varepsilon}\mathbf{F} . \tag{2.47}$$

2.3.3. Stress

The traction **t** on a plane bisecting the body is given by,

$$\mathbf{t} = \boldsymbol{\sigma}\cdot\mathbf{n} , \tag{2.48}$$

where $\boldsymbol{\sigma}$ is the *Cauchy stress tensor* and $\mathbf{n}$ is the outward unit normal vector to the plane. It can be shown that by the conservation of angular momentum that this tensor is symmetric ($\sigma_{ij} = \sigma_{ji}$) [3]. The Cauchy stress tensor, a spatial tensor, is the actual physical stress, that is, the force per unit deformed area. To simplify the equations of continuum mechanics, especially when working in the material configuration, several other stress measures are often used. The *Kirchhoff stress tensor* is defined as

$$\boldsymbol{\tau} = J\boldsymbol{\sigma} \,. \tag{2.49}$$

The *first Piola-Kirchhoff stress tensor* is given as

$$\mathbf{P} = J\boldsymbol{\sigma}\mathbf{F}^{-T} \,. \tag{2.50}$$

Note that $\mathbf{P}$, like $\mathbf{F}$, is not symmetric. Also, like $\mathbf{F}$, $\mathbf{P}$ is known as a *two-point* tensor, meaning it is neither a material nor a spatial tensor. Since we have two strain tensors, one spatial and one material tensor, it would be useful to have similar stress measures. The Cauchy stress is a spatial tensor and the *second Piola-Kirchhoff (2nd PK) stress tensor*, defined as

$$\mathbf{S} = J\mathbf{F}^{-1}\boldsymbol{\sigma}\mathbf{F}^{-T} \,, \tag{2.51}$$

is a material tensor. The inverse relations are:

$$\boldsymbol{\sigma} = \frac{1}{J}\boldsymbol{\tau}, \quad \boldsymbol{\sigma} = \frac{1}{J}\mathbf{P}\mathbf{F}^{T}, \quad \boldsymbol{\sigma} = \frac{1}{J}\mathbf{F}\mathbf{S}\mathbf{F}^{T} \,. \tag{2.52}$$

In many practical applications it is physically relevant to separate the hydrostatic stress and the deviatoric stress $\tilde{\boldsymbol{\sigma}}$ of the Cauchy stress tensor:

$$\boldsymbol{\sigma} = \tilde{\boldsymbol{\sigma}} + p\mathbf{1} \,. \tag{2.53}$$

Here, the pressure is defined as $p = \frac{1}{3}\operatorname{tr}\boldsymbol{\sigma}$. Note that the deviatoric Cauchy stress tensor satisfies $\operatorname{tr}\tilde{\boldsymbol{\sigma}} = 0$.

The directional derivative of the 2nd PK stress tensor needs to be calculated for the linearization of the finite element equations. For a hyperelastic material, a linear relationship between the directional derivative of $\mathbf{S}$ and the linearized strain $D\mathbf{E}[\mathbf{u}]$ can be obtained:

$$D\mathbf{S}[\mathbf{u}] = \boldsymbol{\mathcal{C}} : D\mathbf{E}[\mathbf{u}] \,. \tag{2.54}$$

Here, $\boldsymbol{\mathcal{C}}$ is a fourth-order tensor known as the *material elasticity tensor*. Its components are given by,

$$\mathcal{C}_{IJKL} = \frac{\partial S_{IJ}}{\partial E_{KL}} = \frac{4\partial^2\Psi}{\partial C_{IJ}\partial C_{KL}} \,, \tag{2.55}$$

where Ψ is the strain-energy density function for the hyperelastic material. The spatial equivalent – the *spatial elasticity tensor* – can be obtained by,

$$c_{ijkl} = \frac{1}{J}F_{iI}F_{jJ}F_{kK}F_{lL}\mathcal{C}_{IJKL} \,. \tag{2.56}$$

2.4. Hyperelasticity

When the constitutive behavior is only a function of the current state of deformation, the material is *elastic*. In the special case when the work done by the stresses during a deformation is only dependent on the initial state and the final state, the material is termed *hyperelastic* and its behavior is path-independent. As a consequence of the path-independence a *strain energy*

function per unit undeformed volume can be defined as the work done by the stresses from the initial to the final configuration:

$$\Psi\left(\mathbf{F}(\mathbf{X}),\mathbf{X}\right)=\int_{t_0}^{t}\mathbf{P}\left(\mathbf{F}(\mathbf{X}),\mathbf{X}\right):\dot{\mathbf{F}}\,dt\,. \tag{2.57}$$

The rate of change of the potential is then given by

$$\dot{\Psi}\left(\mathbf{F}(\mathbf{X}),\mathbf{X}\right)=\mathbf{P}:\dot{\mathbf{F}}\,. \tag{2.58}$$

Or alternatively,

$$P_{iJ}=\sum_{i,J=1}^{3}\frac{\partial\Psi}{\partial F_{iJ}}\dot{F}_{iJ}\,. \tag{2.59}$$

Comparing (2.58) with (2.59) reveals that

$$\mathbf{P}\left(\mathbf{F}(\mathbf{X}),\mathbf{X}\right)=\frac{\partial\Psi\left(\mathbf{F}(\mathbf{X}),\mathbf{X}\right)}{\partial\mathbf{F}}\,. \tag{2.60}$$

This general constitutive equation can be further simplified by observing that, as a consequence of the objectivity requirement, Ψ may only depend on **F** through the stretch tensor **U** and must be independent of the rotation component **R**. For convenience, however, Ψ is often expressed as a function of $\mathbf{C}=\mathbf{U}^2=\mathbf{F}^T\mathbf{F}$. Noting that $\frac{1}{2}\dot{\mathbf{C}}=\dot{\mathbf{E}}$ is work conjugate to the second Piola-Kirchhoff stress **S**, establishes the following general relationships for hyperelastic materials:

$$\dot{\Psi}=\frac{\partial\Psi}{\partial\mathbf{C}}:\dot{\mathbf{C}}=\frac{1}{2}\mathbf{S}:\dot{\mathbf{C}},\quad \boxed{\mathbf{S}\left(\mathbf{C}(\mathbf{X}),\mathbf{X}\right)=2\frac{\partial\Psi}{\partial\mathbf{C}}=\frac{\partial\Psi}{\partial\mathbf{E}}}\,. \tag{2.61}$$

2.4.1. Isotropic Hyperelasticity

The hyperelastic constitutive equations discussed so far are unrestricted in their application. Isotropic material symmetry is defined by requiring the constitutive behavior to be independent of the material axis chosen and, consequently, Ψ must only be a function of the invariants of **C**,

$$\Psi\left(\mathbf{C}(\mathbf{X}),\mathbf{X}\right)=\Psi\left(I_1,I_2,I_3,\mathbf{X}\right), \tag{2.62}$$

where the invariants of **C** are defined here as,

$$I_1=\operatorname{tr}\mathbf{C}=\mathbf{C}:\mathbf{I},\ I_2=\frac{1}{2}\left[\left(\operatorname{tr}\mathbf{C}\right)^2-\operatorname{tr}\mathbf{C}^2\right],\ I_3=\det\mathbf{C}=J^2. \tag{2.63}$$

As a result of the isotropic restriction, the second Piola-Kirchhoff stress tensor can be written as,

$$\mathbf{S}=2\frac{\partial\Psi}{\partial\mathbf{C}}=2\frac{\partial\Psi}{\partial I_1}\frac{\partial I_1}{\partial\mathbf{C}}+2\frac{\partial\Psi}{\partial I_2}\frac{\partial I_2}{\partial\mathbf{C}}+2\frac{\partial\Psi}{\partial I_3}\frac{\partial I_3}{\partial\mathbf{C}}\,. \tag{2.64}$$

The second order tensors formed by the derivatives of the invariants with respect to **C** can be evaluated as follows:

$$\frac{\partial I_1}{\partial\mathbf{C}}=\mathbf{I},\ \frac{\partial I_2}{\partial\mathbf{C}}=I_1\mathbf{I}-\mathbf{C},\ \frac{\partial I_3}{\partial\mathbf{C}}=I_3\mathbf{C}^{-1}. \tag{2.65}$$

Introducing expressions (2.65) into equation (2.64) enables the second Piola-Kirchhoff stress to be evaluated as,

$$\mathbf{S}=2\left\{\left(\Psi_1+I_1\Psi_2+I_2\Psi_3\right)\right)\mathbf{I}-\left(\Psi_2+I_1\Psi_3\right)\mathbf{C}\right\}+\Psi_3\mathbf{C}^2\,, \tag{2.66}$$

where $\Psi_I = \partial\Psi / \partial I_1$, $\Psi_2 = \partial\Psi / \partial I_2$, and $\Psi_3 = \partial\Psi / \partial I_3$.

The Cauchy stresses can now be obtained from the second Piola-Kirchhoff stresses by using (2.52):

$$\boldsymbol{\sigma} = 2\left\{\left(\Psi_1 + I_1\Psi_2 + I_2\Psi_3\right)\right)\mathbf{b} - \left(\Psi_2 + I_1\Psi_3\right)\mathbf{b}^2\right\} + \Psi_3\mathbf{b}^3. \tag{2.67}$$

Note that in this equation Ψ_1, Ψ_2, and Ψ_3 still involve derivatives with respect to the invariants of **C**. However, since the invariants of **b** are identical to those of **C**, the quantities Ψ_1, Ψ_2 and Ψ_3 may also be considered to be the derivatives with respect to the invariants of **b**.

2.4.2. Isotropic Elasticity in Principal Directions

For isotropic materials, the principal directions of the strain and stress tensors are the same. Let the eigenvalues of $\mathbf{C}$ be denoted by λ_i^2 ($i = 1,2,3$), then the strain energy density may be given as a function of these eigenvalues, $\Psi\left(\lambda_1^2, \lambda_2^2, \lambda_3^2\right)$. To derive the expression for the stress, recognize that

$$\frac{\partial\lambda_i^2}{\partial\mathbf{C}} = \mathbf{N}_i \otimes \mathbf{N}_i \equiv \mathbf{A}_i, \tag{2.68}$$

where the $\mathbf{N}_i$ are the eigenvectors of $\mathbf{C}$. It follows that the second Piola-Kirchhoff stress may be represented as

$$\mathbf{S} = \sum_{i=1}^{3} S_i \mathbf{A}_i, \tag{2.69}$$

where

$$S_i = 2\frac{\partial\Psi}{\partial\lambda_i^2}. \tag{2.70}$$

To evaluate the material elasticity tensor, recognize that

$$\frac{\partial\mathbf{A}_i}{\partial\mathbf{C}} = \frac{1}{\lambda_i^2 - \lambda_j^2}\left(\mathbf{A}_i \overline{\underline{\otimes}} \mathbf{A}_j + \mathbf{A}_j \overline{\underline{\otimes}} \mathbf{A}_i\right) + \frac{1}{\lambda_i^2 - \lambda_k^2}\left(\mathbf{A}_i \overline{\underline{\otimes}} \mathbf{A}_k + \mathbf{A}_k \overline{\underline{\otimes}} \mathbf{A}_i\right), \tag{2.71}$$

where i, j, k form a permutation over $1,2,3$. Then it can be shown that the material elasticity tensor is given by

$$\begin{aligned}\mathcal{C} = &\sum_{i=1}^{3} 4\frac{\partial^2\Psi}{\partial\lambda_i^2\partial\lambda_i^2}\mathbf{A}_i \otimes \mathbf{A}_i \\ &+ \sum_{i=1}^{3}\sum_{j=i+1}^{3} 4\frac{\partial^2\Psi}{\partial\lambda_i^2\partial\lambda_j^2}\left(\mathbf{A}_i \otimes \mathbf{A}_j + \mathbf{A}_j \otimes \mathbf{A}_i\right) \\ &+ \sum_{i=1}^{3}\sum_{j=i+1}^{3} 2\frac{S_i - S_j}{\lambda_i^2 - \lambda_j^2}\left(\mathbf{A}_i \overline{\underline{\otimes}} \mathbf{A}_j + \mathbf{A}_j \overline{\underline{\otimes}} \mathbf{A}_i\right)\end{aligned} \tag{2.72}$$

When eigenvalues coincide, L'Hospital's rule may be used to evalue the coefficient in the last term,

$$\lim_{\lambda_j^2 \to \lambda_i^2} 2\frac{S_i - S_j}{\lambda_i^2 - \lambda_j^2} = 4\left(\frac{\partial^2\Psi}{\partial\lambda_j^2\partial\lambda_j^2} - \frac{\partial^2\Psi}{\partial\lambda_i^2\partial\lambda_j^2}\right). \tag{2.73}$$

The double summations in (2.72) are arranged such that the summands represent fourth-order tensors with major and minor symmetries.

In the spatial frame, the Cauchy stress is given by

$$\boldsymbol{\sigma} = \sum_{i=1}^{3} \sigma_i \mathbf{a}_i \tag{2.74}$$

where

$$\mathbf{a}_i = \mathbf{n}_i \otimes \mathbf{n}_i \,, \tag{2.75}$$

and $\mathbf{n}_i = \left(\mathbf{F}\cdot\mathbf{N}_i\right)/\lambda_i$ are the eigenvectors of $\mathbf{b}$. The principal normal stresses are

$$\sigma_i = \frac{\lambda_i}{J}\frac{\partial \Psi}{\partial \lambda_i} \,. \tag{2.76}$$

The spatial elasticity tensor is given by

$$\begin{aligned} \boldsymbol{c} = & \sum_{i=1}^{3}\left(J^{-1}\lambda_i^2 \frac{\partial^2 \Psi}{\partial \lambda_i^2} - \sigma_i \right) \mathbf{a}_i \otimes \mathbf{a}_i \\ & + \sum_{i=1}^{3}\sum_{j=i+1}^{3} J^{-1}\lambda_i\lambda_j \frac{\partial^2 \Psi}{\partial \lambda_i \partial \lambda_j}\left(\mathbf{a}_i \otimes \mathbf{a}_j + \mathbf{a}_j \otimes \mathbf{a}_i\right) \\ & + \sum_{i=1}^{3}\sum_{j=i+1}^{3} 2\frac{\lambda_j^2\sigma_i - \lambda_i^2\sigma_j}{\lambda_i^2 - \lambda_j^2}\left(\mathbf{a}_i \,\underline{\overline{\otimes}}\, \mathbf{a}_j + \mathbf{a}_j \,\underline{\overline{\otimes}}\, \mathbf{a}_i\right) \end{aligned} \tag{2.77}$$

2.4.3. Nearly-Incompressible Hyperelasticity

A material is considered incompressible if it shows no change in volume during deformation, or otherwise stated, if $J = 1$ holds throughout the entire body. It can be shown [1] that if the material is incompressible the hyperelastic constitutive equation becomes

$$\mathbf{S} = 2\frac{\partial \tilde{\Psi}}{\partial \mathbf{C}} + pJ\mathbf{C}^{-1} \,, \tag{2.78}$$

where $\tilde{\Psi} = \Psi\left(\tilde{\mathbf{C}}\right)$ is the deviatoric strain energy function and p is the hydrostatic pressure. The presence of J may seem unnecessary, but retaining J has the advantage that equation (2.78) remains valid in the nearly incompressible case. Further, in practical terms, a finite element analysis rarely enforces $J = 1$ in a pointwise manner, and hence its retention may be important for the evaluation of stresses.

The process of defining constitutive equations in the case of nearly incompressible hyperelasticity is simplified by adding a volumetric energy component $U\left(J\right)$ to the distortional component $\tilde{\Psi}\left(\mathbf{C}\right)$:

$$\Psi\left(\mathbf{C}\right) = \tilde{\Psi}\left(\mathbf{C}\right) + U\left(J\right) \,. \tag{2.79}$$

The second Piola-Kirchhoff tensor for a material defined by (2.79) is obtained in the standard manner with the help of equation (2.64).

$$\begin{aligned}\mathbf{S} &= 2\frac{\partial\Psi}{\partial\mathbf{C}} \\ &= 2\frac{\partial\tilde{\Psi}}{\partial\mathbf{C}} + 2\frac{dU}{dJ}\frac{\partial J}{\partial C} \\ &= 2\frac{\partial\tilde{\Psi}}{\partial\mathbf{C}} + pJ\mathbf{C}^{-1},\end{aligned} \tag{2.80}$$

where the pressure p is defined as

$$p = \frac{dU}{dJ}. \tag{2.81}$$

An example for U that will be used later in the definition of the constitutive models is

$$U(J) = \frac{1}{2}\kappa(\ln J)^2. \tag{2.82}$$

The parameter κ will be used later as a penalty factor that will enforce the (nearly-) incompressible constraint. However, κ can represent a true material coefficient, namely the bulk modulus, for a compressible material that happens to have a hyperelastic strain energy function in the form of (2.79). In the case where the dilatational energy is given by (2.82), the pressure is

$$p = \kappa\frac{\ln J}{J}. \tag{2.83}$$

Equation (2.80) can be further developed by applying the chain rule to the first term:

$$\mathbf{S} = pJ\mathbf{C}^{-1} + J^{-2/3}\,\mathrm{Dev}\,\tilde{\mathbf{S}}, \tag{2.84}$$

where the *fictitious second Piola-Kirchoff* tensor [4] is defined by,

$$\tilde{\mathbf{S}} = 2\frac{\partial\tilde{\Psi}}{\partial\tilde{\mathbf{C}}}, \tag{2.85}$$

and Dev is the deviator operator in the reference frame:

$$\mathrm{Dev}(\bullet) = (\bullet) - \frac{1}{3}\left((\bullet):\mathbf{C}\right)\mathbf{C}^{-1}. \tag{2.86}$$

The Cauchy stress can then be obtained from equation $(2.52)_3$:

$$\boldsymbol{\sigma} = p\mathbf{I} + \mathrm{dev}\,\tilde{\boldsymbol{\sigma}}. \tag{2.87}$$

where

$$\tilde{\boldsymbol{\sigma}} = \frac{2}{J}\tilde{\mathbf{F}}\frac{\partial\tilde{\Psi}}{\partial\tilde{\mathbf{C}}}\tilde{\mathbf{F}}^T \tag{2.88}$$

2.4.4. Transversely Isotropic Hyperelasticity

Transverse isotropy can be introduced by adding a vector field representing the material preferred direction explicitly into the strain energy [5]. We require that the strain energy depends on a unit vector field $\mathbf{A}$, which describes the local fiber direction in the undeformed configuration. When the material undergoes deformation, the vector $\mathbf{A}(\mathbf{X})$ may be described by a unit vector field $\mathbf{a}(\varphi(\mathbf{X}))$. In general, the fibers will also undergo length change. The fiber stretch, λ, can be determined in terms of the deformation gradient and the fiber direction in the undeformed configuration,

$$\lambda\mathbf{a} = \mathbf{F}\cdot\mathbf{A}. \tag{2.89}$$

Also, since $\mathbf{a}$ is a unit vector,

$$\lambda^2 = \mathbf{A}\cdot\mathbf{C}\cdot\mathbf{A}. \tag{2.90}$$

The strain energy function for a transversely isotropic material, $\Psi(\mathbf{C},\mathbf{A},\mathbf{X})$ is an isotropic function of $\mathbf{C}$ and $\mathbf{A}\otimes\mathbf{A}$. It can be shown [3] that the following set of invariants are sufficient to describe the material fully:

$$I_1 = \operatorname{tr}\mathbf{C}, \quad I_2 = \frac{1}{2}\left[\left(\operatorname{tr}\mathbf{C}\right)^2 - \operatorname{tr}\mathbf{C}^2\right], \quad I_3 = \det C = J^2, \tag{2.91}$$

$$I_4 = \mathbf{A}\cdot\mathbf{C}\cdot\mathbf{A}, \quad I_5 = \mathbf{A}\cdot\mathbf{C}^2\cdot\mathbf{A}. \tag{2.92}$$

The strain energy function can be written in terms of these invariants such that

$$\Psi(\mathbf{C},\mathbf{A},\mathbf{X}) = \Psi\left(I_1(\mathbf{C}), I_2(\mathbf{C}), I_3(\mathbf{C}), I_4(\mathbf{C},\mathbf{A}), I_5(\mathbf{C},\mathbf{A})\right). \tag{2.93}$$

The second Piola-Kirchhoff can now be obtained in the standard manner:

$$\mathbf{S} = 2\frac{\partial\Psi}{\partial\mathbf{C}} = 2\sum_{i=1}^{5}\frac{\partial\Psi}{\partial I_i}\frac{\partial I_i}{\partial\mathbf{C}}. \tag{2.94}$$

In the transversely isotropic constitutive models described in Chapter 5 it is further assumed that the strain energy function can be split into the following terms:

$$\Psi(\mathbf{C},\mathbf{A}) = \Psi_1(I_1, I_2, I_3) + \Psi_2(I_4) + \Psi_3(I_1, I_2, I_3 I_4). \tag{2.95}$$

The strain energy function Ψ_1 represents the material response of the isotropic ground substance matrix, Ψ_2 represents the contribution from the fiber family (e.g. collagen), and Ψ_3 is the contribution from interactions between the fibers and matrix. The form (2.95) generalizes many constitutive equations that have been successfully used in the past to describe biological soft tissues e.g. [6-8]. While this relation represents a large simplification when compared to the general case, it also embodies almost all of the material behavior that one would expect from transversely isotropic, large deformation matrix-fiber composites.

2.5. Biphasic Material

Biphasic materials may be used to model deformable porous media. A biphasic material represents a mixture of a porous permeable solid and an interstitial fluid. Each constituent is intrinsically incompressible, but the mixture may change volume as interstitial fluid is exchanged with the pore space of the solid. Biphasic materials require the explicit modeling of fluid that permeates the solid. The biphasic material model is useful to simulate materials that show flow-dependent viscoelastic behavior resulting from the frictional interactions of the fluid and solid. Several biological materials such as cartilage can be described more accurately this way.

2.5.1. Governing Equations

Consider a mixture consisting of a solid constituent and a fluid constituent. Both constituents are considered to be intrinsically incompressible, but the mixture can change volume when fluid enters or leaves the porous solid matrix [9, 10]. According to the kinematics of the continuum [11], each constituent α of a mixture ($\alpha = s$ for the solid and $\alpha = w$ for the fluid) has a separate motion $\boldsymbol{\varphi}^{\alpha}\left(\mathbf{X}^{\alpha}, t\right)$ which places particles of each mixture constituent, originally located at $\mathbf{X}^{\alpha}$, in the current configuration $\mathbf{x}$ according to

$$\mathbf{x} = \boldsymbol{\varphi}^{\alpha}\left(\mathbf{X}^{\alpha}, t\right). \tag{2.96}$$

For the purpose of finite element analyses, the motion of the solid matrix, $\alpha = s$, is of particular interest.

The governing equations that enter into the statement of virtual work are the conservation of linear momentum and the conservation of mass, for the mixture as a whole. Under quasi-static conditions, in the absence of external body forces, the conservation of momentum reduces to

$$\operatorname{div}\boldsymbol{\sigma} = \mathbf{0}, \tag{2.97}$$

where $\boldsymbol{\sigma}$ is the Cauchy stress for the mixture. Since the mixture is porous, this stress may also be written as

$$\boldsymbol{\sigma} = -p\mathbf{I} + \boldsymbol{\sigma}^{e}, \tag{2.98}$$

where p is the fluid pressure and $\boldsymbol{\sigma}^{e}$ is the effective or extra stress, resulting from the deformation of the solid matrix. Conservation of mass for the mixture requires that

$$\operatorname{div}\left(\mathbf{v}^{s} + \mathbf{w}\right) = 0, \tag{2.99}$$

where $\mathbf{v}^{s} = \partial\boldsymbol{\varphi}^{s}/\partial t$ is the solid matrix velocity and $\mathbf{w}$ is the flux of the fluid relative to the solid matrix. Let the solid matrix displacement be denoted by $\mathbf{u}$, then $\mathbf{v}^{s} = \dot{\mathbf{u}}$.

To relate the relative fluid flux $\mathbf{w}$ to the fluid pressure and solid deformation, it is necessary to employ the equation of conservation of linear momentum for the fluid,

$$-\varphi^{w}\operatorname{grad} p + \hat{\mathbf{p}}_{d}^{w} = \mathbf{0}, \tag{2.100}$$

where φ^{w} is the solid matrix porosity, and $\hat{\mathbf{p}}_{d}^{w}$ is the momentum exchange between the solid and fluid constituents, typically representing the frictional interaction between these constituents. This equation neglects the viscous stress of the fluid in comparison to $\hat{\mathbf{p}}_{d}^{w}$. The most common

constitutive relation is $\hat{\mathbf{p}}_d^w = -\varphi^w \mathbf{k}^{-1} \cdot \mathbf{w}$, where the second order, symmetric tensor $\mathbf{k}$ is the hydraulic permeability of the mixture. When combined with Eq.(2.100), it produces

$$\mathbf{w} = -\mathbf{k} \cdot \text{grad}\, p \,, \tag{2.101}$$

which is equivalent to Darcy's law. In general, $\mathbf{k}$ may be a function of the deformation.

2.6. Biphasic-Solute Material

A biphasic-solute material is an extension of the biphasic material model that also includes transport and mechano-chemical effects of a neutral solute. Transport of a solute in a porous medium includes diffusion, resulting from gradients in the solute concentration, and convection of the solute by the solvent, as a result of fluid pressure gradients. Mechano-chemical effects describe phenomena such as osmotic pressurization and swelling.

2.6.1. Governing Equations

The governing equations adopted in this finite element implementation of neutral solute transport in deformable porous media are based on the framework of mixture theory [11, 12]. A single solute is considered in this presentation for notational simplicity, though the extension of equations to multiple solutes is straightforward. Various forms of the governing equations have been presented in the prior literature [13, 14], though a presentation that incorporates all the desired features of this implementation has not been reported previously and is thus detailed here.

The fundamental modeling assumptions adopted in this treatment are quasi-static conditions for momentum balance (negligible effects of inertia), intrinsic incompressibility of all constituents (invariant true densities), isothermal conditions, negligible volume fraction of solute relative to the solid and solvent, and negligible effects of solute and solvent viscosities (friction within constituents) relative to frictional interactions between constituents. These assumptions are often made in studies of biological tissues and cells. External body forces and chemical reactions are not considered.

The three constituents of the mixture are the porous-permeable solid matrix ($\alpha = s$), the solvent ($\alpha = w$), and the solute ($\alpha = u$). The motion of the solid matrix is described by the displacement vector $\mathbf{u}$, the pressure of the interstitial fluid (solvent+solute) is p, and the solute concentration (on a solution-volume basis) is c. The total (or mixture) stress may be described by the Cauchy stress tensor $\boldsymbol{\sigma} = -p\mathbf{I} + \boldsymbol{\sigma}^e$, where $\mathbf{I}$ is the identity tensor and $\boldsymbol{\sigma}^e$ is the stress arising from the strain in the porous solid matrix. Because it is porous, the solid matrix is compressible since the volume of pores changes as interstitial fluid enters or leaves the matrix. Under the conditions outlined above, the balance of linear momentum for the mixture reduces to

$$\operatorname{div}\boldsymbol{\sigma} = -\operatorname{grad} p + \operatorname{div}\boldsymbol{\sigma}^e = \mathbf{0}\,. \tag{2.102}$$

Similarly, the equations of balance of linear momentum for the solvent and solute are given by

$$\begin{aligned} \rho^w \operatorname{grad}\tilde{\mu}^w + \mathbf{f}^{ws}\cdot\left(\mathbf{v}^s - \mathbf{v}^w\right) + \mathbf{f}^{wu}\cdot\left(\mathbf{v}^u - \mathbf{v}^w\right) &= \mathbf{0}, \\ -\rho^u \operatorname{grad}\tilde{\mu}^u + \mathbf{f}^{us}\cdot\left(\mathbf{v}^s - \mathbf{v}^u\right) + \mathbf{f}^{uw}\cdot\left(\mathbf{v}^w - \mathbf{v}^u\right) &= \mathbf{0}, \end{aligned} \tag{2.103}$$

where ρ^α is the apparent density (mass of α per volume of the mixture), $\tilde{\mu}^\alpha$ is the mechano-chemical potential and $\mathbf{v}^\alpha$ is the velocity of constituent α. $\mathbf{f}^{\alpha\beta}$ is the diffusive drag tensor between constituents α and β representing momentum exchange via frictional interactions, which satisfies $\mathbf{f}^{\beta\alpha} = \mathbf{f}^{\alpha\beta}$. An important feature of these relations is the incorporation of

momentum exchange term between the solute and solid matrix, $\mathbf{f}^{us}\cdot\left(\mathbf{v}^{s}-\mathbf{v}^{u}\right)$, which is often neglected in other treatments but plays an important role for describing solid-solute interactions [13, 15, 16]. These momentum equations show that the driving force for the transport of solvent or solute is the gradient in its mechano-chemical potential, which is resisted by frictional interactions with other constituents.

The mechano-chemical potential is the sum of the mechanical and chemical potentials. The chemical potential μ^{α} of α represents the rate at which the mixture free energy changes with increasing mass of α. The mechanical potential represents the rate at which the mixture free energy density changes with increasing volumetric strain of α. In a mixture of intrinsically incompressible constituents, where the volumetric strain is idealized to be zero, this potential is given by $\left(p-p_0\right)/\rho_T^{\alpha}$, where ρ_T^{α} is the true density of α (mass of α per volume of α), which is invariant for incompressible constituents, and p_0 is some arbitrarily set reference pressure (e.g., ambient pressure).

From classical physical chemistry, the general form of a constitutive relation for the chemical potential is $\mu^{\alpha}=\mu_0^{\alpha}\left(\theta\right)+\left(R\theta/M^{\alpha}\right)\ln a^{\alpha}$ [17], where R is the universal gas constant, θ is the absolute temperature, M^{α} is the molecular weight (invariant) and a^{α} is the activity of constituent α (a non-dimensional quantity); $\mu_0^{\alpha}\left(\theta\right)$ is the chemical potential at some arbitrary reference state, at a given temperature. For solutes, physical chemistry treatments let $a^{u}=\gamma c/c_0$, where c_0 is the solute concentration in some standard reference state (an invariant, typically $c_0=1\text{M}$), and γ is the non-dimensional activity coefficient, which generally depends on the current state (e.g., concentration) but reduces to unity under the assumption of ideal physico-chemical behavior [17]. Since this representation is strictly valid for free solutions only, whereas solutes may be partially excluded from some of the interstitial space of a porous solid matrix, Mauck et al. [13] extended this representation of the solute activity to let $a^{u}=\gamma c/\kappa c_0$, where the solubility κ represents the fraction of the pore space which is accessible to the solute ($0<\kappa\le 1$). In this extended form, it becomes clear that even under ideal behavior ($\gamma=1$), the solute activity may be affected by the solubility. Indeed, for neutral solutes, the solubility also represents the partition coefficient of the solute between the tissue and external bath [18, 19].

When accounting for the fact that the solute volume fraction is negligible compared to the solvent volume fraction [17, 20], the general expressions for $\tilde{\mu}^{w}$ and $\tilde{\mu}^{u}$ take the form

$$\begin{aligned}\tilde{\mu}^{w}&=\mu_0^{w}\left(\theta\right)+\frac{1}{\rho_T^{w}}\left(p-p_0-R\theta\Phi c\right),\\ \tilde{\mu}^{u}&=\mu_0^{u}\left(\theta\right)+\frac{R\theta}{M}\ln\frac{\gamma c}{\kappa c_0},\end{aligned}\tag{2.104}$$

where Φ is the osmotic coefficient (a non-dimensional function of the state), which deviates from unity under non-ideal physico-chemical behavior. Therefore, a complete description of the physico-chemical state of solvent and solute requires constitutive relations for Φ and the

effective solubility $\tilde{\kappa} = \kappa / \gamma$, which should generally depend on the solid matrix strain and the solute concentration.

It is also necessary to satisfy the balance of mass for each of the constituents. In the absence of chemical reactions, the statement of balance of mass for constituent α reduces to

$$\frac{\partial \rho^{\alpha}}{\partial t} + \operatorname{div}\left(\rho^{\alpha}\mathbf{v}^{\alpha}\right) = 0 . \tag{2.105}$$

The apparent density may be related to the true density via $\rho^{\alpha} = \varphi^{\alpha}\rho_T^{\alpha}$, where φ^{α} is the volume fraction of α in the mixture. Due to mixture saturation (no voids), the volume fractions add up to unity. Since the volume fraction of solute is considered negligible ($\varphi^u \ll \varphi^s, \varphi^w$), it follows that $\sum_{\alpha}\varphi^{\alpha} \approx \varphi^s + \varphi^w = 1$. Since ρ_T^{α} of an incompressible constituent is invariant in space and time, these relations may be combined to produce the mixture balance of mass relation,

$$\operatorname{div}\left(\mathbf{v}^s + \mathbf{w}\right) = 0 , \tag{2.106}$$

where $\mathbf{w} = \varphi^w\left(\mathbf{v}^w - \mathbf{v}^s\right)$ is the volumetric flux of solvent relative to the solid. The balance of mass for the solute may also be written as

$$\frac{\partial\left(\varphi^w c\right)}{\partial t} + \operatorname{div}\left(\mathbf{j} + \varphi^w c\,\mathbf{v}^s\right) = 0 , \tag{2.107}$$

where $\mathbf{j} = \varphi^w c\left(\mathbf{v}^u - \mathbf{v}^s\right)$ is the molar flux of solute relative to the solid. This mass balance relation is obtained by recognizing that the solute apparent density (mass per mixture volume) is related to its concentration (moles per solution volume) via $\rho^u = \left(1 - \varphi^s\right)Mc \approx \varphi^w Mc$. Finally, it can be shown via standard arguments that the mass balance for the solid matrix reduces to

$$\varphi^s = \frac{\varphi_r^s}{J} , \tag{2.108}$$

where φ_r^s is the solid volume fraction in the reference state, $J = \det\mathbf{F}$ and $\mathbf{F} = \mathbf{I} + \operatorname{Grad}\mathbf{u}$ is the deformation gradient of the solid matrix.

Inverting the momentum balance equations in (2.103), it is now possible to relate the solvent and solute fluxes to the driving forces according to

$$\begin{aligned} \mathbf{w} &= -\tilde{\mathbf{k}} \cdot \left(\rho_T^w \operatorname{grad}\tilde{\mu}^w + Mc\frac{\mathbf{d}}{d_0}\operatorname{grad}\tilde{\mu}^u \right) \\ \mathbf{j} &= \mathbf{d} \cdot \left(-\frac{M}{R\theta}\varphi^w c \operatorname{grad}\tilde{\mu}^u + \frac{c}{d_0}\mathbf{w} \right) \end{aligned} \tag{2.109}$$

where $\mathbf{d}$ is the solute diffusivity tensor in the mixture (solid+solution), d_0 is its (isotropic) diffusivity in free solution; $\tilde{\mathbf{k}}$ is the hydraulic permeability tensor of the solution (solvent+solute) through the porous solid matrix, which depends explicitly on concentration according to

$$\tilde{\mathbf{k}} = \left[\mathbf{k}^{-1} + \frac{R\theta c}{\varphi^w d_0} \left(\mathbf{I} - \frac{\mathbf{d}}{d_0} \right) \right]^{-1}, \tag{2.110}$$

where $\mathbf{k}$ represents the hydraulic permeability tensor of the solvent through the solid matrix. The permeability and diffusivity tensors are related to the diffusive drag tensors appearing in (2.103) according to

$$\begin{aligned} \mathbf{k} &= \left(\varphi^w\right)^2 \left(\mathbf{f}^{ws}\right)^{-1} \\ \mathbf{d}_0 &= R\theta\varphi^w c \left(\mathbf{f}^{uw}\right)^{-1} \equiv d_0 \mathbf{I}, \\ \mathbf{d} &= R\theta\varphi^w c \left(\mathbf{f}^{us} + \mathbf{f}^{uw}\right)^{-1} \end{aligned} \tag{2.111}$$

though these explicit relationships are not needed here since $\mathbf{k}$, $\mathbf{d}$ and d_0 may be directly specified in a particular analysis. Since the axiom of entropy inequality requires that the tensors $\mathbf{f}^{\alpha\beta}$ be positive semi-definite (see appendix of [21]), it follows that d_0 must be greater than or equal to the largest eigenvalue of $\mathbf{d}$. Constitutive relations are needed for these transport properties, which relate them to the solid matrix strain and solute concentration. Note that the relations in (2.111) represent generalizations of Darcy's law for fluid permeation through porous media, and Fick's law for solute diffusion in porous media or free solution.

2.6.2. Continuous Variables

In principle, the objective of the finite element analysis is to solve for the three unknowns, $\mathbf{u}$, p and c, using the partial differential equations that enforce mixture momentum balance in (2.102) , mixture mass balance in (2.106), and solute mass balance in (2.107). The remaining solvent and solute momentum balances in (2.109), and solid mass balance in (2.108), have been reduced to relations that may be substituted into the three partial differential equations as needed. Solving these equations requires the application of suitable boundary conditions that are consistent with mass, momentum and energy balances across boundary surfaces or interfaces. When defining boundaries or interfaces on the solid matrix (the conventional approach in solid mechanics), whose outward unit normal is $\mathbf{n}$, mass and momentum balance relations demonstrate that the mixture traction $\mathbf{t} = \boldsymbol{\sigma} \cdot \mathbf{n}$ and normal flux components $w_n = \mathbf{w} \cdot \mathbf{n}$ and $j_n = \mathbf{j} \cdot \mathbf{n}$ must be continuous across the interface [20, 22]. Therefore, $\mathbf{t}$, w_n and j_n may be prescribed as boundary conditions.

Combining momentum and energy balances across an interface also demonstrates that $\tilde{\mu}^w$ and $\tilde{\mu}^u$ must be continuous [20, 23], implying that these mechano-chemical potentials may be prescribed as boundary conditions. However, because of the arbitrariness of the reference states μ_0^w, μ_0^u, p_0 and c_0, and the ill-conditioning of the logarithm function in the limit of small solute concentration, the mechano-chemical potentials do not represent practical choices for primary variables in a finite element implementation. An examination of (2.104) also shows that continuity of these potentials across an interface does not imply continuity of the fluid pressure p or solute concentration c. Therefore, pressure and concentration are also unsuitable as nodal variables in a finite element analysis and they must be replaced by alternative choices. Based on

the similar reasoning presented by Sun et al. [24], an examination of the expressions in (2.104) shows that continuity may be enforced by using

$$\tilde{p} = p - R\theta\Phi c,$$
$$\tilde{c} = \frac{c}{\tilde{\kappa}}, \tag{2.112}$$

where $\tilde{p}$ is the effective fluid pressure and $\tilde{c}$ is the effective solute concentration in the mixture. Note that $\tilde{p}$ represents that part of the fluid pressure which does not result from osmotic effects (since the term $R\theta\Phi c$ may be viewed as the osmotic pressure contribution to p), and $\tilde{c}$ is a straightforward measure of the solute activity, since $a^u = \tilde{c}/c_0$. Therefore these alternative variables have clear physical meanings.

Since the unknowns are now given by $\mathbf{u}$, $\tilde{p}$ and $\tilde{c}$, the governing partial differential equations may be rewritten in the form

$$\operatorname{grad}\left(\tilde{p} + R\theta\Phi\tilde{\kappa}\tilde{c}\right) + \operatorname{div}\boldsymbol{\sigma}^e = \mathbf{0},$$
$$\operatorname{div}\left(\mathbf{v}^s + \mathbf{w}\right) = 0, , \tag{2.113}$$
$$\frac{\partial\left(\varphi^w\tilde{\kappa}\tilde{c}\right)}{\partial t} + \operatorname{div}\left(\mathbf{j} + \varphi^w\tilde{\kappa}\tilde{c}\,\mathbf{v}^s\right) = 0,$$

where

$$\mathbf{w} = -\tilde{\mathbf{k}}\cdot\left(\operatorname{grad}\tilde{p} + R\theta\frac{\tilde{\kappa}}{d_0}\mathbf{d}\cdot\operatorname{grad}\tilde{c}\right),$$
$$\mathbf{j} = \tilde{\kappa}\mathbf{d}\cdot\left(-\varphi^w\operatorname{grad}\tilde{c} + \frac{\tilde{c}}{d_0}\mathbf{w}\right), \tag{2.114}$$
$$\tilde{\mathbf{k}} = \left[\mathbf{k}^{-1} + \frac{R\theta}{\varphi^w}\frac{\tilde{\kappa}\tilde{c}}{d_0}\left(\mathbf{I} - \frac{\mathbf{d}}{d_0}\right)\right]^{-1}.$$

Constitutive equations are needed to relate $\boldsymbol{\sigma}^e$, $\mathbf{k}$, $\mathbf{d}$, d_0, $\tilde{\kappa}$ and Φ to the solid matrix strain and effective solute concentration.

2.7. Mixture of Solids

A solid material may consist of a heterogeneous mixture of various solid constituents that are constrained to move together. If each constituent is denoted by the superscript σ, a constrained mixture satisfies $\mathbf{v}^\sigma = \mathbf{v}^s$ for all σ, where $\mathbf{v}^s$ is the velocity of the solid mixture. For example, a fiber-reinforced material may consist of a mixture of fibers and a ground matrix. In general, the constitutive relation for such a constrained mixture of solids may be a complex function of the mass fraction of each constituent as well as the ultrastructure of the constituents and their mutual interactions. The mass fraction of each constituent may be represented by the apparent density ρ_r^σ, which is the ratio of the mass of σ to the volume of the mixture in the reference configuration, in an elemental region. In the framework of hyperelasticity, the general representation for the strain energy density for such a solid mixture may have the form

$$\Psi = \Psi\left(\mathbf{F}^{(1)},\cdots,\mathbf{F}^{(n)},\rho_r^{(1)},\cdots,\rho_r^{(n)}\right), \tag{2.115}$$

where $\mathbf{F}^{\sigma}$ is the deformation gradient of constituent σ and n is the number of solid constituents in the mixture. Though the solid constituents are constrained to move together, their deformation gradients are not necessarily the same, depending on how the various solid constituents of a constrained mixture were assembled [25].

With no loss of generality, it may be assumed that the strain energy density of the mixture is the summation of the strain energy densities of all the constituents,

$$\Psi\left(\mathbf{F}^{(1)},\cdots,\mathbf{F}^{(n)},\rho_r^{(1)},\cdots,\rho_r^{(n)}\right) = \sum_{\sigma=1}^{n}\Psi^{\sigma}\left(\mathbf{F}^{(1)},\cdots,\mathbf{F}^{(n)},\rho_r^{(1)},\cdots,\rho_r^{(n)}\right), \tag{2.116}$$

where Ψ^{σ} is the strain energy density of constituent σ.

Now, *as a special case*, we may assume that the simplest form of the constitutive relation for a mixture of constrained solids is

$$\Psi\left(\mathbf{F}^{(1)},\cdots,\mathbf{F}^{(n)},\rho_r^{(1)},\cdots,\rho_r^{(n)}\right) = \sum_{\sigma=1}^{n}\Psi^{\sigma}\left(\mathbf{F}^{\sigma},\rho_r^{\sigma}\right). \tag{2.117}$$

This special form assumes that there are no explicit dependencies among the various solid constituents of the mixture. Thus, Ψ^{σ} depends only on the deformation gradient and mass content of σ.

Furthermore, if we assume that $\mathbf{F}^{\sigma} = \mathbf{F}$ for all σ (implying no residual stresses in the solid mixture), then the general form for Ψ further reduces to

$$\Psi = \sum_{\sigma=1}^{n}\Psi^{\sigma}\left(\mathbf{F},\rho_r^{\sigma}\right). \tag{2.118}$$

Consequently, the stress tensor for the mixture becomes

$$\boldsymbol{\sigma} = J^{-1}\frac{\partial\Psi}{\partial\mathbf{F}}\cdot\mathbf{F}^{T} = \sum_{\sigma=1}^{n}J^{-1}\frac{\partial\Psi^{\sigma}}{\partial\mathbf{F}}\cdot\mathbf{F}^{T} = \sum_{\sigma=1}^{n}\boldsymbol{\sigma}^{\sigma}. \tag{2.119}$$

In other words, the stress in the solid mixture may be evaluated from the sum of the stresses in each mixture constituent using the same hyperelasticity relation as for a single, pure solid constituent. The fact that Ψ^{σ} also depends on ρ_r^{σ} implies that the material properties appearing in the constitutive relation for $\boldsymbol{\sigma}^{\sigma}$ are dependent on the mass content of solid σ in the mixture.

For nearly-incompressible solids, using a reasoning similar to that which led to (2.118), the uncoupled strain energy density for the solid mixture may be of the form

$$\Psi = U\left(J\right) + \sum_{\sigma=1}^{n}\tilde{\Psi}^{\sigma}\left(\tilde{\mathbf{F}},\rho_r^{\sigma}\right), \tag{2.120}$$

where $U\left(J\right)$ is the volumetric energy component, $\tilde{\Psi} = \sum_{\sigma}\tilde{\Psi}^{\sigma}$ is the distortional energy component, and $\tilde{\mathbf{F}}$ is the distortional part of the deformation gradient, as described in Section 2.4.3.

2.8. Equilibrium Swelling

When the interstitial fluid of a porous medium contains one or more solutes, an osmotic pressure may be produced in the fluid if the osmolarity of the interstitial fluid is non-uniform, or if it is different from that of the external bathing solution surrounding the porous medium. In general, since the osmolarity of the interstitial fluid may vary over time in transient problems, the analysis of such swelling effects may be addressed using, for example, the biphasic-solute material model described in Section 2.6. However, if we are only interested in the steady-state response for such types of materials, when solvent and solute fluxes have subsided, the analysis may be simplified considerably.

The Cauchy stress tensor for a mixture of a porous solid and interstitial fluid is given by

$$\boldsymbol{\sigma} = -p\mathbf{I} + \boldsymbol{\sigma}^e, \tag{2.121}$$

where p is he fluid pressure and $\boldsymbol{\sigma}^e$ is the stress in the solid matrix resulting from solid strain. When steady-state conditions are achieved, the fluid pressure p results exclusively from osmotic effects and ambient conditions (i.e., it does not depend on the loading history). Thus, in analogy to (2.112), $p = \tilde{p} + R\theta\Phi c$ where $\tilde{p}$ is the mechanical pressure resulting from ambient conditions and $R\theta\Phi c$ is the osmotic pressure resulting from the osmolarity c of the solution.

The osmotic pressure p may produce swelling of the solid matrix, which is opposed by the solid matrix stress. This becomes more apparent when considering, for example, the case of a traction-free body. The traction is given by $\mathbf{t} = \boldsymbol{\sigma}\cdot\mathbf{n}$, where $\mathbf{n}$ is the unit outward normal to the boundary. When $\mathbf{t} = \mathbf{0}$, the relation of (2.121) produces $p = \mathbf{n}\cdot\boldsymbol{\sigma}^e\cdot\mathbf{n}$, clearly showing that the osmotic pressure p is balanced by the swelling solid matrix.

The interstitial osmolarity (number of moles of solute per volume of interstitial fluid) may be related to the solute and solid content according to

$$c = \frac{c_r}{J - \varphi_r^s}, \tag{2.122}$$

where c_r is the number of moles of solute per volume of the mixture in the reference configuration, φ_r^s is the volume fraction of the solid in the reference configuration, and $J = \det\mathbf{F}$ is the relative volume of the porous solid matrix. Neither c_r nor φ_r^s depend on the solid matrix deformation, thus (2.122) provides the explicit dependence of c on J. This relation shows that the osmolarity of the interstitial fluid is dependent on the relative change in volume of the solid matrix with deformation. Effectively, under equilibrium swelling conditions, the term $-p\mathbf{I}$ in (2.121) represents an elastic stress and may be treated in this manner when analyzing equilibrium swelling conditions.

Since p also depends on the osmotic coefficient, if we assume that Φ depends on the solid strain at most via a dependence on J, we may thus state generically that $p = p(J)$ under equilibrium swelling. It follows that the elasticity tensor for $\boldsymbol{\sigma}$ is

$$\boldsymbol{c} = -\left(p + J\frac{dp}{dJ} \right)\mathbf{I}\otimes\mathbf{I} + 2p\mathbf{I}\,\underline{\bar{\otimes}}\,\mathbf{I} + \boldsymbol{c}^e, \tag{2.123}$$

where $\boldsymbol{c}^e$ is the elasticity tensor of $\boldsymbol{\sigma}^e$.

2.8.1. Perfect Osmometer

Consider a porous medium with an interstitial fluid that consists of a solvent and one or more solutes, whose boundary is permeable to the solvent but not to the solutes (e.g., a biological cell). Since solutes are trapped within such a medium, c_r is a constant in this type of problem. Since the boundary is permeable to the solvent, $\tilde{p}$ must be continuous across the boundary. Assuming ideal physicochemical conditions, $\Phi = 1$, and zero ambient pressure, this continuity requirement implies that $p = R\theta\left(c - c^*\right)$, where c^* is the osmolarity of the external environment. Using (2.122), it follows that

$$p = R\theta\left(\frac{c_r}{J - \varphi_r^s} - c^* \right). \tag{2.124}$$

The reference configuration (the stress-free configuration of the solid) is achieved when $J = 1$ and $p = 0$, from which it follows that $c_r = \left(1 - \varphi_r^s\right)c_0^*$, where c_0^* is the value of c^* in the reference state. Therefore (2.124) may also be written as

$$p = R\theta c^*\left(\frac{1-\varphi_r^s}{J-\varphi_r^s}\frac{c_0^*}{c^*} - 1 \right), \tag{2.125}$$

and this expression may be substituted into (2.123) to evaluate the corresponding elasticity tensor.

A perfect osmometer is a porous material whose interstitial fluid behaves ideally and whose solid matrix exhibits negligible resistance to swelling ($\boldsymbol{\sigma}^e \approx \mathbf{0}$). In that case $p = 0$ and (2.125) may be rearranged to yield

$$J = \left(1 - \varphi_r^s\right)\frac{c_0^*}{c^*} + \varphi_r^s. \tag{2.126}$$

This equation is known as the Boyle-van't Hoff relation for a perfect osmometer. It predicts that variations in the relative volume of such as medium with changes in external osmolarity c^* is an affine function of c_0^*/c^*, with the intercept at the origin representing the solid volume fraction and the slope representing the fluid volume fraction, in the reference configuration.

FEBio implements the relation of (2.125) for the purpose of modeling equilibrium swelling even when solid matrix stresses are not negligible. The name "perfect osmometer" is adopted for this model because it reproduces the Boyle-van't Hoff response in the special case when $\boldsymbol{\sigma}^e = \mathbf{0}$.

2.8.2. Cell Growth

The growth of cells requires the active uptake of soluble mass to provide the building blocks for various intracellular structures, such as the cytoskeleton or chromosomes, and growth contributes

to the osmolarity of the intracellular space. The resulting mechano-chemical gradient drives solvent into the cell as well, contributing to its volumetric growth.

Cell growth may be modeled using the "perfect osmometer" framework by simply increasing the mass of the intracellular solid matrix and membrane-impermeant solute. This is achieved by using (2.124) to model the osmotic pressure and allowing the parameters φ_r^s and c_r (normally constant) to increase over time as a result of growth. Since cell growth is often accompanied by cell division, and since daughter cells typically achieve the same solid and solute content as their parent, it may be convenient to assume that φ_r^s and c_r increase proportionally, though this is not an obligatory relationship. To ensure that the initial configuration is a stress-free reference configuration, let $c_r = \left(1-\varphi_r^s\right)c^*$ in the initial state prior to growth.

2.8.3. Donnan Equilibrium Swelling

Consider a porous medium whose solid matrix holds a fixed electrical charge and whose interstitial fluid consists of a solvent and two monovalent counter-ions (such as Na^+ and Cl^-). The boundaries of the medium are permeable to the solvent and ions. The fixed charge density is denoted by c^F; it is a measure of the number of fixed charges per volume of the interstitial fluid in the current configuration. This charge density may be either negative or positive, thereby producing an imbalance in the concentration of anions and cations in the interstitial fluid. To determine the osmolarity of the interstitial fluid, it is necessary to equate the mechano-chemical potential of the solvent and the mechano-electrochemical potential of the ions between the porous medium and its surrounding bath. When assuming ideal physicochemical behavior, the interstitial osmolarity (resulting from the interstitial ions) is given by

$$c = \sqrt{\left(c^F\right)^2 + \left(2c^*\right)^2}\ , \tag{2.127}$$

where c^* is the salt concentration in the bath. Alternatively, we note that the osmolarity of the bath is $\bar{c}^* = 2c^*$. Though this expression may be equated with (2.122), the resulting value of c_r is not constant in this case, since ions may transport into or out of the pore space; therefore that relation is not useful here.

However, since the number of charges fixed to the solid matrix is invariant, we may manipulate (2.122) to produce a relation between the fixed charge density in the current configuration, c^F, and the corresponding value in the reference configuration, c_r^F,

$$c^F = \frac{1-\varphi_r^s}{J-\varphi_r^s} c_r^F\ . \tag{2.128}$$

Now the osmotic pressure resulting from the difference in osmolarity between the porous medium and its surrounding bath is given by

$$p = R\theta\left(\sqrt{\left(\frac{1-\varphi_r^s}{J-\varphi_r^s} c_r^F\right)^2 + \left(\bar{c}^*\right)^2} - \bar{c}^*\right). \tag{2.129}$$

This expression may be substituted into (2.123) to evaluate the corresponding elasticity tensor.

When the osmotic pressure results from an imbalance in osmolarity produced by a fixed charge density, it is called a Donnan osmotic pressure. The analysis associated with this relation is called Donnan equilibrium.

Chapter 3. The Nonlinear FE Method

This chapter discusses the basic principles of the nonlinear finite element method. The chapter begins with a short introduction to the weak formulation and the principle of virtual work. Next, the important concept of linearization is discussed and applied to the principle of virtual work. Finally the Newton-Raphson procedure and its application to the nonlinear finite element method are described.

3.1. Weak formulation for solid materials

Generally, the finite element formulation is established in terms of a weak form of the differential equations under consideration. In the context of solid mechanics this implies the use of the virtual work equation:

$$\delta W = \int_v \boldsymbol{\sigma} : \delta \mathbf{d} dv - \int_v \mathbf{f} \cdot \delta \mathbf{v} dv - \int_{\partial v} \mathbf{t} \cdot \delta \mathbf{v} da = 0 . \tag{3.1}$$

Here, $\delta \mathbf{v}$ is a virtual velocity and $\delta \mathbf{d}$ is the virtual rate of deformation tensor. This equation is known as the *spatial virtual work equation* since it is formulated using spatial quantities only. We can also define the *material virtual work equation* by expressing the principle of virtual work using only material quantities.

$$\delta W = \int_V \mathbf{S} : \delta \dot{\mathbf{E}} dV - \int_V \mathbf{f}_0 \cdot \delta \mathbf{v} dV - \int_{\partial V} \mathbf{t}_0 \cdot \delta \mathbf{v} dA = 0 \tag{3.2}$$

Here, $\mathbf{f}_0 = J\mathbf{f}$ is the body force per unit undeformed volume and $\mathbf{t}_0 = \mathbf{t}\left(da / dA\right)$ is the traction vector per unit initial area.

3.1.1. Linearization

Equation (3.1) is the starting point for the nonlinear finite element method. It is highly nonlinear and any method attempting to solve this equation, such as the Newton-Raphson method, necessarily has to be iterative.

To linearize the finite element equations, the directional derivative of the virtual work in equation (3.1) must be calculated. In an iterative procedure, the quantity ϕ will be approximated by a trial solution ϕ_k. Linearization of the virtual work equation around this trial solution gives

$$\delta W\left(\phi_k, \delta \mathbf{v}\right) + D\delta W\left(\phi_k, \delta \mathbf{v}\right)\left[\mathbf{u}\right] = 0 . \tag{3.3}$$

The directional derivative of the virtual work will eventually lead to the definition of the stiffness matrix. In order to proceed, it is convenient to split the virtual work into an internal and external virtual work component:

$$D\delta W\left(\phi, \delta \mathbf{v}\right)\left[\mathbf{u}\right] = D\delta W_{\text{int}}\left(\phi, \delta \mathbf{v}\right)\left[\mathbf{u}\right] - D\delta W_{\text{ext}}\left(\phi, \delta \mathbf{v}\right)\left[\mathbf{u}\right], \tag{3.4}$$

where

$$\delta W_{\text{int}}\left(\phi, \delta \mathbf{v}\right) = \int_v \boldsymbol{\sigma} : \delta \mathbf{d} dv , \tag{3.5}$$

and

$$\delta W_{\text{ext}}\left(\varphi,\delta\mathbf{v}\right)=\int_{v}\mathbf{f}\cdot\delta\mathbf{v}dv+\int_{\partial v}\mathbf{t}\cdot\delta\mathbf{v}da\,. \tag{3.6}$$

The result is listed here without details of the derivation – see [1] for details. The linearization of the internal virtual work is given by

$$D\delta W_{\text{int}}\left(\phi,\delta\mathbf{v}\right)\left[\mathbf{u}\right]=\int_{v}\delta\mathbf{d}:\mathbb{D}:\varepsilon dv+\int_{v}\boldsymbol{\sigma}:\left[\left(\nabla\mathbf{u}\right)^{T}\nabla\delta\mathbf{v}\right]dv\,. \tag{3.7}$$

Notice that this equation is symmetric in $\delta\mathbf{v}$ and $\mathbf{u}$. This symmetry will, upon discretization, yield a symmetric tangent matrix.

The external virtual work has contributions from both body forces and surface tractions. The precise form of the linearized external virtual work depends on the form of these forces. For surface tractions, normal pressure forces may be represented in FEBio. The linearized external work for this type of traction is given by

$$\begin{aligned}D\delta W_{\text{ext}}^{p}\left(\phi,\delta\mathbf{v}\right)\left[\mathbf{u}\right]=&\frac{1}{2}\int_{A_{\xi}}p\frac{\partial\mathbf{x}}{\partial\xi}\cdot\left[\left(\frac{\partial\mathbf{u}}{\partial\eta}\times\delta\mathbf{v}\right)+\left(\frac{\partial\delta\mathbf{v}}{\partial\eta}\times\mathbf{u}\right)\right]d\xi d\eta\\&-\frac{1}{2}\int_{A_{\xi}}p\frac{\partial\mathbf{x}}{\partial\eta}\cdot\left[\left(\frac{\partial\mathbf{u}}{\partial\xi}\times\delta\mathbf{v}\right)+\left(\frac{\partial\delta\mathbf{v}}{\partial\xi}\times\mathbf{u}\right)\right]d\xi d\eta\end{aligned}\,. \tag{3.8}$$

Discretization of this equation will also lead to a symmetric component of the tangent matrix.

FEBio currently supports gravity as a body force, $\mathbf{f}=\rho\mathbf{g}$. Since this force is independent of the geometry, the contribution to the linearized external work is zero. Another type of body force implemented in FEBio is the centrifugal force. For a body rotating with a constant angular speed ω, about an axis passing through the point $\mathbf{c}$ and directed along the unit vector $\mathbf{n}$, the body force is given by $\mathbf{f}=\rho\omega^{2}\mathbf{r}$, where $\mathbf{r}$ is the vector distance from a point $\mathbf{x}$ to the axis of rotation,

$$\mathbf{r}=\left(\mathbf{I}-\mathbf{n}\otimes\mathbf{n}\right)\cdot\left(\mathbf{x}-\mathbf{c}\right) \tag{3.9}$$

◇

The resulting linearized external work is given by

$$D\delta W_{\text{ext}}^{f}\left(\phi,\delta\mathbf{v}\right)\left[\mathbf{u}\right]=\int_{v}\rho\omega^{2}\delta\mathbf{v}\cdot\left(\mathbf{I}-\mathbf{n}\otimes\mathbf{n}\right)\cdot\mathbf{u}dv\,, \tag{3.10}$$

which produces a symmetric expression that will yield a symmetric matrix.

3.1.2. Discretization

The basis of the finite element method is that the domain of the problem (that is, the volume of the object under consideration) is divided into smaller subunits, called *finite elements*. In the case of *isoparametric elements* it is further assumed that each element has a local coordinate system, named the *natural coordinates*, and the coordinates and shape of the element are discretized using the same functions. The discretization process is established by interpolating the geometry in terms of the coordinates $\mathbf{X}_a$ of the *nodes* that define the geometry of a finite element, and the *shape functions*:

$$\mathbf{X} = \sum_{a=1}^{n} N_a\left(\xi_1, \xi_2, \xi_3\right)\mathbf{X}_a \,, \tag{3.11}$$

where n is the number of nodes and ξ_i are the natural coordinates. Similarly, the motion is described in terms of the current position $\mathbf{x}_a\left(t\right)$ of the *same* particles:

$$\mathbf{x}\left(t\right) = \sum_{a=1}^{n} N_a \mathbf{x}_a\left(t\right). \tag{3.12}$$

Quantities such as displacement, velocity and virtual velocity can be discretized in a similar way.

In deriving the discretized equilibrium equations, the integrations performed over the entire volume can be written as a sum of integrations constrained to the volume of an element. For this reason, the discretized equations are defined in terms of integrations over a particular element e. The discretized equilibrium equations for this particular element per node is given by

$$\delta W^{(e)}\left(\phi, N_a \delta\mathbf{v}\right) = \delta\mathbf{v}_a \cdot \left(\mathbf{T}_a^{(e)} - \mathbf{F}_a^{(e)}\right), \tag{3.13}$$

where

$$\begin{aligned} T_a^{(e)} &= \int_{v^{(e)}} \sigma \nabla N_a dv, \text{ and} \\ F_a^{(e)} &= \int_{v^{(e)}} N_a \mathbf{f} dv + \int_{\partial v^{(e)}} N_a \mathbf{t} da \,. \end{aligned} \tag{3.14}$$

The linearization of the internal virtual work can be split into a *material* and an *initial stress* component [1]:

$$\begin{aligned} D\delta W_{\text{int}}^{(e)}\left(\phi, \delta\mathbf{v}\right)\left[\mathbf{u}\right] &= \int_{v^{(e)}} \delta\mathbf{d} : \square : \varepsilon dv + \int_{v^{(e)}} \boldsymbol{\sigma} : \left[\left(\nabla\mathbf{u}\right)^T \nabla\delta\mathbf{v}\right] dv \\ &= D\delta W_c^{(e)}\left(\phi, \delta\mathbf{v}\right)\left[\mathbf{u}\right] + D\delta W_\sigma^{(e)}\left(\phi, \delta\mathbf{v}\right)\left[\mathbf{u}\right]. \end{aligned} \tag{3.15}$$

The constitutive component can be discretized as follows:

$$D\delta W_c^{(e)}\left(\phi, \delta\mathbf{v}\right)\left[\mathbf{u}\right] = \delta\mathbf{v}_a \cdot \left(\int_{v^{(e)}} \mathbf{B}_a^T \mathbf{D} \mathbf{B}_b dv\right)\mathbf{u}_b \,. \tag{3.16}$$

The term in parentheses defines the constitutive component of the tangent matrix relating node a to node b in element e:

$$\mathbf{K}_{c,ab}^{(e)} = \int_{v^{(e)}} \mathbf{B}_a^T \mathbf{D} \mathbf{B}_b dv \,. \tag{3.17}$$

Here, the linear strain-displacement matrix $\mathbf{B}$ relates the displacements to the small-strain tensor in Voigt Notation:

$$\underline{\boldsymbol{\varepsilon}} = \sum_{a=1}^{n} \mathbf{B}_a \mathbf{u}_a \,. \tag{3.18}$$

Or, written out completely,

$$\mathbf{B}_a = \begin{bmatrix} \partial N_a / \partial x & 0 & 0 \\ 0 & \partial N_a / \partial y & 0 \\ 0 & 0 & \partial N_a / \partial z \\ \partial N_a / \partial y & \partial N_a / \partial x & 0 \\ 0 & \partial N_a / \partial z & \partial N_a / \partial y \\ \partial N_a / \partial z & 0 & \partial N_a / \partial z \end{bmatrix}. \tag{3.19}$$

The spatial constitutive matrix $\mathbf{D}$ is constructed from the components of the fourth-order tensor $\boldsymbol{c}$ using the following table; $\mathbf{D}_{IJ} = \boldsymbol{c}_{ijkl}$ where

I/J	**i/k**	**j/l**
1	1	1
2	2	2
3	3	3
4	1	2
5	2	3
6	1	3

The initial stress component can be written as follows:

$$D\delta W_{\sigma}^{(e)}\left(\phi, N_a \delta \mathbf{v}\right)\left[N_b \mathbf{u}_b\right] = \int_{v^{(e)}} \left(\nabla N_a \cdot \boldsymbol{\sigma} \nabla N_b\right) \mathbf{I} dv \,. \tag{3.20}$$

For the pressure component of the external virtual work, we find

$$D\delta W_{p}^{(e)}\left(\phi, N_a \delta \mathbf{v}_a\right)\left[N_b \mathbf{u}_b\right] = \delta \mathbf{v}_a \cdot \mathbf{K}_{p,ab}^{(e)} \mathbf{u}_b \,, \tag{3.21}$$

where,

$$\mathbf{K}_{p,ab}^{(e)} = \boldsymbol{\mathcal{E}} \mathbf{k}_{p,ab}^{(e)}, \quad \mathbf{k}_{p,ab}^{(e)} = \frac{1}{2}\int_{A_\xi} p \frac{\partial \mathbf{x}}{\partial \xi}\left(\frac{\partial N_a}{\partial \eta} N_b - \frac{\partial N_b}{\partial \eta} N_a\right) d\xi d\eta \;. \tag{3.22}$$

$$+\frac{1}{2}\int_{A_\xi} p \frac{\partial \mathbf{x}}{\partial \eta}\left(\frac{\partial N_a}{\partial \xi} N_b - \frac{\partial N_b}{\partial \xi} N_a\right) d\xi d\eta$$

3.2. Weak formulation for biphasic materials

A weak form of the statement conservation of linear momemtum for the quasi-static case is obtained by using Eqs.(2.97) and (2.99):

$$\int_b \left[\delta \mathbf{v}^s \cdot \operatorname{div} \boldsymbol{\sigma} + \delta p \operatorname{div}\left(\mathbf{v}^s + \mathbf{w} \right) \right] dv = 0 , \tag{3.23}$$

where b is the domain of interest defined on the solid matrix, $\delta \mathbf{v}^s$ is a virtual velocity of the solid and δp is a virtual pressure of the fluid [26]. dv is an elemental volume of b. Using the divergence theorem, this expression may be rearranged as

$$\delta W = \int_b \boldsymbol{\sigma} : \delta \mathbf{d}^s dv - \int_{\partial b} \delta \mathbf{v}^s \cdot \mathbf{t} da + \int_b \left(\mathbf{w} \cdot \operatorname{grad} \delta p - \delta p \operatorname{div} \mathbf{v}^s \right) dv - \int_{\partial b} \delta p \, w_n da = 0 , \tag{3.24}$$

where $\delta \mathbf{d}^s = \left(\operatorname{grad} \delta \mathbf{v}^s + \operatorname{grad}^T \delta \mathbf{v}^s \right) / 2$ is the virtual rate of deformation tensor, $\mathbf{t} = \boldsymbol{\sigma} \cdot \mathbf{n}$ is the total traction on the surface ∂b, and $w_n = \mathbf{w} \cdot \mathbf{n}$ is the component of the fluid flux normal to ∂b, with $\mathbf{n}$ representing the unit outward normal to ∂b. da represents an elemental area of ∂b. In this type of problem, essential boundary conditions are prescribed for $\mathbf{u}$ and p, and natural boundary conditions are prescribed for $\mathbf{t}$ and w_n. In the expression of Eq.(3.24), $\delta W \left(\boldsymbol{\varphi}^s, p, \delta \mathbf{v}^s, \delta p \right)$ represents the virtual work.

3.2.1. Linearization

Since the system of equations in Eq.(3.24) is highly nonlinear, its solution requires an iterative scheme such as Newton's method. This requires the linearization of δW at some trial solution $\left(\boldsymbol{\varphi}_k^s, p_k \right)$, along an increment $\Delta \mathbf{u}$ in $\boldsymbol{\varphi}^s$ and an increment Δp in p,

$$\delta W + D\delta W \left[\Delta \mathbf{u} \right] + D\delta W \left[\Delta p \right] = 0 , \tag{3.25}$$

where $Df \left[\Delta q \right]$ represents the directional derivative of f along Δq. For convenience, the virtual work may be separated into its internal and external parts,

$$\delta W = \delta W_{\text{int}} - \delta W_{\text{ext}} , \tag{3.26}$$

where

$$\delta W_{\text{int}} = \int_b \boldsymbol{\sigma} : \delta \mathbf{d}^s dv + \int_b \left(\mathbf{w} \cdot \operatorname{grad} \delta p - \delta p \operatorname{div} \mathbf{v}^s \right) dv , \tag{3.27}$$

and

$$\delta W_{\text{ext}} = \int_{\partial b} \delta \mathbf{v}^s \cdot \mathbf{t} da + \int_{\partial b} \delta p \, w_n da . \tag{3.28}$$

The evaluation of the directional derivatives can be performed following a standard approach [1]. For the internal part of the virtual work, the directional derivative along $\Delta \mathbf{u}$ yields

$$\begin{aligned} D\delta W_{\text{int}} \left[\Delta \mathbf{u} \right] = & \int_b \delta \mathbf{d}^s : \boldsymbol{c} : \Delta \boldsymbol{\varepsilon} dv + \int_b \boldsymbol{\sigma} : \left(\operatorname{grad}^T \Delta \mathbf{u} \cdot \operatorname{grad} \delta \mathbf{v}^s \right) dv \\ & - \int_b \delta p \left(\left[\left(\operatorname{div} \Delta \mathbf{u} \right) \mathbf{I} - \operatorname{grad}^T \Delta \mathbf{u} \right] : \operatorname{grad} \mathbf{v}^s + \operatorname{div} \dot{\overline{\Delta \mathbf{u}}} \right) dv , \\ & - \int_b \operatorname{grad} \delta p \cdot \left(\boldsymbol{k} : \Delta \boldsymbol{\varepsilon} \right) \cdot \operatorname{grad} p dv \end{aligned} \tag{3.29}$$

where $\boldsymbol{c}$ is the fourth-order spatial elasticity tensor for the mixture and $\Delta\boldsymbol{\varepsilon} = \left(\operatorname{grad}\Delta\mathbf{u} + \operatorname{grad}^T \Delta\mathbf{u}\right)/2$. Based on the relation of Eq.(2.98), the spatial elasticity tensor may also be expanded as

$$\boldsymbol{c} = \boldsymbol{c}^e + p\left(-\mathbf{I}\otimes\mathbf{I} + 2\mathbf{I}\,\underline{\overline{\otimes}}\,\mathbf{I}\right), \tag{3.30}$$

where $\boldsymbol{c}^e$ is the spatial elasticity tensor for the solid matrix [27]. It is related to the material elasticity tensor $\mathcal{C}^e$ via

$$\boldsymbol{c}^e = J^{-1}\left(\mathbf{F}\,\underline{\otimes}\,\mathbf{F}\right):\mathcal{C}^e:\left(\mathbf{F}^T\,\underline{\otimes}\,\mathbf{F}^T\right), \tag{3.31}$$

where $\mathbf{F}$ is the deformation gradient of the solid matrix, $\mathcal{C}^e = \partial\mathbf{S}^e/\partial\mathbf{E}$ where $\mathbf{E}$ is the Lagrangian strain tensor and $\mathbf{S}^e$ is the second Piola-Kirchhoff stress tensor, related to the Cauchy stress tensor via $\boldsymbol{\sigma}^e = J^{-1}\mathbf{F}\cdot\mathbf{S}^e\cdot\mathbf{F}^T$.

Similarly, $\boldsymbol{k}$ is a fourth-order tensor that represents the spatial measure of the rate of change of permeability with strain. It is related to its material frame equivalent $\mathcal{K}$ via

$$\boldsymbol{k} = J^{-1}\left(\mathbf{F}\,\underline{\otimes}\,\mathbf{F}\right):\mathcal{K}:\left(\mathbf{F}^T\,\underline{\otimes}\,\mathbf{F}^T\right), \tag{3.32}$$

where $\mathcal{K} = \partial\mathbf{K}/\partial\mathbf{E}$ and $\mathbf{K}$ is the permeability tensor in the material frame, such that $\mathbf{k} = J^{-1}\mathbf{F}\cdot\mathbf{K}\cdot\mathbf{F}^T$. Since $\mathbf{K}$ and $\mathbf{E}$ are symmetric tensors, it follows that $\boldsymbol{k}$ and $\mathcal{K}$ exhibit two minor symmetries (e.g., $k_{jikl} = k_{ijkl}$ and $\mathcal{K}_{ijlk} = \mathcal{K}_{ijkl}$). However, unlike the elasticity tensor, it is not necessary that these tensors exhibit major symmetry (e.g., $\mathcal{K}_{klij} \neq \mathcal{K}_{ijkl}$ in general).

The directional derivative of δW_{int} along Δp is given by

$$D\delta W_{\text{int}}\left[\Delta p\right] = -\int_b \operatorname{grad}\delta p\cdot\mathbf{k}\cdot\operatorname{grad}\Delta p\,dv - \int_b \Delta p\operatorname{div}\delta\mathbf{v}^s\,dv\,. \tag{3.33}$$

Note that letting $p = 0$ and $\delta p = 0$ in the above equations recovers the virtual work relations for nonlinear elasticity of compressible solids. The resulting simplified equation emerging from Eq.(3.29) is symmetric to interchanges of $\Delta\mathbf{u}$ and $\delta\mathbf{v}^s$, producing a symmetric stiffness matrix in the finite element formulation [1]. However, the general relations of Eqs.(3.29) and (3.33) do not exhibit symmetry to interchanges of $\left(\Delta\mathbf{u},\Delta p\right)$ and $\left(\delta\mathbf{v}^s,\delta p\right)$, implying that the finite element stiffness matrix for a solid-fluid mixture is not symmetric under general conditions.

The directional derivatives of the external virtual work δW_{ext} depend on the type of boundary conditions being considered. For a prescribed total normal traction t_n, where $\mathbf{t} = t_n\mathbf{n}$,

$$\delta W_{ext}^t = \int_{\partial b}\delta\mathbf{v}^s\cdot t_n\mathbf{n}\,da\,, \tag{3.34}$$

and

$$\begin{aligned} D\delta W_{ext}^t\left[\Delta\mathbf{u}\right] &= \int_{\partial b}\delta\mathbf{v}^s\cdot t_n\left(\mathbf{g}_1\times\frac{\partial\Delta\mathbf{u}}{\partial\eta^2} - \mathbf{g}_2\times\frac{\partial\Delta\mathbf{u}}{\partial\eta^1}\right)\frac{da}{\left|\mathbf{g}_1\times\mathbf{g}_2\right|}, \\ D\delta W_{ext}^t\left[\Delta p\right] &= 0, \end{aligned} \tag{3.35}$$

where

$$\mathbf{g}_\alpha = \frac{\partial\mathbf{x}}{\partial\eta^\alpha}, \quad \alpha = 1,2 \tag{3.36}$$

are covariant basis (tangent) vectors on ∂b, such that

$$\mathbf{n} = \frac{\mathbf{g}_1 \times \mathbf{g}_2}{\left|\mathbf{g}_1 \times \mathbf{g}_2\right|}. \tag{3.37}$$

For a prescribed normal effective traction t_n^e, where $\mathbf{t} = \left(-p + t_n^e\right)\mathbf{n}$ and p is not prescribed, then

$$\delta W_{ext}^e = \int_{\partial b} \delta \mathbf{v}^s \cdot \left(-p + t_n^e\right)\mathbf{n}\, da, \tag{3.38}$$

and

$$\begin{aligned} D\delta W_{ext}^e\left[\Delta\mathbf{u}\right] &= \int_{\partial b} \delta \mathbf{v}^s \cdot \left(-p + t_n^e\right)\left(\mathbf{g}_1 \times \frac{\partial \Delta\mathbf{u}}{\partial \eta^2} - \mathbf{g}_2 \times \frac{\partial \Delta\mathbf{u}}{\partial \eta^1}\right)\frac{da}{\left|\mathbf{g}_1 \times \mathbf{g}_2\right|}, \\ D\delta W_{ext}^e\left[\Delta p\right] &= -\int_{\partial b} \delta \mathbf{v}^s \cdot \Delta p\, \mathbf{n}\, da. \end{aligned} \tag{3.39}$$

Finally, for a prescribed normal fluid flux $w_n = \mathbf{w} \cdot \mathbf{n}$,

$$\delta W_{ext}^w = \int_{\partial b} \delta p\, w_n\, da, \tag{3.40}$$

and

$$\begin{aligned} D\delta W_{ext}^w\left[\Delta\mathbf{u}\right] &= \int_{\partial b} \delta p\, w_n\, \mathbf{n} \cdot \left(\mathbf{g}_1 \times \frac{\partial \Delta\mathbf{u}}{\partial \eta^2} - \mathbf{g}_2 \times \frac{\partial \Delta\mathbf{u}}{\partial \eta^1}\right)\frac{da}{\left|\mathbf{g}_1 \times \mathbf{g}_2\right|}, \\ D\delta W_{ext}^w\left[\Delta p\right] &= 0. \end{aligned} \tag{3.41}$$

3.2.2. Discretization

Let

$$\begin{aligned} \delta \mathbf{v}^s &= \sum_{a=1}^{m} N_a \delta \mathbf{v}_a, \quad \delta p = \sum_{a=1}^{m} N_a \delta p_a, \\ \Delta\mathbf{u} &= \sum_{b=1}^{m} N_b \Delta\mathbf{u}_b, \quad \Delta p = \sum_{b=1}^{m} N_b \Delta p_b, \end{aligned} \tag{3.42}$$

where N_a represents the interpolation functions over an element, $\delta\mathbf{v}_a, \delta p_a, \Delta\mathbf{u}_b$ and Δp_b respectively represent nodal values of $\delta\mathbf{v}^s, \delta p, \Delta\mathbf{u}$ and Δp, and m is the number of nodes in an element. Then the discretized form of δW_{int} in Eq.(3.27) may be written as

$$\delta W_{\text{int}} = \sum_{e=1}^{n_e} \sum_{k=1}^{n_{\text{int}}^{(e)}} W_k J_\eta \sum_{a=1}^{m} \left[\delta\mathbf{v}_a \quad \delta p_a\right] \cdot \begin{bmatrix} \mathbf{r}_a^u \\ r_a^p \end{bmatrix}, \tag{3.43}$$

where n_e is the number of elements in b, $n_{\text{int}}^{(e)}$ is the number of integration points in the $e-$th element, W_k is the quadrature weight associated with the $k-$th integration point, and J_η is the Jacobian of the transformation from the spatial frame to the parametric space of the element. In the above expression,

$$\mathbf{r}_a^u = \boldsymbol{\sigma} \cdot \nabla N_a \quad r_a^p = \mathbf{w} \cdot \nabla N_a - N_a \operatorname{div}\left(\mathbf{v}^s\right) \tag{3.44}$$

and it is understood that J_η, $\mathbf{r}_a^u$ and r_a^p are evaluated at the parametric coordinates of the $k-$th integration point.

Similarly, the discretized form of $D\delta W_{\text{int}}$ in Eqs.(3.29) and (3.33) may be written as

$$-D\delta W_{\text{int}} = \sum_{e=1}^{n_e}\sum_{k=1}^{n_{\text{int}}^{(e)}} W_k J_\eta \sum_{a=1}^{m}\left[\delta\mathbf{v}_a \quad \delta p_a\right]\cdot\sum_{b=1}^{m}\begin{bmatrix}\mathbf{K}_{ab}^{uu} & \mathbf{k}_{ab}^{up}\\ \mathbf{k}_{ab}^{pu} & k_{ab}^{pp}\end{bmatrix}\cdot\begin{bmatrix}\Delta\mathbf{u}_b\\ \Delta p_b\end{bmatrix}, \tag{3.45}$$

where

$$\begin{aligned}
\mathbf{K}_{ab}^{uu} &= \nabla N_a\cdot\boldsymbol{c}\cdot\nabla N_b + \left(\nabla N_a\cdot\boldsymbol{\sigma}\cdot\nabla N_b\right)\mathbf{I},\\
\mathbf{k}_{ab}^{up} &= -N_b\nabla N_a,\\
\mathbf{k}_{ab}^{pu} &= -\left(\nabla N_a\cdot\boldsymbol{k}\cdot\nabla N_b\right)\cdot\operatorname{grad} p - N_a\left[\left(\operatorname{div}\mathbf{v}^s + \frac{1}{\Delta t}\right)\mathbf{I} - \operatorname{grad}^T\mathbf{v}^s\right]\cdot\nabla N_b,\\
k_{ab}^{pp} &= -\nabla N_a\cdot\mathbf{k}\cdot\nabla N_b,
\end{aligned} \tag{3.46}$$

and Δt is a discrete increment in time. In a numerical implementation, it has been found that evaluating $\operatorname{div}\left(\mathbf{v}^s\right)$ from $\dot{J}/J$, where $J = \det\mathbf{F}$, yields more accurate solutions than evaluating it from the trace of $\operatorname{grad}\mathbf{v}^s$ [28].

For the various types of contributions to the external virtual work, a similar discretization produces

$$\delta W_{\text{ext}} = \sum_{e=1}^{n_e}\sum_{k=1}^{n_{\text{int}}^{(e)}} W_k J_\eta \sum_{a=1}^{m}\left[\delta\mathbf{v}_a \quad \delta p_a\right]\cdot\begin{bmatrix}\mathbf{r}_a^u\\ r_a^p\end{bmatrix}, \tag{3.47}$$

and

$$-D\delta W_{\text{ext}} = \sum_{e=1}^{n_e}\sum_{k=1}^{n_{\text{int}}^{(e)}} W_k J_\eta \sum_{a=1}^{m}\left[\delta\mathbf{v}_a \quad \delta p_a\right]\cdot\sum_{b=1}^{m}\begin{bmatrix}\mathbf{K}_{ab}^{uu} & \mathbf{k}_{ab}^{up}\\ \mathbf{k}_{ab}^{pu} & k_{ab}^{pp}\end{bmatrix}\cdot\begin{bmatrix}\Delta\mathbf{u}_b\\ \Delta p_b\end{bmatrix}, \tag{3.48}$$

where

$$J_\eta = \left|\mathbf{g}_1\times\mathbf{g}_2\right|. \tag{3.49}$$

In this case, m represents the number of nodes on an element face. For a prescribed normal traction t_n as given in (3.34)-(3.35),

$$\begin{aligned}
&\mathbf{r}_a^u = t_n N_a\mathbf{n}, \quad r_a^u = 0,\\
&\mathbf{K}_{ab}^{uu} = t_n N_a\frac{1}{J_\eta}\boldsymbol{\mathcal{A}}\left\{\frac{\partial N_b}{\partial\eta^1}\mathbf{g}_2 - \frac{\partial N_b}{\partial\eta^2}\mathbf{g}_1\right\}, \quad \mathbf{k}_{ab}^{up} = \mathbf{0},\\
&\mathbf{k}_{ab}^{pu} = \mathbf{0}, \quad k_{ab}^{pp} = 0,
\end{aligned} \tag{3.50}$$

where $\boldsymbol{\mathcal{A}}\left\{\mathbf{v}\right\} = -\boldsymbol{\mathcal{E}}\cdot\mathbf{v}$ is the skew-symmetric tensor whose dual vector is $\mathbf{v}$ and $\boldsymbol{\mathcal{E}}$ is the third-order permutation pseudo-tensor. For a prescribed traction t_n^e as given in (3.38)-(3.39),

$$\begin{aligned}
&\mathbf{r}_a^u = \left(-p + t_n^e\right)N_a\mathbf{n}, \quad r_a^u = 0,\\
&\mathbf{K}_{ab}^{uu} = \left(-p + t_n^e\right)N_a\frac{1}{J_\eta}\boldsymbol{\mathcal{A}}\left\{\frac{\partial N_b}{\partial\eta^1}\mathbf{g}_2 - \frac{\partial N_b}{\partial\eta^2}\mathbf{g}_1\right\}, \quad \mathbf{k}_{ab}^{up} = N_a N_b\mathbf{n},\\
&\mathbf{k}_{ab}^{pu} = \mathbf{0}, \quad k_{ab}^{pp} = 0.
\end{aligned} \tag{3.51}$$

For a prescribed normal fluid flux w_n as given in (3.40)-(3.41),

$$\begin{aligned}
&\mathbf{r}_a^u = \mathbf{0}, \quad r_a^u = w_n N_a, \\
&\mathbf{K}_{ab}^{uu} = \mathbf{0}, \quad \mathbf{k}_{ab}^{up} = \mathbf{0}, \\
&\mathbf{k}_{ab}^{pu} = w_n N_a \frac{1}{J_\eta} \mathbf{n} \times \left(\frac{\partial N_b}{\partial \eta^1} \mathbf{g}_2 - \frac{\partial N_b}{\partial \eta^2} \mathbf{g}_1 \right), \quad k_{ab}^{pp} = 0.
\end{aligned} \tag{3.52}$$

3.3. Weak formulation for biphasic-solute materials

The virtual work integral for this problem is given by

$$\delta W = -\int_b \delta \mathbf{v} \cdot \operatorname{div} \boldsymbol{\sigma}\, dv - \int_b \delta \tilde{p} \operatorname{div}\left(\mathbf{v}^s + \mathbf{w}\right) dv - \int_b \delta \tilde{c} \left[\frac{\partial\left(\phi^w \tilde{\kappa} \tilde{c}\right)}{\partial t} + \operatorname{div}\left(\mathbf{j} + \phi^w \tilde{\kappa} \tilde{c}\, \mathbf{v}^s\right) \right] dv, \tag{3.53}$$

where $\delta \mathbf{v}$ is the virtual velocity of the solid, $\delta \tilde{p}$ is the virtual effective fluid pressure, and $\delta \tilde{c}$ is the virtual molar energy of the solute. b represents the mixture domain in the spatial frame and dv is an elemental mixture volume in b. In the last integral of δW, note that

$$\frac{\partial\left(\phi^w \tilde{\kappa} \tilde{c}\right)}{\partial t} + \operatorname{div}\left(\phi^w \tilde{\kappa} \tilde{c}\, \mathbf{v}^s\right) = \frac{1}{J} \frac{D^s}{Dt}\left(J \phi^w \tilde{\kappa} \tilde{c}\right), \tag{3.54}$$

where $D^s f / Dt \equiv \partial f / \partial t + \mathbf{v}^s \cdot \operatorname{grad} f$ is the material time derivative of a scalar function f in the spatial frame, following the solid. Similarly, note that $\operatorname{div} \mathbf{v}^s = J^{-1}\left(D^s J / Dt\right)$. Using the divergence theorem, the virtual work integral may be separated into internal and external contributions, $\delta W = \delta W_{\text{int}} - \delta W_{\text{ext}}$, where

$$\begin{aligned}
\delta W_{\text{int}} &= \int_b \boldsymbol{\sigma} : \delta \mathbf{d}^s\, dv + \int_b \left(\mathbf{w} \cdot \operatorname{grad} \delta \tilde{p} - \frac{\delta \tilde{p}}{J} \frac{D^s J}{Dt} \right) dv + \int_b \left[\mathbf{j} \cdot \operatorname{grad} \delta \tilde{c} - \frac{\delta \tilde{c}}{J} \frac{D^s}{Dt}\left(J \phi^w \tilde{\kappa} \tilde{c}\right) \right] dv, \\
\delta W_{\text{ext}} &= \int_{\partial b} \left(\delta \mathbf{v} \cdot \mathbf{t} + \delta \tilde{p}\, w_n + \delta \tilde{c}\, j_n \right) da,
\end{aligned} \tag{3.55}$$

with δW_{ext} being evaluated on the domain's boundary surface ∂b. In the first expression $\delta \mathbf{d}^s = \left(\operatorname{grad} \delta \mathbf{v} + \operatorname{grad}^T \delta \mathbf{v}\right) / 2$ represents the virtual solid rate of deformation.

To solve this nonlinear system using an iterative Newton scheme, the virtual work must be linearized at trial solutions, along increments in $\mathbf{u}$, $\tilde{p}$ and $\tilde{c}$,

$$\delta W + D\delta W\left[\Delta \mathbf{u}\right] + D\delta W\left[\Delta \tilde{p}\right] + D\delta W\left[\Delta \tilde{c}\right] \approx 0, \tag{3.56}$$

where, for any function $f(q)$, $Df\left[\Delta q\right]$ represents the directional derivative of f along Δq [1]. To operate the directional derivative on the integrand of δW_{int}, it is first necessary to convert the integrals from the spatial to the material domain [1]:

$$\delta W_{\text{int}} = \int_B \mathbf{S} : \delta \dot{\mathbf{E}}\, dV + \int_B \left(\mathbf{W} \cdot \operatorname{Grad} \delta \tilde{p} - \delta \tilde{p} \frac{\partial J}{\partial t} \right) dV + \int_B \left[\mathbf{J} \cdot \operatorname{Grad} \delta \tilde{c} - \delta \tilde{c} \frac{\partial}{\partial t}\left(J \phi^w \tilde{\kappa} \tilde{c}\right) \right] dV, \tag{3.57}$$

where B represents the mixture domain in the material frame, dV is an elemental mixture volume in B, and

$$\begin{aligned}\mathbf{S} &= J\,\mathbf{F}^{-1}\cdot\boldsymbol{\sigma}\cdot\mathbf{F}^{-T},\\ \delta\dot{\mathbf{E}} &= \mathbf{F}^{T}\cdot\delta\mathbf{d}^{s}\cdot\mathbf{F},\\ \mathbf{W} &= J\,\mathbf{F}^{-1}\cdot\mathbf{w},\\ \mathbf{J} &= J\,\mathbf{F}^{-1}\cdot\mathbf{j}.\end{aligned} \tag{3.58}$$

The second Piola-Kirchhoff stress tensor $\mathbf{S}$, and material flux vectors $\mathbf{W}$ and $\mathbf{J}$, are respectively related to $\boldsymbol{\sigma}$, $\mathbf{w}$ and $\mathbf{j}$ by the Piola transformations for tensors and vectors [1, 29]. Substituting (3.58) into (2.114) produces

$$\begin{aligned}\mathbf{W} &= -\tilde{\mathbf{K}}\cdot\left(\operatorname{Grad}\tilde{p} + R\theta\frac{\tilde{\kappa}}{d_0}J^{-1}\mathbf{C}\cdot\mathbf{D}\cdot\operatorname{Grad}\tilde{c}\right),\\ \mathbf{J} &= \tilde{\kappa}\mathbf{D}\cdot\left(-\phi^{w}\operatorname{Grad}\tilde{c} + \frac{\tilde{c}}{d_0}J^{-1}\mathbf{C}\cdot\mathbf{W}\right),\end{aligned} \tag{3.59}$$

where $\tilde{\mathbf{K}}$ and $\mathbf{D}$ are the material representations of the permeability and diffusivity tensors, related to $\tilde{\mathbf{k}}$ and $\mathbf{d}$ via the Piola transformation,

$$\begin{aligned}\tilde{\mathbf{K}} &= J\,\mathbf{F}^{-1}\cdot\tilde{\mathbf{k}}\cdot\mathbf{F}^{-T}\\ \mathbf{D} &= J\,\mathbf{F}^{-1}\cdot\mathbf{d}\cdot\mathbf{F}^{-T}\end{aligned}. \tag{3.60}$$

The linearization of δW_{int} is rather involved and a summary of the resulting lengthy expressions is provided below. In consideration of the dearth of experimental data relating $\tilde{\kappa}$ and Φ to the complete state of solid matrix strain (such as $\mathbf{C}$), this implementation assumes that the dependence of these functions on the strain is restricted to a dependence on the relative volume $J = \left(\det\mathbf{C}\right)^{1/2}$. Furthermore, it is assumed that the free solution diffusivity d_0 is independent of the strain.

The linearization of δW_{ext} is described in Section 3.3.2. Following the linearization procedure, the resulting expressions may be discretized by nodally interpolating $\mathbf{u}$, $\tilde{p}$ and $\tilde{c}$ over finite elements, producing a set of equations in matrix form, as described in Section 3.3.2.

The formulation presented in this study is implemented in FEBio by introducing an additional module dedicated to solute transport in deformable porous media. Classes are implemented to describe material functions for $\boldsymbol{\sigma}^{e}$, $\mathbf{k}$, $\mathbf{d}$ (and d_0), $\tilde{\kappa}$ and Φ, which allow the formulation of any desired constitutive relation for these functions of $\mathbf{C}$ and $\tilde{c}$, along with corresponding derivatives of these functions with respect to $\mathbf{C}$ and $\tilde{c}$. The implementation accepts essential boundary conditions on $\mathbf{u}$, $\tilde{p}$ and $\tilde{c}$, or natural boundary conditions on $\mathbf{t}$, w_n and j_n; initial conditions may also be specified for $\tilde{p}$ and $\tilde{c}$. Analysis results for pressure and concentration may be displayed either as $\tilde{p}$ and $\tilde{c}$, or as p and c by inverting the relations of (2.112).

3.3.1. Linearization of Internal Virtual Work

The virtual work integral δW_{int} in (3.57) may be linearized term by term along increments in $\Delta\mathbf{u}$, $\Delta\tilde{p}$ and $\Delta\tilde{c}$ using the general form

$$D\left(\int_B F dV\right)[\Delta q] = \int_B DF[\Delta q]\, dV = \int_b f dv\,. \tag{3.61}$$

For notational simplicity, the integral sign is omitted and the linearization of each term is presented in the form $DF[\Delta q]dV = f\, dv$.

3.3.1.1. Linearization along $\Delta\mathbf{u}$

The linearization of the first term in δW_{int} along $\Delta\mathbf{u}$ yields

$$\left(\mathbf{S}:\delta\dot{\mathbf{E}}\right)[\Delta\mathbf{u}]dV = \left[\delta\mathbf{d}^s : \boldsymbol{c} : \Delta\boldsymbol{\varepsilon} + \boldsymbol{\sigma} : \left(\text{grad}^T\, \Delta\mathbf{u}\cdot\text{grad}\,\delta\mathbf{v}\right)\right]dv\,, \tag{3.62}$$

where $\boldsymbol{c}$ is the spatial elasticity tensor of the mixture,

$$\boldsymbol{c} = \boldsymbol{c}^e - \left(\tilde{p} + R\theta\Phi\tilde{\kappa}\tilde{c}\right)\left(\mathbf{I}\otimes\mathbf{I} - 2\mathbf{I}\,\underline{\overline{\otimes}}\,\mathbf{I}\right) - R\theta\tilde{c}\, J\,\frac{\partial\left(\Phi\tilde{\kappa}\right)}{\partial J}\mathbf{I}\otimes\mathbf{I}\,, \tag{3.63}$$

and $\boldsymbol{c}^e$ is the spatial elasticity tensor of the solid matrix,

$$\boldsymbol{c}^e = J^{-1}\left(\mathbf{F}\,\underline{\otimes}\,\mathbf{F}\right) : 2\frac{\partial\mathbf{S}^e}{\partial\mathbf{C}} : \left(\mathbf{F}^T\,\underline{\otimes}\,\mathbf{F}^T\right). \tag{3.64}$$

The linearization of the second term is

$$D\left(\mathbf{W}\cdot\text{Grad}\,\delta\tilde{p}\right)[\Delta\mathbf{u}]dV = \text{grad}\,\delta\tilde{p}\cdot\mathbf{w}_u'\, dv\,, \tag{3.65}$$

where

$$\begin{aligned}\mathbf{w}_u' \equiv J^{-1}\mathbf{F}\cdot D\mathbf{W}[\Delta\mathbf{u}] &= -\left(\tilde{\boldsymbol{k}} : \Delta\boldsymbol{\varepsilon}\right)\cdot\left(\text{grad}\,\tilde{p} + R\theta\frac{\tilde{\kappa}}{d_0}\mathbf{d}\cdot\text{grad}\,\tilde{c}\right)\\ &-\frac{R\theta}{d_0}\tilde{\mathbf{k}}\cdot\left(J^2\frac{\partial\left(J^{-1}\tilde{\kappa}\right)}{\partial J}\left(\text{div}\,\Delta\mathbf{u}\right)\mathbf{I} + 2\tilde{\kappa}\,\Delta\boldsymbol{\varepsilon}\right)\cdot\mathbf{d}\cdot\text{grad}\,\tilde{c} - \tilde{\kappa}\frac{R\theta}{d_0}\tilde{\mathbf{k}}\cdot\left(\boldsymbol{d} : \Delta\boldsymbol{\varepsilon}\right)\cdot\text{grad}\,\tilde{c}\end{aligned}\,, \tag{3.66}$$

with

$$\begin{aligned}\tilde{\boldsymbol{k}} &= J^{-1}\left(\mathbf{F}\,\underline{\otimes}\,\mathbf{F}\right) : 2\frac{\partial\tilde{\mathbf{K}}}{\partial\mathbf{C}} : \left(\mathbf{F}^T\,\underline{\otimes}\,\mathbf{F}^T\right),\\ \boldsymbol{d} &= J^{-1}\left(\mathbf{F}\,\underline{\otimes}\,\mathbf{F}\right) : 2\frac{\partial\mathbf{D}}{\partial\mathbf{C}} : \left(\mathbf{F}^T\,\underline{\otimes}\,\mathbf{F}^T\right),\end{aligned} \tag{3.67}$$

representing the spatial tangents, with respect to the strain, of the effective permeability and solute diffusivity, respectively. These fourth-order tensors exhibit minor symmetries but not major symmetry, as described recently [21]. Since $\tilde{\mathbf{K}}$ is given by substituting $(2.114)_3$ into $(3.60)_1$, the evaluation of $\tilde{\boldsymbol{k}}$ is rather involved and it can be shown that

$$\tilde{\boldsymbol{k}} = 2\left(\tilde{\mathbf{k}}\otimes\mathbf{I} - 2\tilde{\mathbf{k}}\,\underline{\overline{\otimes}}\,\mathbf{I}\right) - \left(\tilde{\mathbf{k}}\,\underline{\otimes}\,\tilde{\mathbf{k}}\right) : \boldsymbol{g}\,, \tag{3.68}$$

where

$$\begin{aligned}\boldsymbol{g} &= 2\left(\mathbf{k}^{-1}\otimes\mathbf{I}-2\mathbf{k}^{-1}\,\overline{\underline{\otimes}}\,\mathbf{I}\right)-\left(\mathbf{k}^{-1}\,\underline{\otimes}\,\mathbf{k}^{-1}\right):\boldsymbol{k}\\ &+\frac{R\theta\tilde{c}}{d_0}J\frac{\partial}{\partial J}\left(\frac{\tilde{\kappa}}{\phi^w}\right)\left(\mathbf{I}-\frac{\mathbf{d}}{d_0}\right)\otimes\mathbf{I}\\ &+\frac{R\theta\tilde{c}}{d_0}\frac{\tilde{\kappa}}{\phi^w}\left(\mathbf{I}\otimes\mathbf{I}-2\mathbf{I}\,\underline{\otimes}\,\mathbf{I}-\frac{1}{d_0}\boldsymbol{d}\right)\end{aligned} \tag{3.69}$$

and

$$\boldsymbol{k} = J^{-1}\left(\mathbf{F}\,\underline{\otimes}\,\mathbf{F}\right):2\frac{\partial\mathbf{K}}{\partial\mathbf{C}}:\left(\mathbf{F}^T\,\underline{\otimes}\,\mathbf{F}^T\right). \tag{3.70}$$

The next term in δW_{int} linearizes to

$$-D\left(\delta\tilde{p}\frac{\partial J}{\partial t}\right)\left[\Delta\mathbf{u}\right]dV = -\delta\tilde{p}\left(\left[\left(\operatorname{div}\Delta\mathbf{u}\right)\mathbf{I}-\operatorname{grad}^T\Delta\mathbf{u}\right]:\operatorname{grad}\mathbf{v}^s+\operatorname{div}\overline{\Delta\mathbf{u}}^{\cdot}\right)dv, \tag{3.71}$$

where

$$\overline{\Delta\mathbf{u}}^{\cdot} \approx \frac{\Delta\mathbf{u}}{\Delta t}, \tag{3.72}$$

and Δt represents the time increment relative to the previous time point. The next term is given by

$$D\left(\mathbf{J}\cdot\operatorname{Grad}\delta\tilde{c}\right)\left[\Delta\mathbf{u}\right]dV = \operatorname{grad}\delta\tilde{c}\cdot\mathbf{j}_u'\,dv, \tag{3.73}$$

where

$$\begin{aligned}\mathbf{j}_u' \equiv J^{-1}\mathbf{F}\cdot D\mathbf{J}\left[\Delta\mathbf{u}\right] &= \left(J\frac{\partial\tilde{\kappa}}{\partial J}\left(\operatorname{div}\Delta\mathbf{u}\right)\mathbf{d}+\tilde{\kappa}\boldsymbol{d}:\Delta\boldsymbol{\varepsilon}\right)\cdot\left(-\phi^w\operatorname{grad}\tilde{c}+\frac{\tilde{c}}{d_0}\mathbf{w}\right)\\ &+\tilde{\kappa}\mathbf{d}\cdot\left(-\phi^s\left(\operatorname{div}\Delta\mathbf{u}\right)\operatorname{grad}\tilde{c}+\frac{\tilde{c}}{d_0}\left(2\Delta\boldsymbol{\varepsilon}-\left(\operatorname{div}\Delta\mathbf{u}\right)\mathbf{I}\right)\cdot\mathbf{w}\right)+\tilde{\kappa}\frac{\tilde{c}}{d_0}\mathbf{d}\cdot\mathbf{w}_u'\end{aligned}. \tag{3.74}$$

The last term is

$$\begin{aligned}D\left(\delta\tilde{c}\frac{\partial\left(J\phi^w\tilde{\kappa}\tilde{c}\right)}{\partial t}\right)\left[\Delta\mathbf{u}\right]dV &= -\delta\tilde{c}\left(\tilde{c}\frac{\partial J}{\partial t}\frac{\partial^2\left(J\phi^w\tilde{\kappa}\right)}{\partial J^2}+\frac{\partial\tilde{c}}{\partial t}\frac{\partial}{\partial J}\left[J\phi^w\left(\tilde{\kappa}+\frac{\partial\tilde{\kappa}}{\partial\tilde{c}}\tilde{c}\right)\right]\right)\operatorname{div}\Delta\mathbf{u}\,dv\\ &-\delta\tilde{c}\frac{\partial\left(J\phi^w\tilde{\kappa}\right)}{\partial J}\left(\left[\left(\operatorname{div}\Delta\mathbf{u}\right)\mathbf{I}-\operatorname{grad}^T\Delta\mathbf{u}\right]:\operatorname{grad}\mathbf{v}^s+\operatorname{div}\overline{\Delta\mathbf{u}}^{\cdot}\right)\tilde{c}\,dv\end{aligned}. \tag{3.75}$$

3.3.1.2. Linearization along $\Delta\tilde{p}$

The linearization of the various terms in δW_{int} along $\Delta\tilde{p}$ yields

$$D\left(\mathbf{S}:\delta\dot{\mathbf{E}}\right)\left[\Delta\tilde{p}\right]dV = -\Delta\tilde{p}\operatorname{div}\delta\mathbf{v}\,dv, \tag{3.76}$$

$$D\left(\mathbf{W}\cdot\operatorname{Grad}\delta\tilde{p}-\delta\tilde{p}\frac{\partial J}{\partial t}\right)\left[\Delta\tilde{p}\right]dV = -\operatorname{grad}\delta\tilde{p}\cdot\tilde{\mathbf{k}}\cdot\operatorname{grad}\Delta\tilde{p}\,dv, \tag{3.77}$$

$$D\left(\mathbf{J}\cdot\mathrm{Grad}\,\delta\tilde{c}-\delta\tilde{c}\frac{\partial\left(J\varphi^{w}\tilde{\kappa}\tilde{c}\right)}{\partial t}\right)\left[\Delta\tilde{p}\right]dV=-\frac{\tilde{\kappa}\tilde{c}}{d_0}\mathrm{grad}\,\delta\tilde{c}\cdot\mathbf{d}\cdot\tilde{\mathbf{k}}\cdot\mathrm{grad}\,\Delta\tilde{p}\,dv\,. \tag{3.78}$$

3.3.1.3. Linearization along $\Delta\tilde{c}$

The linearization of the first term in δW_{int} along $\Delta\tilde{c}$ yields

$$D\left(\mathbf{S}:\delta\dot{\mathbf{E}}\right)\left[\Delta\tilde{c}\right]dV=\Delta\tilde{c}\left(\boldsymbol{\sigma}_c{}'_c:\delta\mathbf{d}-R\theta\frac{\partial\left(\Phi\tilde{\kappa}\tilde{c}\right)}{\partial\tilde{c}}\mathrm{div}\,\delta\mathbf{v}\right)dv\,, \tag{3.79}$$

where

$$\boldsymbol{\sigma}_c{}'=J^{-1}\mathbf{F}\cdot\frac{\partial\mathbf{S}^e}{\partial\tilde{c}}\cdot\mathbf{F}^T \tag{3.80}$$

represents the spatial tangent of the stress with respect to the effective concentration. The next term is

$$D\left(\mathbf{W}\cdot\mathrm{Grad}\,\delta\tilde{p}\right)\left[\Delta\tilde{c}\right]dV=\mathrm{grad}\,\delta\tilde{p}\cdot\mathbf{w}'_c\,dv\,, \tag{3.81}$$

where

$$\begin{aligned}\mathbf{w}'_c\equiv J^{-1}\mathbf{F}\cdot D\mathbf{W}\left[\Delta\tilde{c}\right]&=-\Delta\tilde{c}\,\tilde{\mathbf{k}}'_c\cdot\left(\mathrm{grad}\,\tilde{p}+R\theta\frac{\tilde{\kappa}}{d_0}\mathbf{d}\cdot\mathrm{grad}\,\tilde{c}\right)\\&-R\theta\tilde{\mathbf{k}}\cdot\left[\Delta\tilde{c}\left(\frac{\partial}{\partial\tilde{c}}\left(\frac{\tilde{\kappa}}{d_0}\right)\mathbf{d}+\frac{\tilde{\kappa}}{d_0}\mathbf{d}'_c\right)\cdot\mathrm{grad}\,\tilde{c}+\frac{\tilde{\kappa}}{d_0}\mathbf{d}\cdot\mathrm{grad}\,\Delta\tilde{c}\right],\end{aligned} \tag{3.82}$$

and

$$\tilde{\mathbf{k}}'_c=J^{-1}\mathbf{F}\cdot\frac{\partial\widetilde{\mathbf{K}}}{\partial\tilde{c}}\cdot\mathbf{F}^T \tag{3.83}$$

is the spatial tangent of the effective hydraulic permeability with respect to the effective concentration.

The next term reduces to

$$-D\left(\delta\tilde{p}\frac{\partial J}{\partial t}\right)\left[\Delta\tilde{c}\right]dV=0\,. \tag{3.84}$$

The following term is

$$D\left(\mathbf{J}\cdot\mathrm{Grad}\,\delta\tilde{c}\right)\left[\Delta\tilde{c}\right]dV=\mathrm{grad}\,\delta\tilde{c}\cdot\mathbf{j}'_c\,dv\,, \tag{3.85}$$

where

$$\begin{aligned}\mathbf{j}'_c&\equiv J^{-1}\mathbf{F}\cdot D\mathbf{J}\left[\Delta\tilde{c}\right]\\&=\Delta\tilde{c}\left(\frac{\partial\tilde{\kappa}}{\partial\tilde{c}}\mathbf{d}+\tilde{\kappa}\mathbf{d}_c{}'\right)\cdot\left(-\phi^{w}\,\mathrm{grad}\,\tilde{c}+\frac{\tilde{c}}{d_0}\mathbf{w}\right),\\&-\phi^{w}\tilde{\kappa}\mathbf{d}\cdot\mathrm{grad}\,\Delta\tilde{c}+\tilde{\kappa}\frac{\tilde{c}}{d_0}\mathbf{d}\cdot\mathbf{w}'_c\end{aligned} \tag{3.86}$$

and

$$\mathbf{d}_c' = J^{-1}\mathbf{F}\cdot\frac{\partial\mathbf{D}}{\partial\tilde{c}}\cdot\mathbf{F}^T \tag{3.87}$$

is the spatial tangent of the diffusivity with respect to the effective concentration.

The last term is

$$\begin{aligned} D\left(\frac{\partial\left(J\phi^w\tilde{\kappa}\tilde{c}\right)}{\partial t}\delta\tilde{c}\right)\left[\Delta\tilde{c}\right]dV = &-\delta\tilde{c}\frac{1}{J}\frac{\partial\left(J\phi^w\right)}{\partial t}\frac{\partial\left(\tilde{\kappa}\tilde{c}\right)}{\partial\tilde{c}}\Delta\tilde{c}\,dv \\ &-\delta\tilde{c}\,\phi^w\left(\frac{\partial^2\left(\tilde{\kappa}\tilde{c}\right)}{\partial\tilde{c}^2}\Delta\tilde{c}\frac{\partial\tilde{c}}{\partial t}+\frac{\partial\left(\tilde{\kappa}\tilde{c}\right)}{\partial\tilde{c}}\dot{\overline{\Delta\tilde{c}}}\right)dv\,, \\ &-\delta\tilde{c}\,\phi^w\frac{\partial J}{\partial t}\frac{\partial}{\partial\tilde{c}}\left(\tilde{c}\frac{\partial\tilde{\kappa}}{\partial J}\right)\Delta\tilde{c}\,dv \end{aligned} \tag{3.88}$$

where

$$\dot{\overline{\Delta\tilde{c}}} \approx \frac{\Delta\tilde{c}}{\Delta t}\,. \tag{3.89}$$

3.3.2. Linearization of External Virtual Work

The linearization of δW_{ext} in (3.55) depends on whether natural boundary conditions are prescribed as area densities or total net values over an area. Thus, in the case when $\mathbf{t}\,da$ (net force), $w_n da$ (net volumetric flow rate), or $j_n da$ (net molar flow rate) are prescribed over the elemental area da, there is no variation in δW_{ext} and it follows that $D\delta W_{\text{ext}} = 0$. Alternatively, in the case when $\mathbf{t}$, w_n or j_n are prescribed, the linearization may be performed by evaluating the integral in the parametric space of the boundary surface ∂b, with parametric coordinates $\left(\eta^1,\eta^2\right)$. Accordingly, for a point $\mathbf{x}\left(\eta^1,\eta^2\right)$ on ∂b, surface tangents (covariant basis vectors) are given by

$$\mathbf{g}_\alpha = \frac{\partial\mathbf{x}}{\partial\eta^\alpha}, \quad \left(\alpha = 1,2\right) \tag{3.90}$$

and the outward unit normal is

$$\mathbf{n} = \frac{\mathbf{g}_1\times\mathbf{g}_2}{\left|\mathbf{g}_1\times\mathbf{g}_2\right|}\,. \tag{3.91}$$

The elemental area on ∂b is $da = \left|\mathbf{g}_1\times\mathbf{g}_2\right| d\eta^1 d\eta^2$. Consequently, the external virtual work integral may be rewritten as

$$\delta W_{\text{ext}} = \int_{\partial b}\left(\delta\mathbf{v}\cdot\mathbf{t} + \delta\tilde{p}\,w_n + \delta\tilde{c}\,j_n\right)\left|\mathbf{g}_1\times\mathbf{g}_2\right| d\eta^1 d\eta^2\,. \tag{3.92}$$

The directional derivative of δW_{ext} may then be applied directly to its integrand, since the parametric space is invariant [1].

If we restrict traction boundary conditions to the special case of normal tractions, then $\mathbf{t} = t_n \mathbf{n}$ where t_n is the prescribed normal traction component. Then it can be shown that the linearization of δW_{ext} along $\Delta\mathbf{u}$ produces

$$D\left(\delta W_{\text{ext}}\right)\left[\Delta\mathbf{u}\right] = \int_{\partial b}\left(t_n \delta\mathbf{v} + w_n \delta\tilde{p}\,\mathbf{n} + j_n \delta\tilde{c}\,\mathbf{n}\right)\cdot\left(\frac{\partial\Delta\mathbf{u}}{\partial\eta^1}\times\mathbf{g}_2 + \mathbf{g}_1\times\frac{\partial\Delta\mathbf{u}}{\partial\eta^2}\right)d\eta^1 d\eta^2 \,. \tag{3.93}$$

The linearizations along $\Delta\tilde{p}$ and $\Delta\tilde{c}$ reduce to zero, $D\left(\delta W_{\text{ext}}\right)\left[\Delta\tilde{p}\right] = 0$ and $D\left(\delta W_{\text{ext}}\right)\left[\Delta\tilde{c}\right] = 0$.

3.3.3. Discretization

To discretize the virtual work relations, let

$$\begin{aligned}
\delta\mathbf{v} &= \sum_{a=1}^{m} N_a \delta\mathbf{v}_a, \quad \Delta\mathbf{u} &= \sum_{b=1}^{m} N_b \Delta\mathbf{u}_b, \\
\delta\tilde{p} &= \sum_{a=1}^{m} N_a \delta\tilde{p}_a, \quad \Delta\tilde{p} &= \sum_{b=1}^{m} N_b \Delta\tilde{p}_b, \\
\delta\tilde{c} &= \sum_{a=1}^{m} N_a \delta\tilde{c}_a, \quad \Delta\tilde{c} &= \sum_{b=1}^{m} N_b \Delta\tilde{c}_b,
\end{aligned} \tag{3.94}$$

where N_a represents the interpolation functions over an element, $\delta\mathbf{v}_a$, $\delta\tilde{p}_a$, $\delta\tilde{c}_a$, $\Delta\mathbf{u}_a$, $\Delta\tilde{p}_a$ and $\Delta\tilde{c}_a$ respectively represent the nodal values of $\delta\mathbf{v}$, $\delta\tilde{p}$, $\delta\tilde{c}$, $\Delta\mathbf{u}$, $\Delta\tilde{p}$ and $\Delta\tilde{c}$; m is the number of nodes in an element.

The discretized form of δW_{int} in (3.55) may be written as

$$\delta W_{\text{int}} = \sum_{e=1}^{n_e}\sum_{k=1}^{n_{\text{int}}^{(e)}} W_k J_\eta \sum_{a=1}^{m}\begin{bmatrix}\delta\mathbf{v}_a & \delta\tilde{p}_a & \delta\tilde{c}_a\end{bmatrix}\cdot\begin{bmatrix}\mathbf{r}_a^u \\ r_a^p \\ r_a^c\end{bmatrix}, \tag{3.95}$$

where n_e is the number of elements in b, $n_{\text{int}}^{(e)}$ is the number of integration points in the $e-$th element, W_k is the quadrature weight associated with the $k-$th integration point, and J_η is the Jacobian of the transformation from the current spatial configuration to the parametric space of the element. In the above expression,

$$\begin{aligned}
\mathbf{r}_a^u &= \boldsymbol{\sigma}\cdot\operatorname{grad} N_a, \\
r_a^p &= \mathbf{w}\cdot\operatorname{grad} N_a - N_a\frac{1}{J}\frac{\partial J}{\partial t}, \\
r_a^c &= \mathbf{j}\cdot\operatorname{grad} N_a - N_a\frac{1}{J}\frac{\partial}{\partial t}\left(J\phi^w\tilde{\kappa}\tilde{c}\right),
\end{aligned} \tag{3.96}$$

and it is understood that J_η, $\mathbf{r}_a^u$, r_a^p and r_a^c are evaluated at the parametric coordinates of the $k-$th integration point. Since the parametric space is invariant, time derivatives are evaluated in a material frame. For example, the time derivative $D^s J\left(\mathbf{x},t\right)/Dt$ appearing in (3.55) becomes

$\partial J\left(\boldsymbol{\eta}_k,t\right)/\partial t$ when evaluated at the parametric coordinates $\boldsymbol{\eta}_k=\left(\eta_k^1,\eta_k^2,\eta_k^3\right)$ of the $k-$th integration point.

Similarly, the discretized form of $D\delta W_{\text{int}}=D\delta W_{\text{int}}\left[\Delta\mathbf{u}\right]+D\delta W_{\text{int}}\left[\Delta\tilde{p}\right]+D\delta W_{\text{int}}\left[\Delta\tilde{c}\right]$ may be written as

$$D\delta W_{\text{int}}=\sum_{e=1}^{n_e}\sum_{k=1}^{n_{\text{int}}^{(e)}}W_k J_\eta\sum_{a=1}^{m}\sum_{b=1}^{m}\left[\delta\mathbf{v}_a \quad \delta\tilde{p}_a \quad \delta\tilde{c}_a\right]\cdot\begin{bmatrix}\mathbf{K}_{ab}^{uu} & \mathbf{k}_{ab}^{up} & \mathbf{k}_{ab}^{uc}\\ \mathbf{k}_{ab}^{pu} & k_{ab}^{pp} & k_{ab}^{pc}\\ \mathbf{k}_{ab}^{cu} & k_{ab}^{cp} & k_{ab}^{cc}\end{bmatrix}\cdot\begin{bmatrix}\Delta\mathbf{u}_b\\ \Delta\tilde{p}_b\\ \Delta\tilde{c}_b\end{bmatrix}, \tag{3.97}$$

where the terms in the first column are the discretized form of the linearization along $\Delta\mathbf{u}$:

$$\mathbf{K}_{ab}^{uu}=\operatorname{grad}N_a\cdot\boldsymbol{c}\cdot\operatorname{grad}N_b+\left(\operatorname{grad}N_a\cdot\boldsymbol{\sigma}\cdot\operatorname{grad}N_b\right)\mathbf{I}, \tag{3.98}$$

$$\mathbf{k}_{ab}^{pu}=\left(\mathbf{w}_b^u\right)^T\cdot\operatorname{grad}N_a+N_a\mathbf{q}_b^{pu}, \tag{3.99}$$

$$\mathbf{k}_{ab}^{cu}=\left(\mathbf{j}_b^u\right)^T\cdot\operatorname{grad}N_a+N_a\mathbf{q}_b^{cu}, \tag{3.100}$$

where

$$, \tag{3.101}$$

$$\begin{aligned}\mathbf{j}_b^u=&\,J\frac{\partial\tilde{\kappa}}{\partial J}\left[\mathbf{d}\cdot\left(-\varphi^w\operatorname{grad}\tilde{c}+\frac{\tilde{c}}{d_0}\mathbf{w}\right)\right]\otimes\operatorname{grad}N_b+\tilde{\kappa}\left(-\varphi^w\operatorname{grad}\tilde{c}+\frac{\tilde{c}}{d_0}\mathbf{w}\right)\cdot\boldsymbol{d}\cdot\operatorname{grad}N_b\\&+\tilde{\kappa}\left(-\varphi^s\left(\mathbf{d}\cdot\operatorname{grad}\tilde{c}\right)\otimes\operatorname{grad}N_b+\frac{\tilde{c}}{d_0}\left[2\left(\operatorname{grad}N_b\cdot\mathbf{w}\right)\mathbf{d}-\left(\mathbf{d}\cdot\mathbf{w}\right)\otimes\operatorname{grad}N_b\right]\right)+\tilde{\kappa}\frac{\tilde{c}}{d_0}\mathbf{d}\cdot\mathbf{w}_b^u\end{aligned}, \tag{3.102}$$

$$\mathbf{q}_b^{pu}=-\left(\operatorname{div}\mathbf{v}^s+\frac{1}{\Delta t}\right)\operatorname{grad}N_b-\operatorname{grad}^T\mathbf{v}^s\cdot\operatorname{grad}N_b, \tag{3.103}$$

$$\mathbf{q}_b^{cu}=-\left(\tilde{c}\frac{\partial J}{\partial t}\frac{\partial^2\left(J\phi^w\tilde{\kappa}\right)}{\partial J^2}+\frac{\partial\tilde{c}}{\partial t}\frac{\partial}{\partial J}\left[J\phi^w\left(\tilde{\kappa}+\frac{\partial\tilde{\kappa}}{\partial\tilde{c}}\tilde{c}\right)\right]\right)\operatorname{grad}N_b+\tilde{c}\frac{\partial\left(J\phi^w\tilde{\kappa}\right)}{\partial J}\mathbf{q}_b^{pu}. \tag{3.104}$$

The terms in the second column of the stiffness matrix in (3.97) are the discretized form of the linearization along $\Delta\tilde{p}$:

$$\mathbf{k}_{ab}^{up}=-N_b\operatorname{grad}N_a, \tag{3.105}$$

$$k_{ab}^{pp}=-\operatorname{grad}N_a\cdot\tilde{\mathbf{k}}\cdot\operatorname{grad}N_b, \tag{3.106}$$

$$k_{ab}^{cp}=-\frac{\tilde{\kappa}\tilde{c}}{d_0}\operatorname{grad}N_a\cdot\mathbf{d}\cdot\tilde{\mathbf{k}}\cdot\operatorname{grad}N_b. \tag{3.107}$$

The terms in the third column of the stiffness matrix in (3.97) are the discretized form of the linearization along $\Delta\tilde{c}$:

$$\mathbf{k}_{ab}^{uc}=N_b\left(\boldsymbol{\sigma}_c'\cdot\operatorname{grad}N_a-R\theta\frac{\partial\left(\Phi\tilde{\kappa}\tilde{c}\right)}{\partial\tilde{c}}\operatorname{grad}N_a\right), \tag{3.108}$$

$$k_{ab}^{pc} = \operatorname{grad} N_a \cdot \mathbf{w}_b^c, \tag{3.109}$$

$$k_{ab}^{cc} = \operatorname{grad} N_a \cdot \mathbf{j}_b^c + N_a q_b^c, \tag{3.110}$$

where

$$\begin{aligned}\mathbf{w}_b^c = &-N_b \tilde{\mathbf{k}}_c' \cdot \left(\operatorname{grad} \tilde{p} + R\theta \frac{\tilde{\kappa}}{d_0} \mathbf{d} \cdot \operatorname{grad} \tilde{c} \right) \\ &-R\theta \tilde{\mathbf{k}} \cdot \left[N_b \left(\frac{\partial}{\partial \tilde{c}} \left(\frac{\tilde{\kappa}}{d_0} \right) \mathbf{d} + \frac{\tilde{\kappa}}{d_0} \mathbf{d}_c' \right) \cdot \operatorname{grad} \tilde{c} + \frac{\tilde{\kappa}}{d_0} \mathbf{d} \cdot \operatorname{grad} N_b \right],\end{aligned} \tag{3.111}$$

$$\mathbf{j}_b^c = N_b \left(\frac{\partial \tilde{\kappa}}{\partial \tilde{c}} \mathbf{d} + \tilde{\kappa} \mathbf{d}_c' \right) \cdot \left(-\phi^w \operatorname{grad} \tilde{c} + \frac{\tilde{c}}{d_0} \mathbf{w} \right) + \tilde{\kappa} \mathbf{d} \cdot \left(-\phi^w \operatorname{grad} N_b + \frac{\tilde{c}}{d_0} \mathbf{w}_b^c \right), \tag{3.112}$$

$$\begin{aligned}q_b^c = &-N_b \frac{1}{J} \frac{\partial \left(J\phi^w \right)}{\partial t} \frac{\partial \left(\tilde{\kappa}\tilde{c} \right)}{\partial \tilde{c}} \\ &-N_b \phi^w \left[\frac{\partial^2 \left(\tilde{\kappa}\tilde{c} \right)}{\partial \tilde{c}^2} \frac{\partial \tilde{c}}{\partial t} + \frac{1}{\Delta t} \frac{\partial \left(\tilde{\kappa}\tilde{c} \right)}{\partial \tilde{c}} + \frac{\partial J}{\partial t} \frac{\partial}{\partial \tilde{c}} \left(\tilde{c} \frac{\partial \tilde{\kappa}}{\partial J} \right) \right].\end{aligned} \tag{3.113}$$

The discretization of δW_{ext} in (3.55) has the form

$$\delta W_{\text{ext}} = \sum_{e=1}^{n_e} \sum_{k=1}^{n_{\text{int}}^{(e)}} W_k J_\eta \sum_{a=1}^{m} \begin{bmatrix} \delta \mathbf{v}_a & \delta \tilde{p}_a & \delta \tilde{c}_a \end{bmatrix} \cdot \begin{bmatrix} N_a t_n \mathbf{n} \\ N_a w_n \\ N_a j_n \end{bmatrix}, \tag{3.114}$$

where $J_\eta = \left| \mathbf{g}_1 \times \mathbf{g}_2 \right|$. The summation is performed over all surface elements on which these boundary conditions are prescribed. The discretization of $-D\delta W_{\text{ext}}$ has the form

$$-D\delta W_{\text{ext}} = \sum_{e=1}^{n_e} \sum_{k=1}^{n_{\text{int}}^{(e)}} W_k J_\eta \sum_{a=1}^{m} \sum_{b=1}^{m} \begin{bmatrix} \delta \mathbf{v}_a & \delta \tilde{p}_a & \delta \tilde{c}_a \end{bmatrix} \cdot \begin{bmatrix} \mathbf{K}_{ab}^{uu} & \mathbf{0} & \mathbf{0} \\ \mathbf{k}_{ab}^{pu} & 0 & 0 \\ \mathbf{k}_{ab}^{cu} & 0 & 0 \end{bmatrix} \cdot \begin{bmatrix} \Delta \mathbf{u}_b \\ \Delta \tilde{p}_b \\ \Delta \tilde{c}_b \end{bmatrix}, \tag{3.115}$$

where

$$\begin{aligned}\mathbf{K}_{ab}^{uu} &= t_n N_a \mathcal{A} \left\{ \frac{\partial N_b}{\partial \eta^1} \mathbf{g}_2 - \frac{\partial N_b}{\partial \eta^2} \mathbf{g}_1 \right\}, \\ \mathbf{k}_{ab}^{pu} &= -w_n N_a \mathcal{A} \left\{ \frac{\partial N_b}{\partial \eta^1} \mathbf{g}_2 - \frac{\partial N_b}{\partial \eta^2} \mathbf{g}_1 \right\} \cdot \mathbf{n}, \\ \mathbf{k}_{ab}^{cu} &= -j_n N_a \mathcal{A} \left\{ \frac{\partial N_b}{\partial \eta^1} \mathbf{g}_2 - \frac{\partial N_b}{\partial \eta^2} \mathbf{g}_1 \right\} \cdot \mathbf{n}.\end{aligned} \tag{3.116}$$

In this expression, $\mathcal{A}\{\mathbf{v}\}$ is the antisymmetric tensor whose dual vector is $\mathbf{v}$ (such that $\mathcal{A}\{\mathbf{v}\} \cdot \mathbf{q} = \mathbf{v} \times \mathbf{q}$ for any vector $\mathbf{q}$).

3.4. Newton-Raphson method

The Newton-Raphson method (also known as "Newton's method", "Full Newton method" or "the Newton method") is the basis for solving the nonlinear finite element equations. This section will describe the *Full Newton method* and the Broyden-Fletcher-Goldfarb-Shanno (BFGS) method [30]. The latter variation is actually a *quasi-Newton method*. It is important since it provides several advantages over the full Newton method and it is this method that is implemented in FEBio [30].

3.4.1. Full Newton Method

The Newton-Raphson equation (3.3) can be written in terms of the discretized equilibrium equations that were derived in the previous section as follows:

$$\delta\mathbf{v}^T \cdot \mathbf{K} \cdot \mathbf{u} = -\delta\mathbf{v}^T \cdot \mathbf{R}\,. \tag{3.117}$$

Since the virtual velocities $\delta\mathbf{v}$ are arbitrary, a discretized Newton-Raphson scheme can be formulated as follows:

$$\mathbf{K}\left(\mathbf{x}_k\right)\cdot\mathbf{u} = -\mathbf{R}\left(\mathbf{x}_k\right); \quad \mathbf{x}_{k+1} = \mathbf{x}_k + \mathbf{u}\,. \tag{3.118}$$

This is the basis of the Newton-Raphson method. For each iteration *k*, both the stiffness matrix and the residual vector are re-evaluated and a displacement increment **u** is calculated by pre-multiplying both sides of the above equation by $\mathbf{K}^{-1}$. This procedure is repeated until some convergence criteria are satisfied.

The formation of the stiffness matrix and, especially, calculation of its inverse, are computationally expensive. Quasi-Newton methods do not require the reevaluation of the stiffness matrix for every iteration. Instead, a quick update is calculated. One particular method that has been quite successful in the field of computational solid mechanics is the BFGS method, which is described in the next section.

3.4.2. BFGS Method

The BFGS method updates the stiffness matrix (or rather its inverse) to provide an approximation to the exact matrix. A displacement increment is defined as

$$\mathbf{d}_k = \mathbf{x}_k - \mathbf{x}_{k-1}\,, \tag{3.119}$$

and an increment in the residual is defined as

$$\mathbf{G}_k = \mathbf{R}_{k-1} - \mathbf{R}_k\,. \tag{3.120}$$

The updated matrix $\mathbf{K}_k$ should satisfy the quasi-Newton equation:

$$\mathbf{K}_k\mathbf{d}_k = \mathbf{G}_k\,. \tag{3.121}$$

In order to calculate this update, as displacement increment is first calculated:

$$\mathbf{u} = \mathbf{K}_{k-1}^{-1}\mathbf{R}_{k-1}\,. \tag{3.122}$$

This displacement vector defines a "direction" for the actual displacement increment. A line search (see next section) can now be applied to determine the optimal displacement increment:

$$\mathbf{x}_k = \mathbf{x}_{k-1} + s\mathbf{u}\,, \tag{3.123}$$

where s is determined from the line search. With the updated position calculated, $\mathbf{R}_k$ can be evaluated. Also, using equations (3.119) and (3.120), $\mathbf{d}_k$ and $\mathbf{G}_k$ can be evaluted. The stiffness update can now be expressed as

$$\mathbf{K}_k^{-1} = \mathbf{A}_k^T \mathbf{K}_{k-1}^{-1} \mathbf{A}_k\,, \tag{3.124}$$

where the matrix $\mathbf{A}$ is an $n \times n$ matrix of the simple form:

$$\mathbf{A}_k = \mathbf{1} + \mathbf{v}_k \mathbf{w}_k^T\,. \tag{3.125}$$

The vectors $\mathbf{v}$ and $\mathbf{w}$ are given by

$$\mathbf{v}_k = -\left(\frac{\mathbf{d}_k^T \mathbf{G}_k}{\mathbf{d}_k^T \mathbf{K}_{k-1} \mathbf{d}_k}\right)^{1/2} \mathbf{K}_{k-1}\mathbf{d}_k - \mathbf{G}_k\,, \tag{3.126}$$

$$\mathbf{w}_k = \frac{\mathbf{d}_k}{\mathbf{d}_k^T \mathbf{G}_k}\,. \tag{3.127}$$

The vector $\mathbf{K}_{k-1}\mathbf{d}_k$ is equal to $s\mathbf{R}_{k-1}$ and has already been calculated.

To avoid numerically dangerous updates, the condition number c of the updating matrix $\mathbf{A}$ is calculated:

$$c = \left(\frac{\mathbf{d}_k^T \mathbf{G}_k}{\mathbf{d}_k^T \mathbf{K}_{k-1} \mathbf{d}_k}\right)^{1/2}\,. \tag{3.128}$$

The update is not performed when this number exceeds a preset tolerance.

Considering the actual computations involved, it should be noted that using the matrix updates defined above, the calculation of the search direction in (3.122) can be rewritten as,

$$\mathbf{u} = \left(\mathbf{1} + \mathbf{w}_{k-1}\mathbf{v}_{k-1}^T\right)\ldots\left(\mathbf{1} + \mathbf{w}_1\mathbf{v}_1^T\right)\mathbf{K}_0^{-1}\left(\mathbf{1} + \mathbf{v}_1\mathbf{w}_1^T\right)\cdots\left(\mathbf{1} + \mathbf{v}_{k-1}\mathbf{w}_{k-1}^T\right)\mathbf{R}_{k-1}\,. \tag{3.129}$$

Hence, the search direction can be computed without explicitly calculating the updated matrices or performing any additional costly matrix factorizations as required in the full Newton-Raphson method.

3.4.3. Line Search Method

A powerful technique often used to improve the convergence rate of Newton based methods is the *line search method*. In this method, the direction of the displacement vector $\mathbf{u}$ is considered as optimal, but the magnitude is controlled by a parameter s:

$$\mathbf{x}_{k+1} = \mathbf{x}_k + s\mathbf{u}\,. \tag{3.130}$$

The value of s is usually chosen so that the total potential energy $W(s) = W(\mathbf{x}_k + s\mathbf{u})$ at the end of the iteration is minimized in the direction of $\mathbf{u}$. This is equivalent to the requirement that the residual force $\mathbf{R}(\mathbf{x}_k + s\mathbf{u})$ at the end of the iteration is orthogonal to $\mathbf{u}$:

$$R(s) = \mathbf{u}^T \mathbf{R}(\mathbf{x}_k + s\mathbf{u}) = 0\,. \tag{3.131}$$

However, in practice it is sufficient to obtain a value of s such that,

$$\left|R(s)\right| < \rho\left|R(0)\right|, \tag{3.132}$$

where typically a value of $\rho = 0.9$ is used. Under normal conditions the value $s = 1$ automatically satisfies equation (3.132) and therefore few extra operations are involved. However, when this is not the case, a more suitable value for *s* needs to be obtained. For this reason it is convenient to approximate $R(s)$ as a quadratic in *s*:

$$R(s) \approx (1-s)R(0) + R(1)s^2 = 0\,, \tag{3.133}$$

which yields a value for *s* as

$$s = \frac{r}{2} \pm \sqrt{\left(\frac{r}{2}\right)^2 - r}\,, \quad r = \frac{R(0)}{R(1)}\,. \tag{3.134}$$

If $r < 0$, the square root is positive and a first improved value for *s* is obtained:

$$s_1 = \frac{r}{2} + \sqrt{\left(\frac{r}{2}\right)^2 - r}\,. \tag{3.135}$$

If $r > 0$ the *s* can be obtained by using the value that minimizes the quadratic function, that is, $s_1 = r/2$. This procedure is now repeated with $R(1)$ replaced by $R(s_1)$ until equation (3.132) is satisfied.

Chapter 4. Element Library

FEBio provides several element types for finite element discretization. This chapter describes these elements in more detail.

4.1. Solid Elements

The 3D solid elements available in FEBio are *isoparametric elements*. All of the solid elements are formulated in a global Cartesian coordinate system. For all these elements, a local coordinate system (so-called *isoparametric coordinates*) is defined as well. The global position vector **x** can be written as a function of the isoparametric coordinates in the following sense:

$$\mathbf{x}(r,s,t)=\sum_{i=1}^{n} N_i(r,s,t)\mathbf{x}_i\,. \tag{4.1}$$

Here, n is the number of nodes, r, s and t are the isoparametric coordinates, N_i are the element shape functions and $\mathbf{x}_i$ are the spatial coordinates of the element nodes. The same parametric interpolation is used for the interpolation of other scalar and vector quantities.

All elements in FEBio are integrated numerically. This implies that integrals over the volume of the element v^e are approximated by a sum:

$$\int_{v^e} f(\mathbf{x})\,dv=\int_{\square^e} f(\mathbf{r})\,J(\mathbf{r})\,d\square \cong \sum_{i=1}^{m} f(\mathbf{r}_i)\,J_i w_i\,. \tag{4.2}$$

Here, $\square$ is the biunit cube, m is the number of integration points, $\mathbf{r}_i$ are the location of the integration points in isoparametric coordinates, J is the Jacobian of the transformation $\mathbf{x}=\mathbf{x}(r,s,t)$, and w_i is a weight associated with the integration point. The integration is performed over the element's volume in the natural coordinate system.

Most fully integrated solid elements are unsuitable for the analysis of (nearly-) incompressible material behavior. To deal with this type of deformation, a three-field element implementation is available in FEBio [31].

4.1.1. Hexahedral elements

FEBio implements an 8-node trilinear hexahedral element. This element is also known as a *brick* element. The shape functions for these elements are defined in function of the isoparametric coordinates r, s and t, and are given below.

$$
\begin{aligned}
N_1 &= \frac{1}{8}(1-r)(1-s)(1-t) \\
N_2 &= \frac{1}{8}(1+r)(1-s)(1-t) \\
N_3 &= \frac{1}{8}(1+r)(1+s)(1-t) \\
N_4 &= \frac{1}{8}(1-r)(1+s)(1-t) \\
N_5 &= \frac{1}{8}(1-r)(1-s)(1+t) \\
N_6 &= \frac{1}{8}(1+r)(1-s)(1+t) \\
N_7 &= \frac{1}{8}(1+r)(1+s)(1+t) \\
N_8 &= \frac{1}{8}(1-r)(1+s)(1+t)
\end{aligned}
\tag{4.3}
$$

4.1.2. Pentahedral Elements

Pentahedral elements (also knows as “wedge” elements) consist of six nodes and five faces. Their shape functions are defined in function of the isoparametric coordinates *r*, *s* and *t* and are given as follows.

$$
\begin{aligned}
N_1 &= \frac{1}{2}(1-r-s)(1-t) \\
N_2 &= \frac{1}{2}r(1-t) \\
N_3 &= \frac{1}{2}s(1-t) \\
N_4 &= \frac{1}{2}(1-r-s)(1+t) \\
N_5 &= \frac{1}{2}r(1+t) \\
N_6 &= \frac{1}{2}s(1+t)
\end{aligned}
\tag{4.4}
$$

4.1.3. Tetrahedral Elements

Linear 4-node tetrahedral elements are also available in FEBio. Their shape functions are defined in function of the isoparametric coordinates *r*, *s* and *t*.

$$
\begin{aligned}
N_1 &= 1 - r - s - t \\
N_2 &= r \\
N_3 &= s \\
N_4 &= t
\end{aligned}
\tag{4.5}
$$

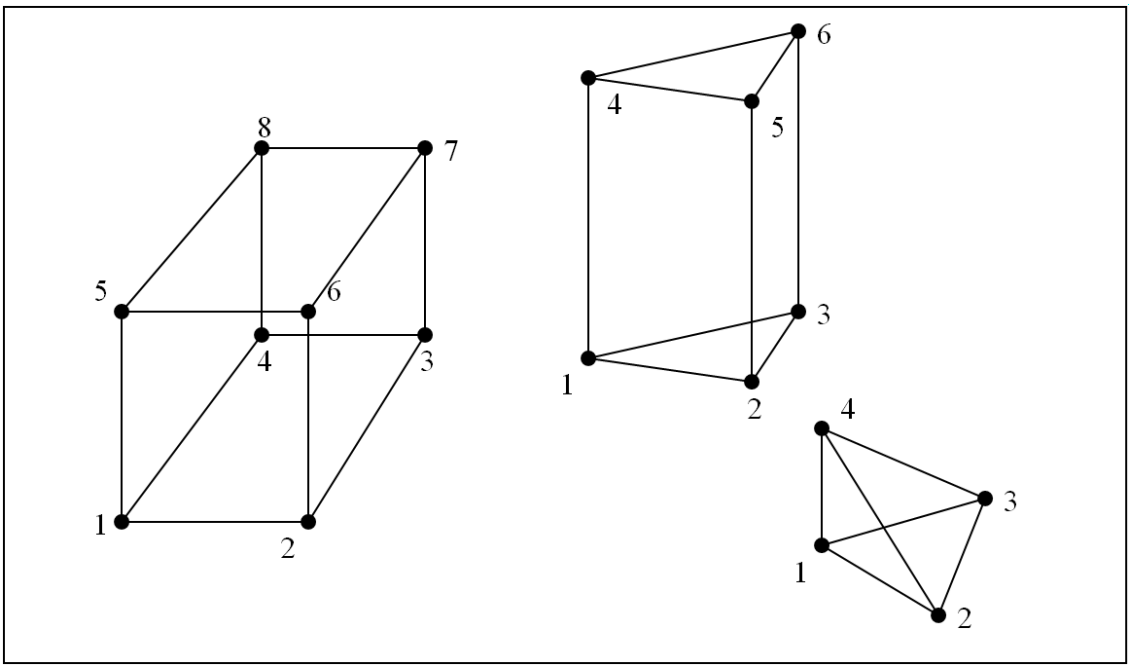

Figure 4-1. Different solid element types that are available in FEBio.

4.2. Shell Elements

Historically, shells have been formulated using two different approaches [32]. The difference between these approaches lies in the way the rotational degrees of freedom are defined. In the first approach, the rotational degrees of freedom are defined as angles. In addition, the plane stress condition needs to be enforced to take thickness variations into account. This approach is very useful for infinitesimal strains, but becomes very difficult to pursue in finite deformation due to the fact that finite rotations do not commute. Another disadvantage of this approach is that it requires a modification to the material formulation to enforce the plane stress condition. For complex materials this modification is very difficult or even impossible to obtain.

The alternative approach is to use an *extensible director* to describe the rotational degrees of freedom. With this approach it is not necessary to enforce the plane-stress condition and the full 3D constitutive relations can be employed. This approach is used in FEBio. A disadvantage of this approach is that it becomes difficult to enforce the unit length of the director throughout the entire element.

The shell formulation implemented in FEBio is still a work in progress. The goal is to implement an extensible director formulation with strain enhancements to deal with the well-known locking effect in incompressible and bending problems [33]. With the current state of the implementation, it is advised to use a fine mesh in such problems.

4.2.1. Shell formulation

In FEBio an extensible director formulation is implemented [33]. Six degrees of freedom are assigned to each shell node: three displacement degrees of freedom and three director degrees of freedom. The position of any point in the shell can be written as:

$$\begin{aligned}
&\mathbf{X}(\xi_i) = \bar{\mathbf{X}}(\xi_\alpha) + \mathbf{D}(\xi_i), \\
&\bar{\mathbf{X}}(\xi_\alpha) = \sum_{a=1}^{n} N_a(\xi_\alpha)\bar{\mathbf{X}}_a, \\
&\mathbf{D}(\xi_i) = \sum_{a=1}^{n} N_a(\xi_\alpha) z_a(\xi_3)\mathbf{D}_a, \\
&z_a(\xi_3) = \frac{1}{2}(1+\xi_3)\left(\frac{h_a^0}{2}\right) - \frac{1}{2}(1-\xi_3)\left(\frac{h_a^0}{2}\right).
\end{aligned} \tag{4.6}$$

It is assumed that Latin indices range from 1 to 3 and that Greek indices range from 1 to 2. The vector **D** is called the *director* and it is assumed that $\|\mathbf{D}_a\| = 1$. (Note that this does not necessarily imply that $\|\mathbf{D}\| = 1$ throughout the entire shell.) The function z_a is the *thickness function* and evaluates the initial thickness of the shell, which at node *a* is given by h_a^0.

Similarly, the displacement is given by

$$\begin{aligned}
&\mathbf{u}(\xi_i) = \bar{\mathbf{u}}(\xi_\alpha) + \mathbf{t}(\xi_i), \\
&\bar{\mathbf{u}}(\xi_\alpha) = \sum_{a=1}^{n} N_a(\xi_\alpha)\bar{\mathbf{u}}_a, \\
&\mathbf{t}(\xi_i) = \sum_{a=1}^{n} N_a(\xi_\alpha) z_a(\xi_3)\mathbf{t}_a.
\end{aligned} \tag{4.7}$$

The current configuration is then determined by

$$\begin{aligned}
&\mathbf{x}(\xi_i) = \bar{\mathbf{x}}(\xi_\alpha) + \mathbf{d}(\xi_i), \\
&\bar{\mathbf{x}}(\xi_\alpha) = \bar{\mathbf{X}}(\xi_\alpha) + \bar{\mathbf{U}}(\xi_\alpha), \\
&\mathbf{d}(\xi_i) = \mathbf{D}(\xi_i) + \mathbf{t}(\xi_i), \\
&\bar{\mathbf{x}}_a = \bar{\mathbf{X}}_a + \bar{\mathbf{u}}_a, \\
&\mathbf{d}_a = \mathbf{D}_a + \mathbf{t}_a.
\end{aligned} \tag{4.8}$$

To take thickness variations into account, it is not required that $\mathbf{d}_a$ is of unit length.

It is assumed that the virtual displacements have a similar interpolation than the actual displacements:

$$\delta\mathbf{u}\left(\xi_i\right)=\sum_{a=1}^{n}N_a\left(\xi_\alpha\right)\delta\overline{\mathbf{u}}_a+\sum_{a=1}^{n}N_a\left(\xi_\alpha\right)z_a\left(\xi_3\right)\delta\mathbf{t}_a\ . \tag{4.9}$$

The gradient of **u** is given by

$$\nabla\mathbf{u}=\sum_{a=1}^{n}\nabla N_a\overline{\mathbf{u}}_a+\sum_{a=1}^{n}\nabla M_a\mathbf{t}_a\ . \tag{4.10}$$

where we have defined $M_a\left(\xi_i\right)=N_a\left(\xi_\alpha\right)z_a\left(\xi_3\right)$. And similarly for the gradient of the virtual displacement,

$$\nabla\delta\mathbf{u}=\sum_{a=1}^{n}\nabla N_a\delta\overline{\mathbf{u}}_a+\sum_{a=1}^{n}\nabla M_a\delta\mathbf{t}_a\ . \tag{4.11}$$

The internal virtual work is now given by

$$\begin{aligned}G_{\text{int}}^{e}&=\int_{\Omega^e}\boldsymbol{\sigma}:\nabla\delta\mathbf{u}dv\\&=\sum_{a=1}^{n}\delta\overline{\mathbf{u}}_a\cdot\int_{\Omega^e}\boldsymbol{\sigma}\cdot\nabla N_a dv+\delta\mathbf{t}_a\cdot\int_{\Omega^e}\boldsymbol{\sigma}\cdot\nabla M_a dv\ .\end{aligned} \tag{4.12}$$

The shell geometry suggests an integration of the following type:

$$\int_{\Omega^e}\left(\bullet\right)dv=\int_{\square}\left(\int_{-1}^{+1}\left(\bullet\right)jd\xi_3\right)d\xi_1 d\xi_2\ . \tag{4.13}$$

where $j=\det\dfrac{\partial\mathbf{x}}{\partial\boldsymbol{\xi}}$ is the Jacobian of the transformation. In FEBio a 3-point Gaussian quadrature rule is used for the through-the-thickness integration.

FEBio currently supports four node quadrilateral and three-node triangular shell elements.

4.2.2. Quadrilateral shells

For quadrilateral shells, the shape functions are given by

$$\begin{aligned}N_1&=\frac{1}{4}\left(1-r\right)\left(1-s\right)\\N_2&=\frac{1}{4}\left(1+r\right)\left(1-s\right)\\N_3&=\frac{1}{4}\left(1+r\right)\left(1+s\right)\\N_4&=\frac{1}{4}\left(1-r\right)\left(1+s\right)\end{aligned} \tag{4.14}$$

4.2.3. Triangular shells

For triangular shell elements, the shape functions are given by

$$\begin{aligned} N_1 &= 1 - r - s \\ N_2 &= r \\ N_3 &= s \end{aligned} \tag{4.15}$$

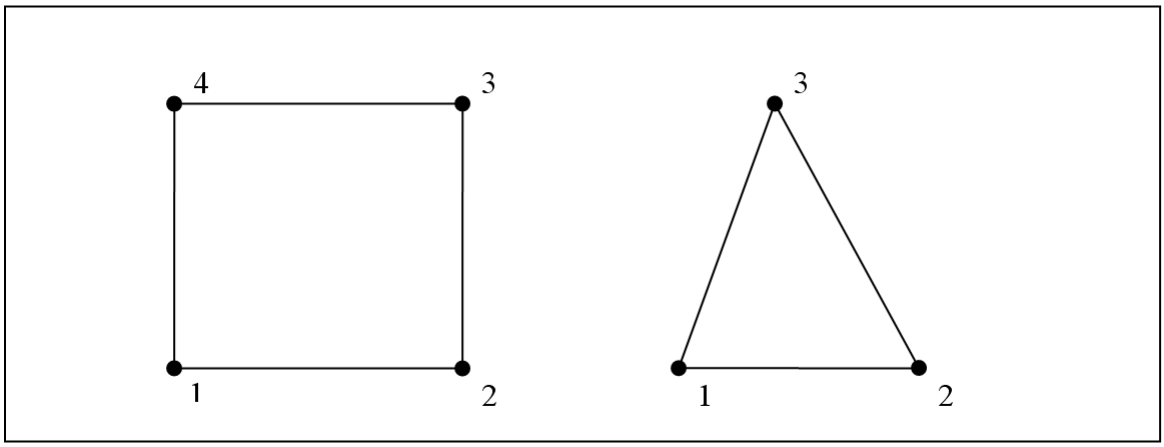

Figure 4-2. Different shell elements available in FEBio

Chapter 5. Constitutive Models

This chapter describes the theoretical background behind the constitutive models that are available in FEBio. Most materials are derived from a hyperelastic strain-energy function. Please consult section 2.4 for more background information on this class of materials.

5.1. Linear Elasticity

In the theory of linear elasticity the Cauchy stress tensor is a linear function of the small strain tensor $\boldsymbol{\varepsilon}$:

$$\boldsymbol{\sigma} = \boldsymbol{c} : \boldsymbol{\varepsilon} \,. \tag{5.1}$$

Here, $\boldsymbol{c}$ is the fourth-order elasticity tensor that contains the material properties. In the most general case this tensor has 21 independent parameters. However, in the presence of material symmetry the number of independent parameters is greatly reduced. For example, in the case of isotropic linear elasticity only two independent parameters remain. In this case, the elasticity tensor is given by $\boldsymbol{c} = \lambda \mathbf{I} \otimes \mathbf{I} + 2\mu \mathbf{I} \underline{\overline{\otimes}} \mathbf{I}$, or equivalently,

$$c_{ijkl} = \lambda \delta_{ij} \delta_{kl} + \mu \left(\delta_{ik} \delta_{jl} + \delta_{il} \delta_{jk} \right) . \tag{5.2}$$

The material coefficients λ and μ are known as the Lamé parameters. Using this equation, the stress-strain relationship can be written as

$$\sigma_{ij} = \lambda \varepsilon_{kk} \delta_{ij} + 2\mu \varepsilon_{ij} \,. \tag{5.3}$$

If the stress and strain are represented inVoigt notation, the constitutive equation can be rewritten in matrix form as

$$\begin{bmatrix} \sigma_{11} \\ \sigma_{22} \\ \sigma_{33} \\ \sigma_{12} \\ \sigma_{23} \\ \sigma_{13} \end{bmatrix} = \begin{bmatrix} \lambda + 2\mu & \lambda & \lambda & 0 & 0 & 0 \\ \lambda & \lambda + 2\mu & \lambda & 0 & 0 & 0 \\ \lambda & \lambda & \lambda + 2\mu & 0 & 0 & 0 \\ 0 & 0 & 0 & \mu & 0 & 0 \\ 0 & 0 & 0 & 0 & \mu & 0 \\ 0 & 0 & 0 & 0 & 0 & \mu \end{bmatrix} \begin{bmatrix} \varepsilon_{11} \\ \varepsilon_{22} \\ \varepsilon_{33} \\ \gamma_{12} \\ \gamma_{23} \\ \gamma_{13} \end{bmatrix} . \tag{5.4}$$

The shear strain measures $\gamma_{ij} = 2\varepsilon_{ij}$ are called the *engineering strains*.

The following table relates the Lamé parameters to the more familiar Young's modulus E and Poisson's ratio ν or to the bulk modulus K and shear modulus G.

	E,ν	λ,μ	K,G
E,ν		$E=\frac{\mu}{\lambda+\mu}(2\mu+3\lambda)$ $\nu=\frac{\lambda}{2(\lambda+\mu)}$	$E=\frac{9KG}{3K+G}$ $\nu=\frac{3K-2G}{6K+2G}$
λ,μ	$\lambda=\frac{\nu E}{(1+\nu)(1-2\nu)}$ $\mu=\frac{E}{2(1+\nu)}$		$\lambda=K-\frac{2}{3}G$ $\mu=G$
K,G	$K=\frac{E}{3(1-2\nu)}$ $G=\frac{E}{2(1+\nu)}$	$K=\lambda+\frac{2}{3}\mu$ $G=\mu$	

The theoretical range of the Young's modulus and Poisson's ratio for an isotropic material have the ranges

$$0<E<\infty\,, \tag{5.5}$$

$$-1\le\nu<0.5\,. \tag{5.6}$$

Materials with Poisson's ratio (close to) 0.5 are known as (nearly-) incompressible materials. For these materials, the bulk modulus approaches infinity. Most materials have a positive Poisson's ratio. However there do exist some materials with a negative ratio. These materials are known as *auxetic* materials and they have the remarkable property that they expand under tension.

The linear stress-strain relationship can also be derived from a strain-energy function such as in the case of hyperelastic materials. In this case the linear strain-energy is given by

$$W=\frac{1}{2}\boldsymbol{\varepsilon}:\boldsymbol{c}:\boldsymbol{\varepsilon}\,. \tag{5.7}$$

The stress is then similarly derived from $\boldsymbol{\sigma}=\frac{\partial W}{\partial\boldsymbol{\varepsilon}}$. In the case of isotropic elasticity, (5.7) can be simplified:

$$W=\frac{1}{2}\lambda\left(\operatorname{tr}\boldsymbol{\varepsilon}\right)^2+\mu\boldsymbol{\varepsilon}:\boldsymbol{\varepsilon}\,. \tag{5.8}$$

The Cauchy stress is now given in tensor form by

$$\boldsymbol{\sigma}=\lambda\left(\operatorname{tr}\boldsymbol{\varepsilon}\right)\mathbf{I}+2\mu\boldsymbol{\varepsilon}\,. \tag{5.9}$$

5.2. Compressible Materials

5.2.1. Isotropic Elasticity

The linear elastic material model as described in section 5.1 is only valid for small strains and small rotations. A first modification to this model to the range of nonlinear deformations is given by the St. Venant-Kirchhoff model [1], which in FEBio is referred to as *isotropic elasticity*. This model is objective for large strains and rotations. For the isotropic case it can be derived from the following hyperelastic strain-energy function:

$$W = \frac{1}{2}\lambda\left(\operatorname{tr}\mathbf{E}\right)^2 + \mu\mathbf{E}:\mathbf{E}\,. \tag{5.10}$$

The second Piola-Kirchhoff stress can be derived from this:

$$\mathbf{S} = \frac{\partial W}{\partial \mathbf{E}} = \lambda\left(\operatorname{tr}\mathbf{E}\right)\mathbf{I} + 2\mu\mathbf{E}\,. \tag{5.11}$$

Note that these equations are similar to the corresponding equations in the linear elastic case, except that the small strain tensor is replaced by the Green-Lagrange elasticity tensor **E**. The material elasticity tensor is then given by,

$$\mathcal{C} = \frac{\partial \mathbf{S}}{\partial \mathbf{E}} = \lambda\mathbf{I}\otimes\mathbf{I} + 2\mu\mathbf{I}\,\underline{\overline{\otimes}}\,\mathbf{I} \tag{5.12}$$

It is important to note that although this model is objective, it should only be used for small strains. For large strains, the response can be somewhat strange if not completely unrealistic. For example, it can be shown that under uni-axial tension the stress becomes infinite and the volume tends to zero for finite strains. Therefore, for large strains it is highly recommended to avoid this material and instead use one of the other non-linear material models described below.

5.2.2. Neo-Hookean Hyperelasticity

This is a compressible neo-Hookean material. It is derived from the following hyperelastic strain energy function [1]:

$$W = \frac{\mu}{2}\left(I_1 - 3\right) - \mu\ln J + \frac{\lambda}{2}\left(\ln J\right)^2. \tag{5.13}$$

The parameters μ and λ are the Lamé parameters from linear elasticity. This model reduces to the isotropic linear elastic model for small strains and rotations.

The Cauchy stress is given by,

$$\boldsymbol{\sigma} = \frac{\mu}{J}\left(\mathbf{b} - \mathbf{I}\right) + \frac{\lambda}{J}\left(\ln J\right)\mathbf{I}\,, \tag{5.14}$$

and the spatial elasticity tensor is given by,

$$\boldsymbol{c} = \frac{\lambda}{J}\mathbf{I}\otimes\mathbf{I} + \frac{2}{J}\left(\mu - \lambda\ln J\right)\mathbf{I}\,\underline{\overline{\otimes}}\,\mathbf{I}\,. \tag{5.15}$$

The neo-Hookean material is an extension of Hooke's law for the case of large deformations. It is useable for certain plastics and rubber-like substances. A generalization of this model is the Mooney-Rivlin material, which is often used to describe the elastic response of biological tissue.

In FEBio this constitutive model uses a standard displacement-based element formulation and a "coupled" strain energy, so care must be taken when modeling materials with nearly-incompressible material behavior to avoid element locking.

5.2.3. Ogden Unconstrained

The Ogden unconstrained material is defined using the following hyperelastic strain energy function:

$$W\left(\lambda_1,\lambda_2,\lambda_3\right)=\frac{1}{2}c_p\left(J-1\right)^2+\sum_{k=1}^{N}\frac{c_k}{m_k^2}\left(\lambda_1^{m_k}+\lambda_2^{m_k}+\lambda_3^{m_k}-3-m_k\ln J\right). \tag{5.16}$$

Here, λ_i are the principal stretches and c_p, c_k and m_k are material parameters.

The Cauchy stress tensor for this material may be obtained using the general formula for isotropic elasticity in principal directions given in (2.74), with

$$\sigma_i=c_p\left(J-1\right)+\sum_{k=1}^{N}\frac{1}{J}\frac{c_i}{m_k}\left(\lambda_i^{m_k}-1\right). \tag{5.17}$$

Similarly, the spatial elasticity tensor is given by

$$\begin{aligned}\boldsymbol{c}=&\sum_{i=1}^{3}\left(c_p+\sum_{k=1}^{N}\frac{1}{J}\frac{c_k}{m_k}\left[\left(m_k-2\right)\lambda_i^{m_k}+2\right]\right)\mathbf{a}_i\otimes\mathbf{a}_i\\&+\sum_{i=1}^{3}\sum_{j=i+1}^{3}c_p\left(2J-1\right)\left(\mathbf{a}_i\otimes\mathbf{a}_j+\mathbf{a}_j\otimes\mathbf{a}_i\right)\\&+\sum_{i=1}^{3}\sum_{j=i+1}^{3}2\frac{\lambda_j^2\sigma_i-\lambda_i^2\sigma_j}{\lambda_i^2-\lambda_j^2}\left(\mathbf{a}_i\,\underline{\overline{\otimes}}\,\mathbf{a}_j+\mathbf{a}_j\,\underline{\overline{\otimes}}\,\mathbf{a}_i\right),\end{aligned} \tag{5.18}$$

where $\mathbf{a}_i=\mathbf{n}_i\otimes\mathbf{n}_i$ and $\mathbf{n}_i$ are the eigenvectors of $\mathbf{b}$. In the limit when eigenvalues coincide,

$$\lim_{\lambda_j\to\lambda_i}2\frac{\sigma_i\lambda_j^2-\sigma_j\lambda_i^2}{\lambda_i^2-\lambda_j^2}=2c_p\left(1-J\right)+\sum_{k=1}^{N}\frac{1}{J}\frac{c_k}{m_k}\left[2+\left(m_k-2\right)\lambda_i^{m_k}\right]. \tag{5.19}$$

In the reference configuration, the elasticity tensor reduces to

$$\boldsymbol{c}\Big|_{\mathbf{b}=\mathbf{I}}=c_p\mathbf{I}\otimes\mathbf{I}+\left(\sum_{k=1}^{N}c_k\right)\mathbf{I}\,\underline{\overline{\otimes}}\,\mathbf{I}, \tag{5.20}$$

which has the form of Hooke's law for infinitesimal isotropic elasticity (see Section 5.1), with equivalent Lamé coefficients $c_p\equiv\lambda$ and $2\mu\equiv\sum_{k=1}^{N}c_k$.

5.2.4. Holmes-Mow

The coupled hyperelastic strain-energy function for this material is given by [34],

$$\Psi\left(I_1, I_2, J\right) = \frac{1}{2}c\left(e^Q - 1\right), \tag{5.21}$$

where I_1 and I_2 are the first and second invariants of the right Cauchy-Green tensor and J the jacobian of the deformation. Furthermore,

$$\begin{aligned} Q &= \frac{\beta}{\lambda + 2\mu}\left[\left(2\mu - \lambda\right)\left(I_1 - 3\right) + \lambda\left(I_2 - 3\right) - \left(\lambda + 2\mu\right)\ln J^2\right] \\ c &= \frac{\lambda + 2\mu}{2\beta} \end{aligned} \tag{5.22}$$

and λ and μ are the Lamé parameters. The corresponding Cauchy stress tensor is

$$\boldsymbol{\sigma} = \frac{1}{2J}e^Q\left(\left[2\mu + \lambda\left(I_1 - 1\right)\right]\mathbf{b} - \lambda\mathbf{b}^2 - \left(\lambda + 2\mu\right)\mathbf{I}\right), \tag{5.23}$$

and the spatial elasticity tensor is

$$\boldsymbol{c} = \frac{4\beta}{\lambda + 2\mu}Je^{-Q}\boldsymbol{\sigma}\otimes\boldsymbol{\sigma} + J^{-1}e^Q\left[\lambda\left(\mathbf{b}\otimes\mathbf{b} - \mathbf{b}\,\underline{\overline{\otimes}}\,\mathbf{b}\right) + \left(\lambda + 2\mu\right)\mathbf{I}\,\underline{\overline{\otimes}}\,\mathbf{I}\right]. \tag{5.24}$$

5.2.5. Donnan Equilibrium Swelling

The swelling pressure is described by the equations for ideal Donnan equilibrium, assuming that the material is porous, with a charged solid matrix, and the external bathing environment consists of a salt solution of monovalent counter-ions. Since osmotic swelling must be resisted by a solid material, this material is not stable on its own. It must be combined with an elastic material that resists the swelling.

The Cauchy stress for this material is the stress from the Donnan equilibrium response [35]:

$$\boldsymbol{\sigma} = -\pi\mathbf{I}, \tag{5.25}$$

where π is the osmotic pressure, given by

$$\pi = R\theta\left(\sqrt{\left(c^F\right)^2 + \left(\overline{c}^*\right)^2} - \overline{c}^*\right), \tag{5.26}$$

and c^F is the fixed charge density in the current configuration, related to the reference configuration via,

$$c^F = \frac{\varphi_0^w}{J - 1 + \varphi_0^w}c_0^F, \tag{5.27}$$

where $J = \det\mathbf{F}$ is the relative volume, R is the universal gas constant and θ is the absolute temperature.

Note that c_0^F may be negative or positive. The gel porosity φ_0^w is unitless and must be in the range $0 < \varphi_0^w < 1$. The corresponding spatial elasticity tensor is [36]

$$\boldsymbol{c} = \frac{R\theta J\left(c^F\right)^2}{\left(J-1+\varphi_0^w\right)\sqrt{\left(c^F\right)^2+\left(\bar{c}^*\right)^2}}\mathbf{I}\otimes\mathbf{I} + R\theta\left[\sqrt{\left(c^F\right)^2+\left(\bar{c}^*\right)^2}-\bar{c}^*\right]\left(2\mathbf{I}\,\underline{\bar{\otimes}}\,\mathbf{I}-\mathbf{I}\otimes\mathbf{I}\right). \tag{5.28}$$

5.2.6. Perfect Osmometer Equilibrium Osmotic Pressure

The swelling pressure is described by the equations for a perfect osmometer, assuming that the material is porous, containing an interstitial solution whose solutes cannot be exchanged with the external bathing environment. Similarly, solutes in the external bathing solution cannot be exchanged with the interstitial fluid of the porous material. Therefore, osmotic pressurization occurs when there is an imbalance between the interstitial and bathing solution osmolarities. Since osmotic swelling must be resisted by a solid matrix, this material is not stable on its own. It must be combined with an elastic material that resists the swelling.

The Cauchy stress for this material is the stress from the perfect osmometer equilibrium response [14]:

$$\mathbf{T} = -\pi\mathbf{I}, \tag{5.29}$$

where π is the osmotic pressure, given by

$$\pi = R\theta\left(\bar{c}-\bar{c}^*\right). \tag{5.30}$$

$\bar{c}$ is the interstitial fluid in the current configuration, related to the reference configuration via,

$$\bar{c} = \frac{\varphi_0^w}{J-1+\varphi_0^w}\bar{c}_0, \tag{5.31}$$

where R is the universal gas constant and θ is the absolute temperature.

Though this material is porous, this is not a full-fledged poroelastic material. The behavior described by this material is strictly valid only after the transient response of interstitial fluid and solute fluxes as subsided. The corresponding spatial elasticity tensor is

$$\boldsymbol{c} = R\theta\left[\frac{J\bar{c}}{J-1+\varphi_0^w}\mathbf{I}\otimes\mathbf{I}+\left(\bar{c}-\bar{c}^*\right)\left(2\mathbf{I}\,\underline{\bar{\otimes}}\,\mathbf{I}-\mathbf{I}\otimes\mathbf{I}\right)\right] \tag{5.32}$$

5.3. Nearly-Incompressible Materials

5.3.1. Mooney-Rivlin Hyperelasticity

This material model is a hyperelastic Mooney-Rivlin type with uncoupled deviatoric and volumetric behavior. The uncoupled strain energy W is given by:

$$W = c_1\left(\tilde{I}_1-3\right)+c_2\left(\tilde{I}_2-3\right)+\frac{1}{2}K\left(\ln J\right)^2. \tag{5.33}$$

Here, c_1 and c_2 are the Mooney-Rivlin material coefficients, $\tilde{I}_1$ and $\tilde{I}_2$ are the invariants of the deviatoric part of the right Cauchy-Green deformation tensor, $\tilde{\boldsymbol{C}} = \tilde{\boldsymbol{F}}^T\tilde{\boldsymbol{F}}$, where $\tilde{\boldsymbol{F}} = J^{(-1/3)}\boldsymbol{F}$, $\boldsymbol{F}$ is the deformation gradient and $J = \det(\boldsymbol{F})$ is the Jacobian of the deformation. When $c_2 = 0$, this model reduces to an uncoupled version of the incompressible neo-Hookean constitutive model.

The Cauchy stress is given by

$$\boldsymbol{\sigma} = p\mathbf{I} + \frac{2}{J}\left[\left(c_1 + c_2\tilde{I}_1\right)\tilde{\mathbf{b}} - c_2\tilde{\mathbf{b}}^2 - \frac{1}{3}\left(c_1\tilde{I}_1 + 2c_2\tilde{I}_2\right)\mathbf{I}\right]. \tag{5.34}$$

The spatial elasticity tensor is given by

$$\boldsymbol{c} = p\left(\mathbf{I}\otimes\mathbf{I} - 2\mathbf{I}\,\underline{\overline{\otimes}}\,\mathbf{I}\right) - \frac{2}{3}\left(\operatorname{dev}\boldsymbol{\sigma}\otimes\mathbf{I} + \mathbf{I}\otimes\operatorname{dev}\boldsymbol{\sigma}\right) + \boldsymbol{c}_w, \tag{5.35}$$

where,

$$\begin{aligned}\boldsymbol{c}_w = {} & \frac{4}{3J}\left(c_1\tilde{I}_1 + 2c_2\tilde{I}_2\right)\left(\mathbf{I}\,\underline{\overline{\otimes}}\,\mathbf{I} - \frac{1}{3}\mathbf{I}\otimes\mathbf{I}\right) + \frac{4c_2}{J}\left(\tilde{\mathbf{b}}\otimes\tilde{\mathbf{b}} - \tilde{\mathbf{b}}\,\underline{\overline{\otimes}}\,\tilde{\mathbf{b}}\right) \\ & - \frac{4c_2}{3J}\left[\left(\tilde{I}_1\tilde{\mathbf{b}} - \tilde{\mathbf{b}}^2\right)\otimes\mathbf{I} + \mathbf{I}\otimes\left(\tilde{I}_1\tilde{\mathbf{b}} - \tilde{\mathbf{b}}^2\right)\right] + \frac{8c_2\tilde{I}_2}{9J}\mathbf{I}\otimes\mathbf{I}.\end{aligned} \tag{5.36}$$

This material model uses a three-field element formulation, interpolating displacements as linear field variables and pressure and volume ratio as piecewise constant in each element [31].

5.3.2. Ogden Hyperelastic

The Ogden material is defined using the following hyperelastic strain energy function:

$$W\left(\lambda_1, \lambda_2, \lambda_3, J\right) = \sum_{i=1}^{N}\frac{c_i}{m_i^2}\left(\tilde{\lambda}_1^{m_i} + \tilde{\lambda}_2^{m_i} + \tilde{\lambda}_3^{m_i} - 3\right) + U\left(J\right). \tag{5.37}$$

Here, $\tilde{\lambda}_i$ are the deviatoric principal stretches and c_i and m_i are material parameters. The term $U\left(J\right)$ is the volumetric component and J is the determinant of the deformation gradient.

Note that the neo-Hookean and Mooney-Rivlin models can also be obtained from the general Ogden strain energy function using special choices for c_i and m_i.

5.3.3. Veronda-Westmann Hyperelasticity

This model is similar to the Mooney-Rivlin model in that it also uses an uncoupled strain energy. However, in this case the strain energy is given by an exponential form:

$$W = C_1\left[e^{\left(C_2\left(\tilde{I}_1 - 3\right)\right)} - 1\right] - \frac{C_1C_2}{2}\left(\tilde{I}_2 - 3\right) + U\left(J\right). \tag{5.38}$$

The dilatational term U is identical to the Mooney-Rivlin model.

The Cauchy stress $\boldsymbol{\sigma}$ is found from

$$\boldsymbol{\sigma} = p\mathbf{I} + \operatorname{dev}\tilde{\boldsymbol{\sigma}}, \tag{5.39}$$

where

$$\tilde{\boldsymbol{\sigma}} = \frac{2}{J}\left[\left(W_1 + I_1 W_2\right)\tilde{\mathbf{b}} - W_2\tilde{\mathbf{b}}^2\right]. \tag{5.40}$$

The strain energy derivatives are given by

$$W_1 = C_1 C_2 e^{C_2(I_1-3)}, \tag{5.41}$$

$$W_2 = -\frac{C_1 C_2}{2}. \tag{5.42}$$

This material model was the result from the research of the elastic response of skin tissue [37].

5.3.4. Arruda-Boyce Hyperelasticity

Arruda and Boyce proposed a model for the deformation of rubber materials [38]. Their main motivation was to develop a model that accurately captures the behavior of rubbers in different loading scenarios and that can be described with a limited number of physically motivated parameters. Their model is based on the Langevin chain statistics, which models a rubber chain segment between chemical crosslinks as a number N of rigid links of equal length l. The parameter N is related to the locking stretch λ_L, the stretch at which the chains reach their full extended state, $\lambda_L = \sqrt{N}$.

Their proposed strain-energy is a truncated Taylor series of the inverse Langevin function. A formulation that retains the first five terms of this function takes on the following form:

$$\tilde{W} = \mu\sum_{i=1}^{5}\frac{\alpha_i}{N^{i-1}}\left(\tilde{I}_1^i - 3^i\right) + U\left(J\right), \tag{5.43}$$

where μ is a shear-modulus like parameter and the coefficients α_i are

$$\alpha_1 = \frac{1}{2},\quad \alpha_2 = \frac{1}{20},\quad \alpha_3 = \frac{11}{1050},\quad \alpha_4 = \frac{19}{7000},\quad \alpha_5 = \frac{519}{673750}. \tag{5.44}$$

The Cauchy stress is given by

$$\boldsymbol{\sigma} = p\mathbf{I} + \frac{2}{J}\operatorname{dev}\left(W_1\tilde{\mathbf{b}}\right) = p\mathbf{I} + \frac{2W_1}{J}\left(\tilde{\mathbf{b}} - \frac{1}{3}\tilde{I}_1\mathbf{I}\right), \tag{5.45}$$

where,

$$W_1 = \frac{\partial\tilde{W}}{\partial\tilde{I}_1} = \mu\sum_{i=1}^{5}\alpha_i i\left(\frac{\tilde{I}_1}{N}\right)^{i-1}. \tag{5.46}$$

5.3.5. Transversely Isotropic Hyperelastic

This constitutive model can be used to represent a material that has a single preferred fiber direction and was developed for application to biological soft tissues [5, 39, 40]. It can be used to model tissues such as tendons, ligaments and muscle. The elastic response of the tissue is assumed to arise from the resistance of the fiber family and an isotropic matrix. It is assumed that the strain energy function can be written as follows:

$$W = F_1\left(\tilde{I}_1, \tilde{I}_2\right) + F_2\left(\tilde{\lambda}\right) + \frac{K}{2}\left[\ln\left(J\right)\right]^2. \tag{5.47}$$

Here $\tilde{I}_1$ and $\tilde{I}_2$ are the first and second invariants of the deviatoric version of the right Cauchy Green deformation tensor $\tilde{\mathbf{C}}$ and $\tilde{\lambda}$ is the deviatoric part of the stretch along the fiber direction ($\tilde{\lambda}^2 = \mathbf{A}\cdot\tilde{\mathbf{C}}\cdot\mathbf{A}$, where $\mathbf{A}$ is the initial fiber direction). The function F_1 represents the material response of the isotropic ground substance matrix, while F_2 represents the contribution from the fiber family. The strain energy of the fiber family is as follows:

$$\begin{aligned}
&\tilde{\lambda}\frac{\partial F_2}{\partial \tilde{\lambda}} = 0, \quad \tilde{\lambda} \le 1; \\
&\tilde{\lambda}\frac{\partial F_2}{\partial \tilde{\lambda}} = C_3\left(e^{C_4\left(\tilde{\lambda}-1\right)} - 1\right), \quad 1 < \tilde{\lambda} < \lambda_m; \\
&\tilde{\lambda}\frac{\partial F_2}{\partial \tilde{\lambda}} = C_5 + C_6\tilde{\lambda}, \quad \tilde{\lambda} \ge \lambda_m .
\end{aligned} \tag{5.48}$$

Here, λ_m is the stretch at which the fibers are straightened, C_3 scales the exponential stresses, C_4 is the rate of uncrimping of the fibers, and C_5 is the modulus of the straightened fibers. C_6 is determined from the requirement that the stress is continuous at λ_m.

This material model uses a three-field element formulation, interpolating displacements as linear field variables and pressure and volume ratio as piecewise constant on each element [31].

5.3.6. Ellipsoidal Fiber Distribution

This constitutive model describes a material that is composed of an ellipsoidal continuous fiber distribution in an uncoupled formulation. The deviatoric part of the stress is given by [35, 41, 42],

$$\tilde{\boldsymbol{\sigma}} = \int_0^{2\pi}\int_0^{\pi} H\left(\tilde{I}_n - 1\right)\tilde{\boldsymbol{\sigma}}_n\left(\mathbf{n}\right)\sin\varphi d\varphi d\theta , \tag{5.49}$$

and the corresponding elasticity tensor is

$$\tilde{c} = \int_0^{2\pi}\int_0^{\pi} H\left(\tilde{I}_n - 1\right)\tilde{c}_n\left(\mathbf{n}\right)\sin\phi d\phi d\theta . \tag{5.50}$$

$\tilde{I}_n = \tilde{\lambda}_n^2 = \mathbf{N}\cdot\tilde{\mathbf{C}}\cdot\mathbf{N}$ is the square of the fiber stretch $\mathbf{F}$, $\mathbf{N}$ is the unit vector along the fiber direction (in the reference configuration), which in spherical angles is directed along $\left(\theta,\varphi\right)$, $\mathbf{n} = \tilde{\mathbf{F}}\cdot\mathbf{N}/\tilde{\lambda}_n$ and $H\left(\bullet\right)$ is the unit step function that enforces the tension-only contribution. The fiber stress is determined from a fiber strain energy function in the usual manner:

$$\tilde{\boldsymbol{\sigma}}_n = 2J^{-1}\tilde{I}_n\frac{\partial\tilde{\Psi}}{\partial\tilde{I}_n}\mathbf{n}\otimes\mathbf{n} , \tag{5.51}$$

whereas the fiber elasticity tensor is

$$\tilde{c}_n = 4J^{-1}\tilde{I}_n^2\frac{\partial^2\tilde{\Psi}}{\partial\tilde{I}_n^2}\mathbf{n}\otimes\mathbf{n}\otimes\mathbf{n}\otimes\mathbf{n} , \tag{5.52}$$

where in this material

$$\tilde{\Psi}\left(\mathbf{n},\tilde{I}_n\right) = \xi\left(\mathbf{n}\right)\left(\tilde{I}_n - 1\right)^{\beta(\mathbf{n})} . \tag{5.53}$$

The materials parameters β and ξ are determined from:

$$\xi(\mathbf{n}) = \left(\frac{\cos^2\theta\sin^2\varphi}{\xi_1^2} + \frac{\sin^2\theta\sin^2\varphi}{\xi_2^2} + \frac{\cos^2\varphi}{\xi_3^2} \right)^{-1/2},$$
$$\beta(\mathbf{n}) = \left(\frac{\cos^2\theta\sin^2\varphi}{\beta_1^2} + \frac{\sin^2\theta\sin^2\varphi}{\beta_2^2} + \frac{\cos^2\varphi}{\beta_3^2} \right)^{-1/2}. \tag{5.54}$$

Since fibers can only sustain tension, this material is not stable on its own. It must be combined with a material that acts as the ground matrix. The total stress is then given by the sum of the fiber stress and the ground matrix stress:

$$\tilde{\boldsymbol{\sigma}} = \tilde{\boldsymbol{\sigma}}_m + \tilde{\boldsymbol{\sigma}}_f . \tag{5.55}$$

5.3.7. Fiber with exponential Power law

This material model describes a constitutive model for fibers, where a single fiber family follows an exponential power law strain energy function. The deviatoric part of the Cauchy stress is given by:

$$\tilde{\boldsymbol{\sigma}} = 2J^{-1}H\left(\tilde{I}_n - 1\right)\tilde{I}_n \frac{\partial\tilde{\Psi}}{\partial\tilde{I}_n}\mathbf{n}\otimes\mathbf{n}, \tag{5.56}$$

and the corresponding spatial elasticity tensor is

$$\tilde{\boldsymbol{c}} = 4J^{-1}H\left(\tilde{I}_n - 1\right)\tilde{I}_n^2 \frac{\partial^2\tilde{\Psi}}{\partial\tilde{I}_n^2}\mathbf{n}\otimes\mathbf{n}\otimes\mathbf{n}\otimes\mathbf{n} \tag{5.57}$$

where $\tilde{I}_n = \tilde{\lambda}_n^2 = \mathbf{N}\cdot\tilde{\mathbf{C}}\cdot\mathbf{N}$ is the square of the fiber stretch, $\mathbf{N}$ is the fiber orientation in the reference configuration,

$$\mathbf{N} = \sin\varphi\cos\theta\mathbf{e}_1 + \sin\varphi\sin\theta\mathbf{e}_2 + \cos\varphi\mathbf{e}_3 \tag{5.58}$$

and $\mathbf{n} = \tilde{\mathbf{F}}\cdot\mathbf{N}/\tilde{\lambda}_n$ and $H(\bullet)$ is the unit step function that enforces the tension-only contribution. The fiber strain energy density is given by

$$\tilde{\Psi} = \frac{\xi}{\alpha\beta}\left(\exp\left[\alpha\left(\tilde{I}_n - 1\right)^\beta\right] - 1\right), \tag{5.59}$$

where $\xi > 0$, $\alpha \geq 0$ and $\beta \geq 2$.

Note: in the limit when $\alpha \to 0$, this expression produces a power law,

$$\lim_{\alpha\to 0}\tilde{\Psi} = \frac{\xi}{\beta}\left(\tilde{I}_n - 1\right)^\beta . \tag{5.60}$$

Note: when $\beta > 2$, the fiber modulus is zero at the strain origin ($\tilde{I}_n = 1$). Therefore, use $\beta > 2$ when a smooth transition in the stress is desired from compression to tension.

5.3.8. Fung Orthotropic

The hyperelastic strain energy function for a Fung Orthotropic material is given by [43, 44]

$$\tilde{\Psi} = \frac{1}{2}c\left(e^{\tilde{Q}} - 1\right) + U\left(J\right), \tag{5.61}$$

where

$$\tilde{Q} = c^{-1}\sum_{a=1}^{3}\left[2\mu_a \mathbf{M}_a : \tilde{\mathbf{E}}^2 + \sum_{b=1}^{3}\lambda_{ab}\left(\mathbf{M}_a : \tilde{\mathbf{E}}\right)\left(\mathbf{M}_b : \tilde{\mathbf{E}}\right)\right]. \tag{5.62}$$

Here, $\tilde{\mathbf{E}} = \frac{1}{2}\left(\tilde{\mathbf{C}} - \mathbf{I}\right)$ and $\mathbf{M}_a = \mathbf{A}_a \otimes \mathbf{A}_a$, where $\mathbf{A}_a$ are orthonormal vectors that define the initial direction of material axes. The orthotropic Lamé coefficients should be chosen such that the stiffness matrix,

$$\begin{bmatrix} \lambda_{11} + 2\mu_1 & \lambda_{12} & \lambda_{13} & 0 & 0 & 0 \\ \lambda_{12} & \lambda_{22} + 2\mu_2 & \lambda_{23} & 0 & 0 & 0 \\ \lambda_{13} & \lambda_{23} & \lambda_{33} + 2\mu_3 & 0 & 0 & 0 \\ 0 & 0 & 0 & \frac{1}{2}\left(\mu_1 + \mu_2\right) & 0 & 0 \\ 0 & 0 & 0 & 0 & \frac{1}{2}\left(\mu_2 + \mu_3\right) & 0 \\ 0 & 0 & 0 & 0 & 0 & \frac{1}{2}\left(\mu_1 + \mu_3\right) \end{bmatrix} \tag{5.63}$$

is positive definite.

5.3.9. Tension-Compression Nonlinear Orthotropic

This material model is based on the following uncoupled hyperelastic strain energy function [45]:

$$\Psi\left(\mathbf{C}, \lambda_1, \lambda_2, \lambda_3\right) = \tilde{\Psi}_{iso}\left(\tilde{\mathbf{C}}\right) + \sum_{i=1}^{3}\tilde{\Psi}_i^{TC}\left(\tilde{\lambda}_i\right) + U\left(J\right). \tag{5.64}$$

The isotropic strain energy $\tilde{\Psi}_{iso}$ and the dilatational energy U are the same as for the Mooney-Rivlin material. The tension-compression term is defined as follows:

$$\tilde{\Psi}_i^{TC}\left(\tilde{\lambda}_i\right) = \begin{cases} \xi_i\left(\tilde{\lambda}_i - 1\right)^{\beta_i}, & \tilde{\lambda}_i > 1 \\ 0, & \tilde{\lambda}_i \le 1 \end{cases}, \xi_i \ge 0 \qquad \text{(no sum on i)} \tag{5.65}$$

The $\tilde{\lambda}_i$ parameters are the deviatoric fiber stretches of the local material fibers,

$$\tilde{\lambda}_i = \left(\mathbf{A}_i \cdot \tilde{\mathbf{C}} \cdot \mathbf{A}_i\right)^{1/2}. \tag{5.66}$$

The local material fibers are defined (in the reference frame) as an orthonormal set of vectors $\mathbf{A}_i$. The corresponding deviatoric part of the Cauchy stress is

$$\tilde{\boldsymbol{\sigma}} = J^{-1}\sum_{i=1}^{3}\frac{1}{\tilde{\lambda}_i}\frac{\partial\tilde{\Psi}}{\partial\tilde{\lambda}_i}\mathbf{a}_i \otimes \mathbf{a}_i \tag{5.67}$$

and the spatial elasticity tensor is

$$\tilde{\boldsymbol{c}} = J^{-1}\sum_{i=1}^{3}\frac{1}{\tilde{\lambda}_i}\frac{\partial}{\partial\tilde{\lambda}_i}\left(\frac{1}{\tilde{\lambda}_i}\frac{\partial\tilde{\Psi}}{\partial\tilde{\lambda}_i}\right)\mathbf{a}_i\otimes\mathbf{a}_i\otimes\mathbf{a}_i\otimes\mathbf{a}_i \tag{5.68}$$

where $\mathbf{a}_i = \tilde{\mathbf{F}}\cdot\mathbf{A}_i$.

5.4. Viscoelasticity

For a viscoelastic material the second Piola Kirchhoff stress can be written as follows [39]:

$$\mathbf{S}(t) = \int_{-\infty}^{t} G(t-s)\frac{d\mathbf{S}^e}{ds}ds\,, \tag{5.69}$$

where $\mathbf{S}^e$ is the elastic stress and $G(t)$ is the relaxation function. Here we consider the special case where the relaxation function is given by

$$G(t) = \gamma_0 + \sum_{i=1}^{N}\gamma_i\exp(-t/\tau_i)\,. \tag{5.70}$$

With this function chosen for the relaxation function, we can write the total stress as

$$\mathbf{S}(t) = \int_{-\infty}^{t}\left(\gamma_0 + \sum_{i=1}^{N}\gamma_i\exp\left((-t+s)/\tau_i\right)\frac{d\mathbf{S}^e}{ds}\right)ds\,. \tag{5.71}$$

Introducing the internal variables,

$$\mathbf{H}^{(i)}(t) = \int_{-\infty}^{t}\exp\left[-(t-s)/\tau_i\right]\frac{d\mathbf{S}^e}{ds}ds\,, \tag{5.72}$$

we can rewrite (5.71) as follows,

$$\mathbf{S}(t) = \gamma_0\mathbf{S}^e(t) + \sum_{i=1}^{N}\gamma_i\mathbf{H}^{(i)}(t)\,. \tag{5.73}$$

In FEBio, $\gamma_0 = 1$, so $\mathbf{S}^e$ is the long-term elastic response of the material.

The question now remains how to evaluate the internal variables. From equation (5.72) it appears that we have to integrate over the entire time domain. However, we can find a recurrence relationship that will allow us to evaluate the internal variables at a time $t+\Delta t$ given the values at time t.

$$\begin{aligned}\mathbf{H}^{(i)}(t+\Delta t) &= \int_{-\infty}^{t+\Delta t}\exp\left[-(t+\Delta t-s)/\tau_i\right]\frac{d\mathbf{S}^e}{ds}ds \\ &= \exp(-\Delta t/\tau_i)\int_{-\infty}^{t}\exp\left[-(t-s)/\tau_i\right]\frac{d\mathbf{S}^e}{ds}ds + \int_{t}^{t+\Delta t}\exp\left[-(t+\Delta t-s)/\tau_i\right]\frac{d\mathbf{S}^e}{ds}ds \\ &= \exp(-\Delta t/\tau_i)\mathbf{H}^{(i)}(t) + \int_{t}^{t+\Delta t}\exp\left[-(t+\Delta t-s)/\tau_i\right]\frac{d\mathbf{S}^e}{ds}ds.\end{aligned} \tag{5.74}$$

The last term can now be simplified using the midpoint rule to approximate the derivate. In that case we find the recurrence relation:

$$\mathbf{H}^{(i)}(t+\Delta t) = \exp(-\Delta t/\tau_i)\mathbf{H}^{(i)}(t) + \frac{1-\exp(-\Delta t/\tau_i)}{\Delta t/\tau_i}\left(\mathbf{S}^e(t+\Delta t) - \mathbf{S}^e(t)\right). \tag{5.75}$$

The following procedure can now be applied to calculate the new stress. Given $\mathbf{S}_n^e$ and $\mathbf{H}_n^{(i)}$ corresponding to time *t*, find $\mathbf{S}_{n+1}^e$ and $\mathbf{H}_{n+1}^{(i)}$ corresponding to time $t+\Delta t$:

1. calculate elastic stress: $\mathbf{S}_{n+1}^e = \dfrac{\partial W^e}{\partial \mathbf{C}_{n+1}}$
2. evaluate internal variables: $\mathbf{H}_{n+1}^i = \exp\left(-\Delta t/\tau_i\right)\mathbf{H}_n^i + \dfrac{1-\exp\left(-\Delta t/\tau_i\right)}{\Delta t/\tau_i}\left(\mathbf{S}_{n+1}^e - \mathbf{S}_n^e\right)$
3. find the total stress: $\mathbf{S}_{n+1} = \gamma_0 \mathbf{S}_{n+1}^e + \sum_{i=1}^{N} \gamma_i \mathbf{H}_{n+1}^i$

5.5. Hydraulic Permeability

Hydraulic permeability is a material function needed for biphasic and biphasic-solute materials.

5.5.1. Constant Isotropic Permeability

When the permeability is isotropic,

$$\mathbf{k} = k\,\mathbf{I}\,.$$

For this material model, k is constant. Generally, this assumption is only reasonable when strains are small.

5.5.2. Holmes-Mow

This isotropic material is similar to the constant isotropic permeability material described above, except that it uses a strain-dependent permeability tensor [34]:

$$\mathbf{k} = k\left(J\right)\mathbf{I}\,,$$

where,

$$k\left(J\right) = k_0\left(\frac{J-\varphi_0}{1-\varphi_0}\right)^{\alpha} e^{\frac{1}{2}M\left(J^2-1\right)}\,.$$

5.5.3. Referentially Isotropic Permeability

This material uses a strain-dependent permeability tensor that accommodates strain-induced anisotropy [21]:

$$\mathbf{k} = \left(k_{0r}\mathbf{I} + \frac{k_{1r}}{J^2}\mathbf{b} + \frac{k_{2r}}{J^4}\mathbf{b}^2\right)\left(\frac{J-\varphi_r^s}{1-\varphi_r^s}\right)e^{M\left(J^2-1\right)/2}\,,$$

Note that the permeability in the reference state $(\mathbf{F}=\mathbf{I})$ is isotropic and given by $\mathbf{k} = \left(k_{0r} + k_{1r} + k_{2r}\right)\mathbf{I}$.

5.5.4. Referentially Orthotropic Permeability

This material uses a strain-dependent permeability tensor that is orthotropic in the reference configuration, and accommodates strain-induced anisotropy [21]:

$$\mathbf{k} = k_0\mathbf{I} + \sum_{a=1}^{3} k_1^a\mathbf{m}_a + k_2^a\left(\mathbf{m}_a\cdot\mathbf{b} + \mathbf{b}\cdot\mathbf{m}_a\right),$$

where,

$$k_0 = k_{0r}\left(\frac{J-\varphi_r^s}{1-\varphi_r^s}\right)^{\alpha_0} e^{M_0\left(J^2-1\right)/2}$$

$$k_1^a = \frac{k_{1r}^a}{J^2}\left(\frac{J-\varphi_r^s}{1-\varphi_r^s}\right)^{\alpha_a} e^{M_a\left(J^2-1\right)/2}, \quad a=1,2,3$$

$$k_2^a = \frac{k_{2r}^a}{2J^4}\left(\frac{J-\varphi_r^s}{1-\varphi_r^s}\right)^{\alpha_a} e^{M_a\left(J^2-1\right)/2}, \quad a=1,2,3.$$

$\mathbf{m}_a$ are second order tensors representing the spatial structural tensors describing the orthogonal planes of symmetry, given by

$$\mathbf{m}_a = \mathbf{F}\cdot\left(\mathbf{V}_a \otimes \mathbf{V}_a\right)\cdot\mathbf{F}^T, \quad a=1-3,$$

where $\mathbf{V}_a$ are orthonormal vectors normal to the planes of symmetry. Note that the permeability in the reference state ($\mathbf{F}=\mathbf{I}$) is given by $\mathbf{k} = k_{0r}\mathbf{I} + \sum_{a=1}^{3}\left(k_{1r}^a + k_{2r}^a\right)\mathbf{V}_a \otimes \mathbf{V}_a$.

5.5.5. Referentially Transversely Isotropic Permeability

This material uses a strain-dependent permeability tensor that is transversely isotropic in the reference configuration, and accommodates strain-induced anisotropy [21]:

$$\begin{aligned}\mathbf{k} = {} & k_{0r}\left(\frac{J-\varphi_r^s}{1-\varphi_r^s}\right)^{\alpha_0} e^{M_0\left(J^2-1\right)/2}\mathbf{I} \\ & + \left(\frac{k_{1r}^T}{J^2}\left(\mathbf{b}-\mathbf{m}\right) + \frac{k_{2r}^T}{2J^4}\left[2\mathbf{b}^2 - \left(\mathbf{m}\cdot\mathbf{b}+\mathbf{b}\cdot\mathbf{m}\right)\right]\right)\left(\frac{J-\varphi_r^s}{1-\varphi_r^s}\right)^{\alpha_T} e^{M_T\left(J^2-1\right)/2} \\ & + \left(\frac{1}{J^2}k_{1r}^A\mathbf{m} + \frac{1}{2J^4}k_{2r}^A\left(\mathbf{m}\cdot\mathbf{b}+\mathbf{b}\cdot\mathbf{m}\right)\right)\left(\frac{J-\varphi_r^s}{1-\varphi_r^s}\right)^{\alpha_A} e^{M_A\left(J^2-1\right)/2},\end{aligned}$$

$\mathbf{m}$ is a second order tensor representing the spatial structural tensor describing the axial direction, given by

$$\mathbf{m} = \mathbf{F}\cdot\left(\mathbf{V}\otimes\mathbf{V}\right)\cdot\mathbf{F}^T,$$

where $\mathbf{V}$ is a unit vector along the axial direction. Note that the permeability in the reference state ($\mathbf{F}=\mathbf{I}$) is given by $\mathbf{k} = \left(k_{0r} + k_{1r}^T + k_{2r}^T\right)\mathbf{I} + \left(k_{1r}^A - k_{1r}^T + k_{2r}^A - k_{2r}^T\right)\left(\mathbf{V}\otimes\mathbf{V}\right)$.

5.6. Solute Diffusivity

Diffusivity materials provide a constitutive relation for the solute diffusivity in a biphasic-solute material. In general, the diffusivity tensor $\mathbf{d}$ may be a function of strain and solute concentration.

5.6.1. Constant Isotropic Diffusivity

When the permeability is isotropic,

$$\mathbf{d} = d\,\mathbf{I}\,.$$

For this material model, d is constant. This assumption is only true when strains are small. Note that the user must specify $d \le d_0$, where d_0 is the solute diffusivity in free solution, since a solute cannot diffuse through the biphasic-solute mixture faster than in free solution.

5.6.2. Constant Orthotropic Diffusivity

When the permeability is orthotropic,

$$\mathbf{d} = \sum_{a=1}^{3} d^a \mathbf{V}_a \otimes \mathbf{V}_a\,,$$

where $\mathbf{V}_a$ are orthonormal vectors normal to the planes of symmetry. For this material model, the d^a are constant. Therefore this model should be used only when strains are small. Note that the user must specify $d^a \le d_0$, where d_0 is the solute diffusivity in free solution, since a solute cannot diffuse through the biphasic-solute mixture faster than in free solution.

5.6.3. Referentially Isotropic Diffusivity

This material uses a strain-dependent diffusivity tensor that is isotropic in the reference configuration and accommodates strain-induced anisotropy:

$$\mathbf{d} = \left(d_{0r}\mathbf{I} + \frac{d_{1r}}{J^2}\mathbf{b} + \frac{d_{2r}}{J^4}\mathbf{b}^2 \right)\left(\frac{J-\varphi_r^s}{1-\varphi_r^s} \right) e^{M\left(J^2-1\right)/2}\,,$$

where J is the jacobian of the deformation, i.e. $J = \det \mathbf{F}$ where $\mathbf{F}$ is the deformation gradient, and $\mathbf{b} = \mathbf{F}\cdot\mathbf{F}^T$ is the left Cauchy-Green tensor. Note that the diffusivity in the reference state ($\mathbf{F} = \mathbf{I}$) is isotropic and given by $\mathbf{d} = \left(d_{0r} + d_{1r} + d_{2r}\right)\mathbf{I}$.

5.6.4. Referentially Orthotropic Diffusivity

This material uses a strain-dependent diffusivity tensor that is orthotropic in the reference configuration and accommodates strain-induced anisotropy:

$$\mathbf{d} = d_0\mathbf{I} + \sum_{a=1}^{3} d_1^a \mathbf{m}_a + d_2^a\left(\mathbf{m}_a\cdot\mathbf{b} + \mathbf{b}\cdot\mathbf{m}_a\right),$$

where,

$$d_0 = d_{0r}\left(\frac{J-\varphi_r^s}{1-\varphi_r^s}\right)^{\alpha_0} e^{M_0\left(J^2-1\right)/2}$$

$$d_1^a = \frac{d_{1r}^a}{J^2}\left(\frac{J-\varphi_r^s}{1-\varphi_r^s}\right)^{\alpha_a} e^{M_a\left(J^2-1\right)/2}, \quad a=1,2,3 \ ,$$

$$d_2^a = \frac{d_{2r}^a}{2J^4}\left(\frac{J-\varphi_r^s}{1-\varphi_r^s}\right)^{\alpha_a} e^{M_a\left(J^2-1\right)/2}, \quad a=1,2,3$$

J is the Jacobian of the deformation, i.e. $J=\det\mathbf{F}$ where $\mathbf{F}$ is the deformation gradient. $\mathbf{m}_a$ are second order tensor representing the spatial structural tensors describing the orthogonal planes of symmetry, given by

$$\mathbf{m}_a = \mathbf{F}\cdot\left(\mathbf{V}_a\otimes\mathbf{V}_a\right)\cdot\mathbf{F}^T, \quad a=1-3,$$

where $\mathbf{V}_a$ are orthonormal vectors normal to the planes of symmetry. Note that the permeability in the reference state ($\mathbf{F}=\mathbf{I}$) is given by $\mathbf{k}=k_{0r}\mathbf{I}+\sum_{a=1}^{3}\left(k_{1r}^a+k_{2r}^a\right)\mathbf{V}_a\otimes\mathbf{V}_a$.

5.7. Solute Solubility

Solubility constitutive equations provide a relation for $\tilde{\kappa}$ as a function of solid matrix strain and solute concentration.

5.7.1. Constant Solubility

For this material model, $\tilde{\kappa}$ is constant.

5.8. Osmotic Coefficient

Solubility constitutive equations provide a relation for Φ as a function of solid matrix strain and solute concentration.

5.8.1. Constant Osmotic Coefficient

For this material model, Φ is constant.

5.9. Active Contraction Model

A time varying "elastance" active contraction model [46] was added to the transversely isotropic materials. When active contraction is activated, the total Cauchy stress $\boldsymbol{\sigma}$ is defined as the sum of the active stress tensor $\boldsymbol{\sigma}^a = T^a \mathbf{a} \otimes \mathbf{a}$ and the passive stress tensor $\boldsymbol{\sigma}^p$:

$$\boldsymbol{\sigma} = \boldsymbol{\sigma}^p + \boldsymbol{\sigma}^a, \tag{5.76}$$

where $\boldsymbol{a}$ is the deformed fiber vector (unit length), defined as $\lambda \mathbf{a} = \mathbf{F} \cdot \mathbf{a}$. The time varying elastance model is a modification of the standard Hill equation that scales the standard equation by an activation curve $C(t)$. The active fiber stress T^a is defined as:

$$T^a = T_{\max} \frac{Ca_0^2}{Ca_0^2 + ECa_{50}^2} C(t), \tag{5.77}$$

where T_{max} = 135.7 KPa is the isometric tension under maximal activation at the peak intracellular calcium concentration of Ca_0 = 4.35 μM. The length dependent calcium sensitivity is governed by the following equation:

$$ECa_{50} = \frac{(Ca_o)_{\max}}{\sqrt{\exp\left[B(l - l_0)\right] - 1}}, \tag{5.78}$$

where $(Ca_0)_{max}$ = 4.35 μM is the maximum peak intracellular calcium concentration, $B = 4.75$ μm^{-1} governs the shape of the peak isometric tension-sarcomere length relation, l_0 = 1.58 μm is the sarcomere length at which no active tension develops, and l is the sarcomere length which is the product of the fiber stretch λ and the sarcomere unloaded length $l_r = 2.04$ μm.

Chapter 6. Contact and Coupling

FEBio allows the user to connect the different parts of the model in various ways. Deformable parts can be connected to rigid bodies. Deformable objects can be brought in contact with each other. Rigid bodies can be connected with rigid joints. This chapter describes the different ways to couple parts together.

6.1. Rigid-Deformable Coupling

In FEBio deformable meshes can be coupled with rigid bodies. The coupling requires a modification of the global stiffness matrix. Additionally, degrees of freedom need to be introduced for the rigid bodies [47]. This section describes the coupling between rigid and deformable bodies.

6.1.1. Kinematics

The position vector **x** of a finite element node may be denoted as,

$$\mathbf{x} = \mathbf{X} + \mathbf{u}\,, \tag{6.1}$$

where **X** is the initial position of the node and **u** the displacement vector. If this node is connected to a rigid body the position can alternatively be written as,

$$\mathbf{x} = \mathbf{r} + \mathbf{a}\,, \tag{6.2}$$

where **r** is the current position of the center of mass of the rigid body and **a** is the relative position of the node to the center of mass. The vector **a** may be written in terms of its initial value $\mathbf{a}_0$ in the undeformed state and a rotation matrix,

$$\mathbf{a} = \mathbf{Q}\mathbf{a}_0\,. \tag{6.3}$$

In an incremental displacement formulation equation (6.2) must be linearized:

$$\Delta\mathbf{u} = \Delta\mathbf{r} + \Delta\mathbf{Q}\mathbf{a}_0\,, \tag{6.4}$$

where the linearization of the rotation matrix can be expressed in a more convenient form,

$$\Delta\mathbf{Q} = \hat{\mathbf{a}}\Delta\boldsymbol{\theta}\,. \tag{6.5}$$

Here is $\Delta\boldsymbol{\theta}^T = \left[\Delta\theta_1, \Delta\theta_2, \Delta\theta_3\right]$ and the matrix $\hat{\mathbf{a}}$ is

$$\hat{\mathbf{a}} = \begin{bmatrix} 0 & a_3 & -a_2 \\ -a_3 & 0 & a_1 \\ a_2 & -a_1 & 0 \end{bmatrix}. \tag{6.6}$$

For a model containing both deformable and rigid nodes the nodal degrees of freedom may be grouped, and the above expressions used to obtain a condensed set of unknowns:

$$\begin{Bmatrix} \Delta\mathbf{u}^D \\ \Delta\mathbf{u}^R \end{Bmatrix} = \begin{bmatrix} \mathbf{I} & \mathbf{0} & \mathbf{0} \\ \mathbf{0} & \mathbf{I} & \hat{\mathbf{a}} \end{bmatrix} \begin{Bmatrix} \Delta\mathbf{u}^D \\ \Delta\mathbf{r} \\ \Delta\boldsymbol{\theta} \end{Bmatrix} = \mathbf{A}\Delta\tilde{\mathbf{u}}\,. \tag{6.7}$$

Substituting this into the discrete form of the principle of virtual work yields expressions for the condensed finite element stiffness matrix and residual vector for the coupled rigid-deformable system:

$$\tilde{\mathbf{K}}\Delta\tilde{\mathbf{u}} = -\tilde{\mathbf{R}}, \quad \tilde{\mathbf{K}} = \mathbf{A}^T\mathbf{K}\mathbf{A}, \quad \tilde{\mathbf{R}} = \mathbf{A}^T\mathbf{R}\,. \tag{6.8}$$

6.1.2. A single rigid body

The global system of equations can now be written as follows (for a single rigid body coupled to a deformable body),

$$\begin{bmatrix} \mathbf{K}^D & \mathbf{K}^{DR} \\ \left(\mathbf{K}^{DR}\right)^T & \mathbf{K}^R \end{bmatrix} \begin{Bmatrix} \Delta\mathbf{u}^D \\ \Delta\mathbf{r} \\ \Delta\boldsymbol{\theta} \end{Bmatrix} = -\begin{Bmatrix} \mathbf{R}^D \\ \mathbf{F}^R \\ \mathbf{M}^R \end{Bmatrix}. \tag{6.9}$$

Here $\mathbf{F}^R$ is formed by adding all the residual vectors of all interface nodes that connect the deformable body to the rigid body,

$$\mathbf{F}^R = \sum_i \mathbf{R}_i^D , \tag{6.10}$$

where i sums over all interface nodes, and

$$\mathbf{M}^R = \sum_i \hat{\mathbf{a}}_i \mathbf{R}_i^D . \tag{6.11}$$

It is recognized that $\mathbf{F}^R$ is simply the total residual force that is applied to the rigid body and $\mathbf{M}^R$ is the total residual torque.

Constructing the stiffness matrix is accomplished in a similar manner. Assume n nodes per element, then the normal element stiffness matrix (in absence of rigid nodes) is given by,

$$\mathbf{k}^{(e)} = \begin{bmatrix} \mathbf{k}_{11} & \cdots & \mathbf{k}_{1n} \\ \vdots & \ddots & \vdots \\ \mathbf{k}_{n1} & \cdots & \mathbf{k}_{nn} \end{bmatrix}, \tag{6.12}$$

where $\mathbf{k}_{ij}$ is the nodal stiffness matrix connecting node i to node j. These nodal stiffness matrices are now assembled into the global stiffness matrix. If node i and j are neither interface nodes their nodal stiffness matrix is assembled into $\mathbf{K}^D$ in the usual manner,

$$\mathbf{K}^D = \sum_e \mathbf{k}_{ij}^{(e)} , \tag{6.13}$$

where the sum now has to interpreted as the finite element assembly operator.

If node j is an interface node, than the nodal stiffness matrix gets assembled in the $\mathbf{K}^{DR}$ matrix:

$$\mathbf{K}^{DR} = \sum_e \left[\mathbf{k}_{ij}^{(e)} \quad \mathbf{k}_{ij}^{(e)} \hat{\mathbf{a}}_j \right]. \tag{6.14}$$

If both nodes belong to the rigid body than the nodal element matrix gets assembled in $\mathbf{K}^R$ as follows,

$$\mathbf{K}^R = \sum_e \begin{bmatrix} \mathbf{k}_{ij}^{(e)} & \mathbf{k}_{ij}^{(e)} \hat{\mathbf{a}}_j \\ \hat{\mathbf{a}}_i^T \mathbf{k}_{ij}^{(e)T} & \hat{\mathbf{a}}_i^T \mathbf{k}_{ij}^{(e)} \hat{\mathbf{a}}_j \end{bmatrix}. \tag{6.15}$$

6.1.3. Multiple Rigid Bodies

The previous results can easily be extended if there are multiple rigid bodies. The following section presents the approach for two rigid bodies, but the results can easily be generalized to N rigid bodies.

For two rigid bodies, the global system of equations takes the following form,

$$\begin{bmatrix} \mathbf{K}^D & \mathbf{K}_1^{DR} & \mathbf{K}_2^{DR} \\ \left(\mathbf{K}_1^{DR}\right)^T & \mathbf{K}_{11}^R & \mathbf{K}_{12}^R \\ \left(\mathbf{K}_2^{DR}\right)^T & \mathbf{K}_{21}^R & \mathbf{K}_{22}^R \end{bmatrix} \begin{Bmatrix} \Delta\mathbf{u}^D \\ \Delta\mathbf{r}_1 \\ \Delta\boldsymbol{\theta}_1 \\ \Delta\mathbf{r}_2 \\ \Delta\boldsymbol{\theta}_2 \end{Bmatrix} = -\begin{Bmatrix} \mathbf{R}^R \\ \mathbf{F}_1 \\ \mathbf{M}_1 \\ \mathbf{F}_2 \\ \mathbf{M}_2 \end{Bmatrix}. \tag{6.16}$$

Care must be taken to assemble the nodal stiffness matrix in the correct global sub-matrix. If node *i* is not an interface node and node *j* is connected to rigid body 1, then their nodal stiffness matrix goes into $\mathbf{K}_1^{DR}$. If, however, node *j* is attached to rigid body 2 then their nodal stiffness matrix goes into $\mathbf{K}_2^{DR}$. If node *i* is connected to rigid body 1 and node *j* is connected to rigid body 2, then their nodal stiffness matrix goes into $\mathbf{K}_{12}^R$, and so on. Note that it is assumed here that a node may only connect to a single rigid body.

6.2. Rigid Joints

A rigid joint is a location in space where two rigid bodies connect. The joint enforces a constraint on the system. This constraint can be written as,

$$\mathbf{c}\left(\mathbf{Y}^c\right) = \varphi^{(1)}\left(\mathbf{Y}^c\right) - \varphi^{(2)}\left(\mathbf{Y}^c\right) = \mathbf{0} \tag{6.17}$$

Here $\mathbf{Y}^c$ is the location of the joint in the reference configuration and $\varphi^{(i)}\left(i=1,2\right)$ is the deformation map of rigid body *i*. Equation (6.17) is a constraint equation that will be added to the total balance of virtual work.

$$G\left(\varphi, w\right) = \sum_{i=1}^{2} G^{\text{int},ext}\left(\varphi^{(i)}, w^{(i)}\right) - \underbrace{\sum_{i=1}^{2} w^{(i)}\left(\mathbf{Y}^c\right)\cdot\mathbf{T}^{(i)}}_{G^c} = 0 \tag{6.18}$$

Here, the $\mathbf{T}^{(i)}$'s are the forces that will prevent the rigid bodies to separate at the joint position and $w^{(i)} = \delta\varphi^{(i)}$. First we note that due to the third law of Newton $\mathbf{T}^{(1)} = -\mathbf{T}^{(2)}$, so that we can write the constraint term as,

$$G^c\left(\varphi, w\right) = -\mathbf{T}^{(1)}\cdot\left(w^{(1)} - w^{(2)}\right)\left(\mathbf{Y}^c\right) \tag{6.19}$$

Note that we can also write this as,

$$G^c\left(\varphi, w\right) = -\mathbf{T}^{(1)}\cdot\delta\mathbf{c} \tag{6.20}$$

The constraint forces are determined by the augmented Lagrangian method and are given by,

$$\mathbf{T} = \boldsymbol{\lambda} + \varepsilon_c \mathbf{c} \tag{6.21}$$

where $\boldsymbol{\lambda}$ is the Lagrange multiplier and ε_c is a user defined penalty factor.
The linearization of (6.20) is given by,

$$\begin{aligned} \Delta G^c(\varphi, w) &= -\Delta\left(\varepsilon_c \mathbf{c} \cdot \delta\mathbf{c}\right) \\ &= -\varepsilon_c \Delta\mathbf{c} \cdot \delta\mathbf{c} \end{aligned} \tag{6.22}$$

Using the rigid body assumption, the quantity $\Delta\mathbf{c}$ can be written as follows,

$$\begin{aligned} \Delta\mathbf{c} &= \Delta\varphi^{(1)}\left(\mathbf{Y}^c\right) - \Delta\varphi^{(2)}\left(\mathbf{Y}^c\right) \\ &= \Delta\mathbf{r}_1 + \hat{\mathbf{y}}_1^c \Delta\boldsymbol{\theta}_1 - \Delta\mathbf{r}_2 - \hat{\mathbf{y}}_2^c \Delta\boldsymbol{\theta}_2 \end{aligned} \tag{6.23}$$

And similarly for $\delta\mathbf{c}$. If we now introduce the vectors,

$$\delta\Phi = \begin{bmatrix} \delta\mathbf{r}_1 \\ \delta\boldsymbol{\theta}_1 \\ \delta\mathbf{r}_2 \\ \delta\boldsymbol{\theta}_2 \end{bmatrix} \quad \mathbf{N} = \begin{bmatrix} \mathbf{T} \\ \hat{\mathbf{y}}_1^T \mathbf{T} \\ -\mathbf{T} \\ -\hat{\mathbf{y}}_2^T \mathbf{T} \end{bmatrix} \tag{6.24}$$

Then we can write the constraint work as,

$$G^c = -\delta\boldsymbol{\Phi}^T \mathbf{N} \tag{6.25}$$

And the stiffness contribution as,

$$\Delta G^c = -\delta\boldsymbol{\Phi}^T \mathbf{K}^c \Delta\boldsymbol{\Phi} \tag{6.26}$$

$$\mathbf{K}^c = \varepsilon_c \begin{bmatrix} \mathbf{I} & \hat{\mathbf{y}}_1 & -\mathbf{I} & -\hat{\mathbf{y}}_2 \\ \hat{\mathbf{y}}_1^T & \hat{\mathbf{y}}_1^T \mathbf{y}_1 & -\mathbf{y}_1^T & -\mathbf{y}_1^T \mathbf{y}_2 \\ -\mathbf{I} & -\mathbf{y}_1 & \mathbf{I} & \mathbf{y}_2 \\ -\mathbf{y}_2^T & -\mathbf{y}_2^T \mathbf{y}_1 & \mathbf{y}_2^T & \mathbf{y}_2^T \mathbf{y}_2 \end{bmatrix} \tag{6.27}$$

6.3. Sliding Interfaces

This section summarizes the theoretical developments of the two body contact problem. After introducing some notation and terminology, the contact integral is presented, which contains the contribution to the virtual work equation from the contact tractions. Since the nonlinear contact problem is solved using a Newton based iterative method, the contact integral is linearized. Next, anticipating a finite element implementation, the contact integral and its linearization are

discretized using a standard finite element approach. Finally the augmented Lagrangian method for enforcing the contact constraints is described.

6.3.1. Contact Kinematics

For the most part the notation of this section follows [48], with a few simplifications here and there since the implementation in FEBio is currently for quasi-static, frictionless, two body contact problem.

The volume occupied by body *i* in the reference configuration is denoted by $\Omega^{(i)} \subset \mathbb{R}^3$ where $i = 1,2$. The boundary of body *i* is denoted by $\Gamma^{(i)}$ and is divided into three regions $\Gamma^{(i)} = \Gamma_\sigma^{(i)} \bigcup \Gamma_u^{(i)} \bigcup \Gamma_c^{(i)}$, where $\Gamma_\sigma^{(i)}$ is the boundary where tractions are applied, $\Gamma_u^{(i)}$ the boundary where the solution is prescribed and $\Gamma_c^{(i)}$ the part of the boundary that will be in contact with the other body. It is assumed that $\Gamma_\sigma^{(i)} \bigcap \Gamma_u^{(i)} \bigcap \Gamma_c^{(i)} = \varnothing$.

The deformation of body *i* is defined by $\varphi^{(i)}$. The boundary of the deformed body *i*, that is the boundary of $\varphi^{(i)}\left(\Omega^{(i)}\right)$ is denoted by $\gamma^{(i)} = \gamma_\sigma^{(i)} \bigcup \gamma_u^{(i)} \bigcup \gamma_c^{(i)}$ where $\gamma_\sigma^{(i)} = \varphi^{(i)}\left(\Gamma_\sigma^{(i)}\right)$ is the boundary in the current configuration where the tractions are applied and similar definitions for $\gamma_u^{(i)}$ and $\gamma_c^{(i)}$. See the figure below for a graphical illustration of the defined regions.

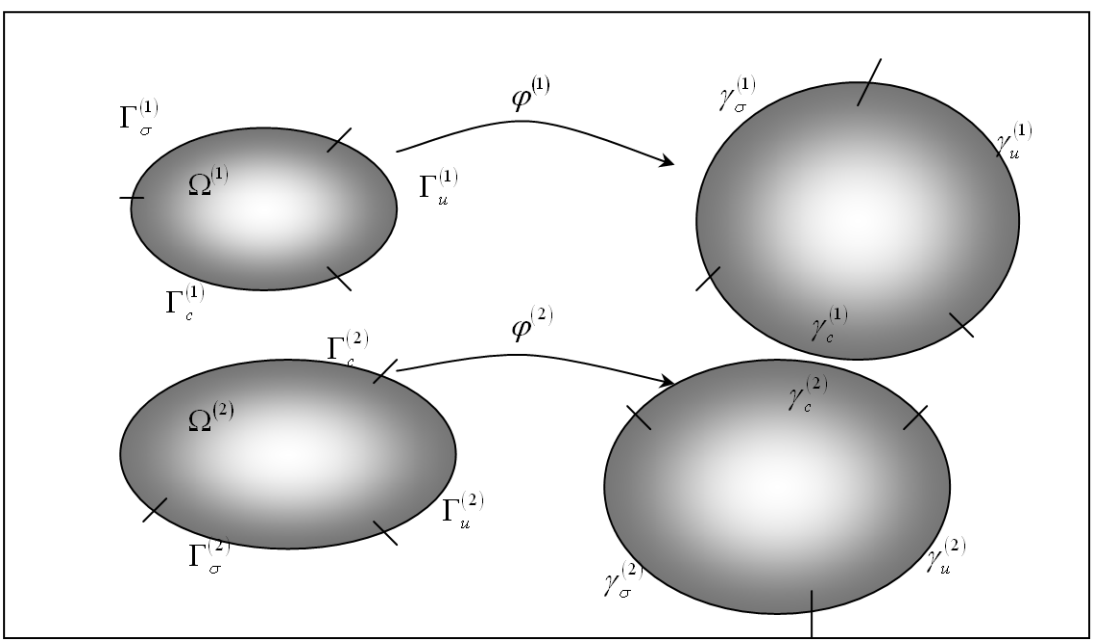

Figure 6-1. The two-body contact problem.

Points in body 1 are denoted by **X** in the reference configuration and **x** in the current configuration. For body 2 these points are denoted by **Y** and **y**. To define contact, the location where the two bodies are in contact with each other must be established. If body 1 is the *slave*

body and body 2 is the *master body*, then for a given point $\mathbf{X}$ on the slave reference contact surface there is a point $\bar{\mathbf{Y}}(\mathbf{X})$ on the master contact surface that is in some sense closest to point $\mathbf{X}$. This closest point is defined in a closest point projection sense:

$$\bar{\mathbf{Y}}(\mathbf{X}) = \arg\min_{\mathbf{Y}\in\Gamma_c^{(2)}} \left\| \varphi^{(1)}(\mathbf{X}) - \varphi^{(2)}(\mathbf{Y}) \right\|. \tag{6.28}$$

With the definition of $\bar{\mathbf{Y}}(\mathbf{X})$ established the *gap function* can be defined, which is a measure for the distance between $\mathbf{X}$ and $\bar{\mathbf{Y}}(\mathbf{X})$,

$$g(\mathbf{X}) = -\mathbf{v}\cdot\left(\varphi^{(1)}(\mathbf{X}) - \varphi^{(2)}\left(\bar{\mathbf{Y}}(\mathbf{X})\right)\right), \tag{6.29}$$

where $\mathbf{v}$ is the local surface normal of surface $\gamma_c^{(2)}$ evaluated at $\bar{\mathbf{y}} = \varphi^{(2)}\left(\bar{\mathbf{Y}}(\mathbf{X})\right)$. Note that $g > 0$ when $\mathbf{X}$ has penetrated body 2, so that the constraint condition to be satisfied at all time is $g \le 0$.

6.3.2. Weak Form of Two Body Contact

The balance of linear momentum can be written for each of the two bodies in the reference configuration,

$$G^{(i)}\left(\varphi^{(i)}, w^{(i)}\right) = \int_{\Omega^{(i)}} GRAD\left[w^{(i)}\right] : \mathbf{P}^{(i)} d\Omega - \int_{\Omega^{(i)}} w^{(i)}\cdot\mathbf{F}^{(i)} d\Omega - \int_{\Gamma_s^{(i)}} w^{(i)}\cdot\mathbf{T}^{(i)} d\Gamma - \int_{\Gamma_c^{(i)}} w^{(i)}\cdot\mathbf{T}^{(i)} d\Gamma = 0 \tag{6.30}$$

where $w^{(i)}$ is a weighting function and $\mathbf{P}$ is the 1st Piola-Kirchhoff stress tensor. The last term corresponds to the virtual work of the contact tractions on body *i*. For notational convenience, the notations φ and w are introduced to denote the collection of the respective mappings $\varphi^{(i)}$ and $w^{(i)}$ (for i=1,2). In other words,

$$\begin{aligned} \varphi &: \bar{\Omega}^{(1)} \bigcup \bar{\Omega}^{(2)} \to \mathbb{R}^3 \\ w &: \bar{\Omega}^{(1)} \bigcup \bar{\Omega}^{(2)} \to \mathbb{R}^3 \end{aligned}. \tag{6.31}$$

The variational principle for the two body system is the sum of (6.30) for body 1 and 2 and can be expressed as,

$$\begin{aligned} G(\varphi, w) &:= \sum_{i=1}^{2} G^{(i)}\left(\varphi^{(i)}, w^{(i)}\right) \\ &= \underbrace{\sum_{i=1}^{2}\left\{\int_{\Omega^{(i)}} GRAD\left[w^{(i)}\right] : \mathbf{P}^{(i)} d\Omega - \int_{\Omega^{(i)}} w^{(i)}\cdot\mathbf{F}^{(i)} d\Omega - \int_{\Gamma_s^{(i)}} w^{(i)}\cdot\mathbf{T}^{(i)} d\Gamma\right\}}_{G^{\text{int},ext}(\varphi,w)} \\ &\quad \underbrace{-\sum_{i=1}^{2}\int_{\Gamma_c^{(i)}} w^{(i)}\cdot\mathbf{T}^{(i)} d\Gamma}_{G^{c}(\varphi,w)} \end{aligned} \tag{6.32}$$

Or in short,

$$G(\varphi, w) = G^{\text{int},ext}(\varphi, w) + G^{c}(\varphi, w). \tag{6.33}$$

Note that the minus sign is included in the definition of the contact integral G^c. The contact integral can be written as an integration over the contact surface of body 1 by balancing linear momentum across the contact surface:

$$\mathbf{t}^{(2)}\left(\bar{\mathbf{y}}\left(\mathbf{x}\right)\right)d\Gamma^{(2)} = -\mathbf{t}^{(1)}\left(\mathbf{x}\right)d\Gamma^{(1)}. \tag{6.34}$$

The contact integral can now be rewritten over the contact surface of body 1:

$$G^c = -\int_{\Gamma_c^{(1)}} \mathbf{t}^{(1)}\left(\mathbf{x}\right)\cdot\left[w^{(1)}\left(\mathbf{x}\right) - w^{(2)}\left(\bar{\mathbf{y}}\left(\mathbf{x}\right)\right)\right]d\Gamma. \tag{6.35}$$

In the case of frictionless contact, the contact traction is taken as perpendicular to surface 2 and therefore can be written as, $\mathbf{t}^{(1)} = t_N\mathbf{v}$ where $\mathbf{v}$ is the (outward) surface normal and t_N is to be determined from the solution strategy. For example in a Lagrange multiplier method the t_N's would be the Lagrange multipliers.

By noting that the variation of the gap function is given by

$$\delta g = -\mathbf{v}\cdot\left(w^{(1)}\left(\mathbf{x}\right) - w^{(2)}\left(\bar{\mathbf{y}}\left(\mathbf{x}\right)\right)\right), \tag{6.36}$$

equation (6.35) can be simplified as,

$$G^c = \int_{\Gamma_c^{(1)}} t_N\delta g d\Gamma. \tag{6.37}$$

6.3.3. Linearization of the Contact Integral

In a Newton-Raphson implementation the contact integral must be linearized with respect to the current configuration:

$$\Delta G^c\left(\varphi, w\right) = \int_{\Gamma_c^{(1)}} \Delta\left(t_N\delta g\right)d\Gamma. \tag{6.38}$$

Examining the normal contact term first, the directional derivative of t_N is given (for the case of the penalty regularization) by:

$$\begin{aligned}\Delta t_N &= \Delta\left\{\varepsilon_N\left\langle g\right\rangle\right\} \\ &= H\left(g\right)\varepsilon_N\Delta g\end{aligned}, \tag{6.39}$$

where ε_N is the penalty factor and $H\left(g\right)$ is the Heaviside function. The quantity $\Delta\left(\delta g\right)$ is given by,

$$\begin{aligned}\Delta\left(\delta g\right) = g\Big[&\mathbf{v}\cdot\delta\varphi_{,\gamma}^{(2)}\left(\bar{\mathbf{Y}}\left(\mathbf{X}\right)\right) + \kappa_{\alpha\gamma}\left(\bar{\mathbf{Y}}\left(\mathbf{X}\right)\right)\delta\bar{\xi}_\alpha\Big]m^{\gamma\beta} \\ &\Big[\mathbf{v}\cdot\Delta\varphi_{,\beta}^{(2)}\left(\bar{\mathbf{Y}}\left(\mathbf{X}\right)\right) + \kappa_{\alpha\beta}\left(\bar{\mathbf{Y}}\left(\mathbf{X}\right)\right)\Delta\bar{\xi}^\alpha\Big] \\ &+\delta\bar{\xi}^\beta\mathbf{v}\cdot\left[\Delta\varphi_{,\beta}^{(2)}\left(\bar{\mathbf{Y}}\left(\mathbf{X}\right)\right)\right] + \Delta\bar{\xi}^\beta\mathbf{v}\cdot\left[\delta\varphi_{,\beta}^{(2)}\left(\bar{\mathbf{Y}}\left(\mathbf{X}\right)\right)\right] \\ &+\kappa_{\alpha\beta}\left(\bar{\mathbf{Y}}\left(\mathbf{X}\right)\right)\delta\bar{\xi}^\beta\Delta\bar{\xi}^\alpha\end{aligned}. \tag{6.40}$$

6.3.4. Discretization of the Contact Integral

The contact integral, which is repeated here,

$$G^c(\varphi, w) = \int_{\Gamma^{(1)}} t_N \delta g d\Gamma, \tag{6.41}$$

will now be discretized using a standard finite element procedure. First it is noted that the integration can be written as a sum over the surface element areas:

$$G^c(\varphi, w) = \sum_{e=1}^{N_{sel}} \int_{\Gamma^{(1)e}} t_N \delta g d\Gamma, \tag{6.42}$$

where N_{sel} is the number of surface elements. The integration can be approximated using a quadrature rule,

$$G^c(\varphi, w) \cong \sum_{e=1}^{N_{sel}} \left\{ \sum_{i=1}^{N_{\text{int}}^e} w^i j(\xi_i) t_N(\xi_i) \delta g(\xi_i) \right\}, \tag{6.43}$$

where N_{int}^e are the number of integration points for element *e*. It is now assumed that the integration points coincide with the element's nodes (e.g. for a quadrilateral surface element we have $\xi_1 = (-1,-1)$, $\xi_2 = (1,-1)$, $\xi_3 = (1,1)$ and $\xi_4 = (-1,1)$). With this quadrature rule, we have

$$\begin{aligned} w^{(1)}(\xi_i) &= \mathbf{c}_i^{(1)} \\ w^{(2)}(\bar{\xi}_i) &= \sum_{j=1}^{n} N_j(\bar{\xi}_i) \mathbf{c}_j^{(2)} \end{aligned}, \tag{6.44}$$

so that,

$$\delta g(\xi_i) = -\mathbf{v} \cdot \left(\mathbf{c}_i^{(1)} - \sum_{j=1}^{n} N_j^{(2)}(\bar{\xi}_i) \mathbf{c}_j^{(2)} \right). \tag{6.45}$$

If the following vectors are defined,

$$\begin{aligned} \delta \mathbf{\Phi}^T &= \left[\mathbf{c}_i^{(1)}, \quad \mathbf{c}_1^{(2)}, \quad \cdots, \quad \mathbf{c}_n^{(2)} \right] \\ \mathbf{N}^T &= \left[\mathbf{v}, \quad -\mathbf{v} N_1^{(2)}, \quad \cdots, \quad -\mathbf{v} N_n^{(2)} \right] \end{aligned}, \tag{6.46}$$

equation (6.43) can then be rewritten as follows,

$$G^c(\varphi, \delta \mathbf{v}) \cong \sum_{e=1}^{N_{sel}} \left\{ \sum_{i=1}^{N_{\text{int}}^e} w^i j(\xi_i) t_N(\xi_i) \delta \mathbf{\Phi}^T \mathbf{N}^T \right\}. \tag{6.47}$$

The specific form for t_N will depend on the method employed for enforcing the contact constraint.

6.3.5. Discretization of the Contact Stiffness

A similar procedure can now be used to calculate the discretized contact stiffness matrix. The linearization of the contact integral is repeated here:

$$\begin{aligned}\Delta G^c(\varphi,w) &= \sum_{e=1}^{N_{sel}} \int_{\Gamma^{(1)e}} \Delta\left(t_N \delta g\right) d\Gamma \\ &= \sum_{e=1}^{N_{sel}} \sum_{i=1}^{N_{\text{int}}^e} w_i\, j\left(\xi_i\right) \Delta\left(t_N \delta g\right)\left(\xi_i\right)\end{aligned} . \tag{6.48}$$

Using matrix notation we can rewrite equation (6.48) as,

$$\Delta W^c(\varphi,\delta\mathbf{v}) = \sum_{e=1}^{N_{sel}} \sum_{i}^{N_{\text{int}}^e} w_i\, j\left(\xi_i\right) \delta\mathbf{\Phi}\cdot\mathbf{k}^c \Delta\mathbf{\Phi}\,, \tag{6.49}$$

where $\delta\mathbf{\Phi}$ is as above and $\Delta\mathbf{\Phi}$ similar to $\delta\mathbf{\Phi}$ with δ replaced with Δ and $\mathbf{k}^c$,

$$\begin{aligned}\mathbf{k}^c &= \varepsilon_N H\left(\lambda_N^k + \varepsilon_N g\right)\mathbf{N}\mathbf{N}^T + t_N \Big\{ g\Big[m^{11}\bar{\mathbf{N}}_1\bar{\mathbf{N}}_1^T \\ &+ m^{12}\left(\bar{\mathbf{N}}_1\bar{\mathbf{N}}_2^T + \bar{\mathbf{N}}_2\bar{\mathbf{N}}_1^T\right) + m^{22}\bar{\mathbf{N}}_2\bar{\mathbf{N}}_2^T\Big] - \mathbf{D}_1\mathbf{N}_1^T \\ &- \mathbf{D}_2\mathbf{N}_2^T - \mathbf{N}_1\mathbf{D}_1^T - \mathbf{N}_2\mathbf{D}_2^T + \kappa_{12}\left(\mathbf{D}_1\mathbf{D}_2^T + \mathbf{D}_2\mathbf{D}_1^T\right)\Big\}\end{aligned} , \tag{6.50}$$

where,

$$\mathbf{N} = \begin{bmatrix} \mathbf{v} \\ -N_1\left(\bar{\xi}\right)\mathbf{v} \\ \vdots \\ -N_4\left(\bar{\xi}\right)\mathbf{v} \end{bmatrix}, \quad \mathbf{T}_\alpha = \begin{bmatrix} \boldsymbol{\tau}_\alpha \\ -N_1\left(\bar{\xi}\right)\boldsymbol{\tau}_\alpha \\ \vdots \\ -N_4\left(\bar{\xi}\right)\boldsymbol{\tau}_\alpha \end{bmatrix}, \quad \mathbf{N}_\alpha = \begin{bmatrix} \mathbf{0} \\ -N_{1,\alpha}\left(\bar{\xi}\right)\mathbf{v} \\ \vdots \\ -N_{4,\alpha}\left(\bar{\xi}\right)\mathbf{v} \end{bmatrix}. \tag{6.51}$$

The following vectors are also defined which depend on the vectors of (6.51):

$$\begin{aligned}\mathbf{D}_1 &= \frac{1}{\det\mathbf{A}}\left[A_{22}\left(\mathbf{T}_1 + g\mathbf{N}_1\right) - A_{12}\left(\mathbf{T}_2 + g\mathbf{N}_2\right)\right] \\ \mathbf{D}_2 &= \frac{1}{\det\mathbf{A}}\left[A_{11}\left(\mathbf{T}_2 + g\mathbf{N}_2\right) - A_{12}\left(\mathbf{T}_1 + g\mathbf{N}_1\right)\right], \\ \bar{\mathbf{N}}_1 &= \mathbf{N}_1 - \kappa_{12}\mathbf{D}_2 \\ \bar{\mathbf{N}}_2 &= \mathbf{N}_2 - \kappa_{12}\mathbf{D}_1\end{aligned} \tag{6.52}$$

where the matrix $\mathbf{A}$ is defined as,

$$A_{ij} = m_{ij} + g\kappa_{ij}\,. \tag{6.53}$$

Here, $m_{ij} = \boldsymbol{\tau}_i \cdot \boldsymbol{\tau}_j$ is the surface metric tensor and $\kappa_{ij} = \mathbf{v}\cdot\varphi_{t,ij}^{(2)}\left(\bar{\mathbf{Y}}\right)$ denotes the components of the surface curvature at $\bar{\xi}$.

6.3.6. Augmented Lagrangian Method

The augmented Lagrangian method is used in FEBio to enforce the contact constraints to a user-specified tolerance. This implies that the normal contact tractions are given by,

$$t_N = \left\langle \lambda_N + \varepsilon_N g \right\rangle. \tag{6.54}$$

Note that this assumption is consistent with the approach that was used in establishing the discretization of the linearization of the contact integral (6.50). In (6.54) ε_N is a penalty factor that is chosen arbitrarily.

The Newton-Raphson iterative method is now used to solve the nonlinear contact problem where Uzawa's method (REF) is employed to calculate the Lagrange multipliers λ_N. This implies that the Lagrange multipliers are kept fixed during the Newton-Raphson iterations. After convergence the multipliers are updated and a new NR procedure is started. This procedure can be summarized by the following four steps.

1. **Initialize** the augmented Lagrangian iteration counter *k*, and the initial guesses for the multipliers:
$$\begin{aligned} \lambda_{N_{n+1}}^{(0)} &= \lambda_{N_n} \\ k &= 0 \end{aligned} . \tag{6.55}$$
2. **Solve** for $\mathbf{d}_{n+1}^{(k)}$, the solution vector corresponding to the fixed *k*th iterate for the multipliers,
$$\mathbf{F}^{\text{int}}\left(\mathbf{d}_{n+1}^{(k)}\right) + \mathbf{F}^{c}\left(\mathbf{d}_{n+1}^{(k)}\right) = \mathbf{F}_{n+1}^{ext}, \tag{6.56}$$

   where the contact tractions used to compute $\mathbf{F}^c$, the contact force, are governed by
$$t_{N_{n+1}}^{(k)} = \left\langle \lambda_{N_{n+1}}^{(k)} + \varepsilon_N g_{n+1}^{k} \right\rangle . \tag{6.57}$$
3. **Update** the Lagrange multipliers and iteration counters:
$$\begin{aligned} \lambda_{N_{n+1}}^{(k+1)} &= \left\langle \lambda_{N_{n+1}}^{(k)} + \varepsilon_N g_{n+1}^{(k)} \right\rangle \\ k &= k+1 \end{aligned} . \tag{6.58}$$
4. **Return** to the solution phase.

Steps 2-4 of the above algorithm are generally repeated until all contact constraints are satisfied to a user-specified tolerance or little change in the solution vector from augmentation to augmentation is noted.

6.3.7. Automatic penalty calculation

The determination of the penalty factor ε_N can be a difficult task, since a good value may depend on both material parameters and geometrical factors. In FEBio the value of this penalty factor can be determined automatically. In this case FEBio will calculate a penalty factor for each facet using the following formula.

$$\varepsilon_i = \frac{f_{SI} K_i A_i^2}{V_i} \tag{6.59}$$

Here, K_i is the effective bulk modulus, A_i the surface area of the facet, V_i the volume of the element to which this facet belongs and f_{SI} a user defined scale factor.

6.3.8. Alternative formulations

As of FEBio version 1.2, two alternative formulations for sliding contact are available. The first method, which is referred to as the *facet-to-facet sliding*, is very similar to the formulation described above. It only differs in that it uses a Gaussian quadrature rule instead of nodal integration. Because of the more accurate integration rule, it was noted that this method in many situations was more stable and resulted in better convergence.

The second alternative differs more significantly from the method described above. It also begins with the definition of a single contact integral over the slave surface.

$$G_c = -\int_{\gamma^{(1)}} \mathbf{t}_c \cdot \left(\delta\varphi^{(1)} - \delta\overline{\varphi}^{(2)}\right) da \tag{6.60}$$

But a different derivation is followed to obtain the linearization of this contact integral. The main reason for this difference is a subtly alternative definition for the gap function. In this method, it is defined as follows.

$$g\left(\mathbf{X}\right) = \mathbf{v}^{(1)} \cdot \left(\varphi^{(1)}\left(\mathbf{X}\right) - \varphi^{(2)}\left(\overline{\mathbf{Y}}\left(\mathbf{X}\right)\right)\right) \tag{6.61}$$

where, $\mathbf{v}^{(1)}$ is the normal of the slave surface (opposed to the master normal as used in the derivation above). In this case, the point $\overline{\mathbf{Y}}\left(\mathbf{X}\right)$ is no longer the closest point projection of $\mathbf{X}$ onto the master surface, but instead is the normal projection along $\mathbf{v}^{(1)}$. The linearization of equation (6.61) now becomes,

$$\delta g = \mathbf{v}^{(1)} \cdot \left(\delta\varphi^{(1)}\left(\mathbf{X}\right) - \delta\overline{\varphi}^{(2)}\left(\mathbf{X}\right) - \boldsymbol{\tau}_i^{(2)}\delta\xi_i\right) \tag{6.62}$$

Where, $\boldsymbol{\tau}_i^{(2)} = \dfrac{\partial\overline{\varphi}^{(2)}}{\partial\eta_i}$ are the tangent vectors to the master surface at $\overline{\mathbf{Y}}\left(\mathbf{X}\right)$. Note that since $\mathbf{v}^{(1)}$ is normal to the slave surface, equation (6.62) does not reduce to equation (6.36).
In one assumes frictionless contact, the contact traction can be written as follows,

$$\mathbf{t}_c = t_n\mathbf{v}^{(1)} = t_n \frac{\boldsymbol{\tau}_1^{(1)} \times \boldsymbol{\tau}_2^{(1)}}{\left\|\boldsymbol{\tau}_1^{(1)} \times \boldsymbol{\tau}_2^{(1)}\right\|} \tag{6.63}$$

where, $\boldsymbol{\tau}_i^{(1)}$ are the tangent vectors to $\gamma^{(1)}$ evaluated at $\mathbf{X}$. Using (6.63) we can rewrite the contact integral as follows.

$$G_c = -\int_{\xi^{(1)}} t_n\left(\delta\varphi^{(1)} - \delta\overline{\varphi}^{(2)}\right) \cdot \left(\boldsymbol{\tau}_1^{(1)} \times \boldsymbol{\tau}_2^{(1)}\right) d\xi \tag{6.64}$$

Where we assumed that the integration domain can be mapped to a 2D parametric domain, $\mathbf{x} = \mathbf{x}\left(\xi_\alpha\right)$.

The linearization of (6.64) now proceeds in the usual fashion. Omitting the details, it can be shown that the linearization of the contact integral results in,

$$
\begin{aligned}
DG_c = & \int_{\xi^{(1)}} \varepsilon \mathbf{v}^{(1)} \cdot \left(\mathbf{u}_2 - \mathbf{u}_1 + \overline{\boldsymbol{\tau}}_\alpha^{(2)} \Delta \overline{\xi}_{(2)}^{\alpha} \right) \left(\delta\varphi_1 - \delta\overline{\varphi}_2 \right) \cdot \left(\boldsymbol{\tau}_1^{(1)} \times \boldsymbol{\tau}_2^{(1)} \right) d\xi \\
& - \int_{\xi^{(1)}} t_n \frac{\partial \mathbf{u}_1}{\partial \xi_\alpha} \left(\left(\mathbf{u}_1 - \mathbf{u}_2 \right) \cdot a^{\alpha\beta} \boldsymbol{\tau}_\beta^{(1)} - a^{\alpha\beta} g \mathbf{v}^{(1)} \cdot \frac{\partial \mathbf{u}_1}{\partial \xi_\beta} \right) d\xi \\
& + \int_{\xi^{(1)}} t_n \left(\delta\varphi_1 - \delta\overline{\varphi}_2 \right) \cdot \left(\frac{\partial \mathbf{u}_1}{\partial \xi_1} \times \boldsymbol{\tau}_2^{(1)} + \boldsymbol{\tau}_1^{(1)} \times \frac{\partial \mathbf{u}_1}{\partial \xi_2} \right) d\xi
\end{aligned}
\tag{6.65}
$$

where, $a_{\alpha\beta} = \boldsymbol{\tau}_\alpha^{(1)} \times \boldsymbol{\tau}_\beta^{(2)}$ and $a^{\alpha\beta} = \left(a^{-1} \right)_{\alpha\beta}$.

The discretization of the contact integral and its linearization now proceeds as usual. We will not derive the details, but it is important to point out that the resulting stiffness matrix for this particular contact formulation is not symmetric. Although this method has shown to give good results, especially in large compression problems, it was desirable to derive a symmetric version as well. Because of this, a slightly different formulation was also developed that does reduce to a symmetric stiffness matrix although this symmetric version did not seem to perform as well as the non-symmetric one.

6.4. Biphasic Contact

6.4.1. Contact Integral

See Section 5.5 for a review of biphasic materials, and [49] for additional details on biphasic contact. The contact interface is defined between surfaces $\gamma^{(1)}$ and $\gamma^{(2)}$. Due to continuity requirements on the traction and fluxes, the external virtual work resulting from contact tractions $\mathbf{t}^{(i)}$ and solvent fluxes $w_n^{(i)}$ ($i = 1, 2$), may be combined into the contact integral

$$
\begin{aligned}
\delta G_c = & \int_{\gamma^{(1)}} \left(\delta \mathbf{v}^{(1)} - \delta \mathbf{v}^{(2)} \right) \cdot \mathbf{t}^{(1)} da^{(1)} \\
& + \int_{\gamma^{(1)}} \left(\delta p^{(1)} - \delta p^{(2)} \right) w_n^{(1)} da^{(1)}
\end{aligned}
\tag{6.66}
$$

In the current implementation, only frictionless contact is taken into consideration, so that the contact traction has only a normal component, $\mathbf{t}^{(i)} = t_n \mathbf{n}^{(i)}$. To evaluate and linearize δG_c, define the covariant basis vectors on each surface as

$$
\mathbf{g}_\alpha^{(i)} = \frac{\partial \mathbf{x}^{(i)}}{\partial \eta_{(i)}^{\alpha}}, \quad \alpha = 1, 2, \tag{6.67}
$$

where $\mathbf{x}^{(i)}$ represents the spatial position of points on $\gamma^{(i)}$, and $\eta_{(i)}^{\alpha}$ represent the parametric coordinates of that point. The unit outward normal on each surface is then given by

$$
\mathbf{n}^{(i)} = \frac{\mathbf{g}_1^{(i)} \times \mathbf{g}_2^{(i)}}{\left| \mathbf{g}_1^{(i)} \times \mathbf{g}_2^{(i)} \right|}. \tag{6.68}
$$

Now the contact integral may be rewritten as

$$\begin{aligned}\delta G_c &= \int_{\gamma^{(1)}} \left(\delta \mathbf{v}^{(1)} - \delta \mathbf{v}^{(2)}\right) t_n \mathbf{g}_1^{(1)} \times \mathbf{g}_2^{(1)} d\eta_{(1)}^1 d\eta_{(1)}^2 \\ &+ \int_{\gamma^{(1)}} \left(\delta p^{(1)} - \delta p^{(2)}\right) w_n^{(1)} \left|\mathbf{g}_1^{(1)} \times \mathbf{g}_2^{(1)}\right| d\eta_{(1)}^1 d\eta_{(1)}^2\end{aligned}, \tag{6.69}$$

and the linearization $D\delta G_c$ of δG_c has the form

$$D\delta G_c = \sum_{i=1}^{2} D\delta G_c\left[\Delta \mathbf{u}^{(i)}\right] + D\delta G_c\left[\Delta p^{(i)}\right] \tag{6.70}$$

6.4.2. Gap Function

The gap function g, representing the distance between the contact surfaces, is defined by

$$\mathbf{x}^{(2)} = \mathbf{x}^{(1)} + g\mathbf{n}^{(1)}, \quad g = \left(\mathbf{x}^{(2)} - \mathbf{x}^{(1)}\right) \cdot \mathbf{n}^{(1)} \tag{6.71}$$

The linearization of variables associated with motion, pressure, and concentration, is given by

$$\begin{aligned}&D\mathbf{x}^{(1)} = \Delta \mathbf{u}^{(1)}, \quad D\mathbf{x}^{(2)} = \Delta \mathbf{u}^{(2)} + \mathbf{g}_\alpha^{(2)} \Delta \eta_{(2)}^\alpha \\ &Dp^{(1)} = \Delta p^{(1)}, \quad Dp^{(2)} = \Delta p^{(2)} + \frac{\partial p^{(2)}}{\partial \eta_{(2)}^\alpha} \Delta \eta_{(2)}^\alpha \\ &D\delta \mathbf{v}^{(1)} = \mathbf{0}, \qquad D\mathbf{v}^{(2)} = \frac{\partial \delta \mathbf{v}^{(2)}}{\partial \eta_{(2)}^\alpha} \Delta \eta_{(2)}^\alpha \\ &D\delta p^{(1)} = 0, \qquad D\delta p^{(2)} = \frac{\partial \delta p^{(2)}}{\partial \eta_{(2)}^\alpha} \Delta \eta_{(2)}^\alpha\end{aligned}, \tag{6.72}$$

where

$$\Delta \eta_{(2)}^\alpha = \left(\Delta \mathbf{u}^{(1)} - \Delta \mathbf{u}^{(2)}\right) \cdot a^{\alpha\beta} \mathbf{g}_\beta^{(1)} - a^{\alpha\beta} g \mathbf{n}^{(1)} \cdot \frac{\partial \Delta \mathbf{u}^{(1)}}{\partial \eta_{(1)}^\beta} \tag{6.73}$$

with $a^{\alpha\beta} = \left(A_{\alpha\beta}\right)^{-1}$ and $A_{\alpha\beta} = \mathbf{g}_\alpha^{(1)} \cdot \mathbf{g}_\beta^{(2)}$.

6.4.3. Penalty Method

Let the normal component of the contact traction be described by the penalty function,

$$t_n = \begin{cases} \varepsilon_n g & g < 0 \\ 0 & g \geq 0 \end{cases}, \tag{6.74}$$

where ε_n is a penalty factor associated with t_n. Similarly, let

$$\begin{aligned}&w_n = \varepsilon_p \pi = \varepsilon_p \left(p^{(1)} - p^{(2)}\right), \qquad t_n < 0 \\ &p^{(i)} = 0, \qquad t_n = 0\end{aligned} \tag{6.75}$$

where ε_p is a penalty factor associated with w_n. It follows that

$$Dt_n = \varepsilon_n \left(\Delta\mathbf{u}^{(2)} - \Delta\mathbf{u}^{(1)} + \mathbf{g}_\alpha^{(2)} \Delta\eta_{(2)}^\alpha \right) \cdot \mathbf{n}^{(1)}$$
$$Dw_n = \varepsilon_p \left(\Delta p^{(1)} - \Delta p^{(2)} - \frac{\partial p^{(2)}}{\partial \eta_{(2)}^\alpha} \Delta\eta_{(2)}^\alpha \right) \quad . \tag{6.76}$$

Given these relations, it can be shown that the directional derivatives of the various terms appearing in the integrand of δG_c are

$$\begin{aligned} D\left(t_n \left(\delta\mathbf{v}^{(1)} - \delta\mathbf{v}^{(2)} \right) \cdot \mathbf{g}_1^{(1)} \times \mathbf{g}_2^{(1)} \right) &= -J_\eta^{(1)} \varepsilon_n \left(\delta\mathbf{v}^{(1)} - \delta\mathbf{v}^{(2)} \right) \cdot \left(\mathbf{n}^{(1)} \otimes \mathbf{n}^{(1)} \right) \cdot \left(\Delta\mathbf{u}^{(1)} - \Delta\mathbf{u}^{(2)} \right) \\ &+ J_\eta^{(1)} t_n \frac{\partial \delta\mathbf{v}^{(2)}}{\partial \eta_{(2)}^\alpha} \cdot \left(\mathbf{n}^{(2)} \otimes \mathbf{g}_{(2)}^\alpha \right) \cdot \left(\Delta\mathbf{u}^{(1)} - \Delta\mathbf{u}^{(2)} \right) \\ &+ t_n \left(\delta\mathbf{v}^{(1)} - \delta\mathbf{v}^{(2)} \right) \cdot \left(\frac{\partial \Delta\mathbf{u}^{(1)}}{\partial \eta_{(1)}^1} \times \mathbf{g}_2^{(1)} + \mathbf{g}_1^{(1)} \times \frac{\partial \Delta\mathbf{u}^{(1)}}{\partial \eta_{(1)}^2} \right) \end{aligned} \quad , \tag{6.77}$$

$$\begin{aligned} D\left(w_n \left(\delta p^{(1)} - \delta p^{(2)} \right) \left| \mathbf{g}_1^{(1)} \times \mathbf{g}_2^{(1)} \right| \right) &= J_\eta^{(1)} \varepsilon_p \left(\delta p^{(1)} - \delta p^{(2)} \right) \left(\Delta p^{(1)} - \Delta p^{(2)} \right) \\ &- J_\eta^{(1)} \left[\varepsilon_p \left(\delta p^{(1)} - \delta p^{(2)} \right) \frac{\partial p^{(1)}}{\partial \eta_{(1)}^\alpha} \mathbf{g}_{(1)}^\alpha + w_n \frac{\partial \delta p^{(2)}}{\partial \eta_{(2)}^\alpha} \mathbf{g}_{(2)}^\alpha \right] \cdot \left(\Delta\mathbf{u}^{(1)} - \Delta\mathbf{u}^{(2)} \right), \\ &+ w_n \left(\delta p^{(1)} - \delta p^{(2)} \right) \mathbf{n}^{(1)} \cdot \left(\frac{\partial \Delta\mathbf{u}^{(1)}}{\partial \eta_{(1)}^1} \times \mathbf{g}_2^{(1)} + \mathbf{g}_1^{(1)} \times \frac{\partial \Delta\mathbf{u}^{(1)}}{\partial \eta_{(1)}^2} \right) \end{aligned} \tag{6.78}$$

where $J_\eta^{(1)} = \left| \mathbf{g}_1^{(1)} \times \mathbf{g}_2^{(1)} \right|$.

6.4.4. Discretization

The contact integral may be discretized as

$$\delta G_c = \sum_{e=1}^{n_e^{(1)}} \sum_{k=1}^{n_{\text{int}}^{(e)}} W_k J_\eta^{(1)} \left[t_n \left(\delta\mathbf{v}^{(1)} - \delta\mathbf{v}^{(2)} \right) \cdot \mathbf{n}^{(1)} + w_n \left(\delta p^{(1)} - \delta p^{(2)} \right) \right] \tag{6.79}$$

The variables may be interpolated over each element face according to

$$\begin{aligned} \delta\mathbf{v}^{(1)} &= \sum_{a=1}^{m^{(1)}} N_a^{(1)} \delta\mathbf{v}_a^{(1)}, & \delta\mathbf{v}^{(2)} &= \sum_{b=1}^{m^{(2)}} N_b^{(2)} \delta\mathbf{v}_b^{(2)} \\ \Delta\mathbf{u}^{(1)} &= \sum_{c=1}^{m^{(1)}} N_c^{(1)} \Delta\mathbf{u}_c^{(1)}, & \Delta\mathbf{u}^{(2)} &= \sum_{d=1}^{m^{(2)}} N_d^{(2)} \Delta\mathbf{u}_d^{(2)} \\ \delta p^{(1)} &= \sum_{a=1}^{m^{(1)}} N_a^{(1)} \delta p_a^{(1)}, & \delta p^{(2)} &= \sum_{b=1}^{m^{(2)}} N_b^{(2)} \delta p_b^{(2)} \\ \Delta p^{(1)} &= \sum_{c=1}^{m^{(1)}} N_c^{(1)} \Delta p_c^{(1)}, & \Delta p^{(2)} &= \sum_{d=1}^{m^{(2)}} N_d^{(2)} \Delta p_d^{(2)} \end{aligned} \quad . \tag{6.80}$$

Then,

$$\delta G_c = \sum_{e=1}^{n_e^{(1)}} \sum_{k=1}^{n_{\text{int}}^{(e)}} W_k J_\eta^{(1)} \left(\sum_{a=1}^{m^{(1)}} \begin{bmatrix} \delta \mathbf{v}_a^{(1)} & \delta p_a^{(1)} \end{bmatrix} \cdot \begin{bmatrix} \mathbf{f}_a^{(1)} \\ w_a^{(1)} \end{bmatrix} + \sum_{b=1}^{m_k^{(2)}} \begin{bmatrix} \delta \mathbf{v}_{b,k}^{(1)} & \delta p_{b,k}^{(1)} \end{bmatrix} \cdot \begin{bmatrix} \mathbf{f}_{b,k}^{(1)} \\ w_{b,k}^{(1)} \end{bmatrix} \right), \tag{6.81}$$

where

$$\begin{aligned} \mathbf{f}_a^{(1)} &= N_a^{(1)} t_n \mathbf{n}^{(1)}, & \mathbf{f}_{b,k}^{(2)} &= -N_b^{(2)} t_n \mathbf{n}^{(1)} \\ w_a^{(1)} &= N_a^{(1)} w_n, & w_{b,k}^{(2)} &= -N_b^{(2)} w_n \end{aligned} . \tag{6.82}$$

Similarly,

$$\begin{aligned} -D\delta G_c = \sum_{e=1}^{n_e^{(1)}} \sum_{k=1}^{n_{\text{int}}^{(e)}} W_k J_\eta^{(1)} & \\ \times \Bigg(\sum_{a=1}^{m^{(1)}} \begin{bmatrix} \delta \mathbf{v}_a^{(1)} & \delta p_a^{(1)} \end{bmatrix} \cdot \Bigg(\sum_{c=1}^{m^{(1)}} \begin{bmatrix} \mathbf{K}_{ac}^{(1,1)} & \mathbf{0} \\ \mathbf{g}_{ac}^{(1,1)} & g_{ac}^{(1,1)} \end{bmatrix} \cdot \begin{bmatrix} \Delta \mathbf{u}_c^{(1)} \\ \Delta p_c^{(1)} \end{bmatrix} \\ + \sum_{d=1}^{m_k^{(2)}} \begin{bmatrix} \mathbf{K}_{ad,k}^{(1,2)} & \mathbf{0} \\ \mathbf{g}_{ad,k}^{(1,2)} & g_{ad,k}^{(1,2)} \end{bmatrix} \cdot \begin{bmatrix} \Delta \mathbf{u}_d^{(2)} \\ \Delta p_d^{(2)} \end{bmatrix} \Bigg) \\ + \sum_{b=1}^{m_k^{(2)}} \begin{bmatrix} \delta \mathbf{v}_{b,k}^{(2)} & \delta p_{b,k}^{(2)} \end{bmatrix} \cdot \Bigg(\sum_{c=1}^{m^{(1)}} \begin{bmatrix} \mathbf{K}_{bc,k}^{(2,1)} & \mathbf{0} \\ \mathbf{g}_{bc,k}^{(2,1)} & g_{bc,k}^{(2,1)} \end{bmatrix} \cdot \begin{bmatrix} \Delta \mathbf{u}_c^{(1)} \\ \Delta p_c^{(1)} \end{bmatrix} \\ + \sum_{d=1}^{m_k^{(2)}} \begin{bmatrix} \mathbf{K}_{bd,k}^{(2,2)} & \mathbf{0} \\ \mathbf{g}_{bd,k}^{(2,2)} & g_{bd,k}^{(2,2)} \end{bmatrix} \cdot \begin{bmatrix} \Delta \mathbf{u}_d^{(2)} \\ \Delta p_d^{(2)} \end{bmatrix} \Bigg) \Bigg) \end{aligned}, \tag{6.83}$$

where

$$\begin{aligned}
\mathbf{K}_{ac}^{(1,1)} &= N_a^{(1)}\left(\varepsilon_n N_c^{(1)}\mathbf{N}^{(1)} + t_n \mathbf{A}_c^{(1)}\right) \\
\mathbf{K}_{ad,k}^{(1,2)} &= -\varepsilon_n N_a^{(1)} N_d^{(2)}\mathbf{N}^{(1)} \\
\mathbf{K}_{bc,k}^{(2,1)} &= -N_c^{(1)}\left(\varepsilon_n N_b^{(2)}\mathbf{N}^{(1)} + t_n \mathbf{M}_b^{(2)}\right) - t_n N_b^{(2)}\mathbf{A}_c^{(1)} \\
\mathbf{K}_{bd,k}^{(2,2)} &= N_d^{(2)}\left(\varepsilon_n N_b^{(2)}\mathbf{N}^{(1)} + t_n \mathbf{M}_b^{(2)}\right)
\end{aligned} , \tag{6.84}$$

$$\begin{aligned}
\mathbf{g}_{ac}^{(1,1)} &= N_a^{(1)}\left(\varepsilon_p N_c^{(1)}\mathbf{p}^{(1)} - w_n \mathbf{A}_c^{(1)}\cdot\mathbf{n}^{(1)}\right) \\
\mathbf{g}_{ad,k}^{(1,2)} &= -\varepsilon_p N_a^{(1)} N_d^{(2)}\mathbf{p}^{(1)} \\
\mathbf{g}_{bc,k}^{(2,1)} &= N_c^{(1)}\left(-\varepsilon_p N_b^{(2)}\mathbf{p}^{(1)} + w_n \mathbf{m}_b^{(2)}\right) + w_n N_b^{(2)}\mathbf{A}_c^{(1)}\cdot\mathbf{n}^{(1)} \\
\mathbf{g}_{bd,k}^{(2,2)} &= N_d^{(2)}\left(\varepsilon_p N_b^{(2)}\mathbf{p}^{(1)} - w_n \mathbf{m}_b^{(2)}\right)
\end{aligned} , \tag{6.85}$$

$$\begin{aligned}
g_{ac}^{(1,1)} &= -\varepsilon_p N_a^{(1)} N_c^{(1)} \\
g_{ad,k}^{(1,2)} &= \varepsilon_p N_a^{(1)} N_d^{(2)} \\
g_{bc,k}^{(2,1)} &= \varepsilon_p N_b^{(2)} N_c^{(1)} \\
g_{bd,k}^{(2,2)} &= -\varepsilon_p N_b^{(2)} N_d^{(2)}
\end{aligned} , \tag{6.86}$$

and

$$\begin{aligned}
\mathbf{N}^{(1)} &= \mathbf{n}^{(1)} \otimes \mathbf{n}^{(1)} \\
\mathbf{A}_c^{(1)} &= \frac{1}{J_\eta^{(1)}}\mathcal{A}\left\{\frac{\partial N_c^{(1)}}{\partial \eta_{(1)}^1}\mathbf{g}_2^{(1)} - \frac{\partial N_c^{(1)}}{\partial \eta_{(1)}^2}\mathbf{g}_1^{(1)}\right\} \\
\mathbf{M}_b^{(2)} &= \mathbf{n}^{(2)} \otimes \mathbf{m}_b^{(2)} \\
\mathbf{m}_b^{(2)} &= \frac{\partial N_b^{(2)}}{\partial \eta_{(2)}^\alpha}\mathbf{g}_{(2)}^\alpha \\
\mathbf{p}^{(1)} &= \frac{\partial p^{(1)}}{\partial \eta_{(1)}^\alpha}\mathbf{g}_{(1)}^\alpha
\end{aligned} . \tag{6.87}$$

6.5. Biphasic-Solute Contact

6.5.1. Contact Integral

See Section 2.6 for a review of biphasic-solute materials. The contact interface is defined between surfaces $\gamma^{(1)}$ and $\gamma^{(2)}$. Due to continuity requirements on the traction and fluxes, the external virtual work resulting from contact tractions $\mathbf{t}^{(i)}$, solvent fluxes $w_n^{(i)}$ and solute fluxes $j_n^{(i)}$ ($i = 1, 2$), may be combined into the contact integral

$$\begin{aligned}\delta G_c &= \int_{\gamma^{(1)}} \left(\delta \mathbf{v}^{(1)} - \delta \mathbf{v}^{(2)}\right) \cdot \mathbf{t}^{(1)} da^{(1)} \\ &+ \int_{\gamma^{(1)}} \left(\delta \tilde{p}^{(1)} - \delta \tilde{p}^{(2)}\right) w_n^{(1)} da^{(1)} \,. \\ &+ \int_{\gamma^{(1)}} \left(\delta \tilde{c}^{(1)} - \delta \tilde{c}^{(2)}\right) j_n^{(1)} da^{(1)}\end{aligned} \tag{6.88}$$

In the current implementation, only frictionless contact is taken into consideration, so that the contact traction has only a normal component, $\mathbf{t}^{(i)} = t_n \mathbf{n}^{(i)}$. To evaluate and linearize δG_c, define the covariant basis vectors on each surface as

$$\mathbf{g}_\alpha^{(i)} = \frac{\partial \mathbf{x}^{(i)}}{\partial \eta_{(i)}^\alpha}, \quad \alpha = 1, 2 \,, \tag{6.89}$$

where $\mathbf{x}^{(i)}$ represents the spatial position of points on $\gamma^{(i)}$, and $\eta_{(i)}^\alpha$ represent the parametric coordinates of that point. The unit outward normal on each surface is then given by

$$\mathbf{n}^{(i)} = \frac{\mathbf{g}_1^{(i)} \times \mathbf{g}_2^{(i)}}{\left|\mathbf{g}_1^{(i)} \times \mathbf{g}_2^{(i)}\right|} \,. \tag{6.90}$$

Now the contact integral may be rewritten as

$$\begin{aligned}\delta G_c &= \int_{\gamma^{(1)}} \left(\delta \mathbf{v}^{(1)} - \delta \mathbf{v}^{(2)}\right) t_n \mathbf{g}_1^{(1)} \times \mathbf{g}_2^{(1)} d\eta_{(1)}^1 d\eta_{(1)}^2 \\ &+ \int_{\gamma^{(1)}} \left(\delta \tilde{p}^{(1)} - \delta \tilde{p}^{(2)}\right) w_n^{(1)} \left|\mathbf{g}_1^{(1)} \times \mathbf{g}_2^{(1)}\right| d\eta_{(1)}^1 d\eta_{(1)}^2 \,, \\ &+ \int_{\gamma^{(1)}} \left(\delta \tilde{c}^{(1)} - \delta \tilde{c}^{(2)}\right) j_n^{(1)} \left|\mathbf{g}_1^{(1)} \times \mathbf{g}_2^{(1)}\right| d\eta_{(1)}^1 d\eta_{(1)}^2\end{aligned} \tag{6.91}$$

and the linearization $D\delta G_c$ of δG_c has the form

$$D\delta G_c = \sum_{i=1}^{2} D\delta G_c \left[\Delta \mathbf{u}^{(i)}\right] + D\delta G_c \left[\Delta \tilde{p}^{(i)}\right] + D\delta G_c \left[\Delta \tilde{c}^{(i)}\right] \tag{6.92}$$

6.5.2. Gap Function

The gap function g, representing the distance between the contact surfaces, is defined by

$$\mathbf{x}^{(2)} = \mathbf{x}^{(1)} + g\mathbf{n}^{(1)}, \quad g = \left(\mathbf{x}^{(2)} - \mathbf{x}^{(1)}\right) \cdot \mathbf{n}^{(1)} \,. \tag{6.93}$$

The linearization of variables associated with motion, pressure, and concentration, is given by

$$
\begin{aligned}
&D\mathbf{x}^{(1)} = \Delta\mathbf{u}^{(1)}, \quad D\mathbf{x}^{(2)} = \Delta\mathbf{u}^{(2)} + \mathbf{g}_{\alpha}^{(2)}\Delta\eta_{(2)}^{\alpha} \\
&D\tilde{p}^{(1)} = \Delta\tilde{p}^{(1)}, \quad D\tilde{p}^{(2)} = \Delta\tilde{p}^{(2)} + \frac{\partial\tilde{p}^{(2)}}{\partial\eta_{(2)}^{\alpha}}\Delta\eta_{(2)}^{\alpha} \\
&D\tilde{c}^{(1)} = \Delta\tilde{c}^{(1)}, \quad D\tilde{c}^{(2)} = \Delta\tilde{c}^{(2)} + \frac{\partial\tilde{c}^{(2)}}{\partial\eta_{(2)}^{\alpha}}\Delta\eta_{(2)}^{\alpha} \\
&D\delta\mathbf{v}^{(1)} = \mathbf{0}, \qquad D\mathbf{v}^{(2)} = \frac{\partial\delta\mathbf{v}^{(2)}}{\partial\eta_{(2)}^{\alpha}}\Delta\eta_{(2)}^{\alpha} \\
&D\delta\tilde{p}^{(1)} = 0, \qquad D\delta\tilde{p}^{(2)} = \frac{\partial\delta\tilde{p}^{(2)}}{\partial\eta_{(2)}^{\alpha}}\Delta\eta_{(2)}^{\alpha} \\
&D\delta\tilde{c}^{(1)} = 0, \qquad D\delta\tilde{c}^{(2)} = \frac{\partial\delta\tilde{c}^{(2)}}{\partial\eta_{(2)}^{\alpha}}\Delta\eta_{(2)}^{\alpha}
\end{aligned}
\quad , \tag{6.94}
$$

where

$$
\Delta\eta_{(2)}^{\alpha} = \left(\Delta\mathbf{u}^{(1)} - \Delta\mathbf{u}^{(2)}\right)\cdot a^{\alpha\beta}\mathbf{g}_{\beta}^{(1)} - a^{\alpha\beta} g\mathbf{n}^{(1)}\cdot\frac{\partial\Delta\mathbf{u}^{(1)}}{\partial\eta_{(1)}^{\beta}} \tag{6.95}
$$

with $a^{\alpha\beta} = \left(A_{\alpha\beta}\right)^{-1}$ and $A_{\alpha\beta} = \mathbf{g}_{\alpha}^{(1)}\cdot\mathbf{g}_{\beta}^{(2)}$.

6.5.3. Penalty Method

Let the normal component of the contact traction be described by the penalty function,

$$
t_n = \begin{cases} \varepsilon_n g & g < 0 \\ 0 & g \geq 0 \end{cases}, \tag{6.96}
$$

where ε_n is a penalty factor associated with t_n. Similarly, let

$$
\begin{aligned}
&w_n = \varepsilon_p \pi = \varepsilon_p\left(\tilde{p}^{(1)} - \tilde{p}^{(2)}\right), && t_n < 0 \\
&\tilde{p}^{(i)} = \tilde{p}^{*}, && t_n = 0
\end{aligned} \tag{6.97}
$$

and

$$
\begin{aligned}
&j_n = \varepsilon_c \chi = \varepsilon_c\left(\tilde{c}^{(1)} - \tilde{c}^{(2)}\right), && t_n < 0 \\
&\tilde{c}^{(i)} = \tilde{c}^{*}, && t_n = 0
\end{aligned} \quad , \tag{6.98}
$$

where ε_p and ε_c are penalty factors associated with w_n and j_n, respectively. It follows that

$$
\begin{aligned}
Dt_n &= \varepsilon_n \left(\Delta\mathbf{u}^{(2)} - \Delta\mathbf{u}^{(1)} + \mathbf{g}_\alpha^{(2)} \Delta\eta_{(2)}^\alpha \right) \cdot \mathbf{n}^{(1)} \\
Dw_n &= \varepsilon_p \left(\Delta\tilde{p}^{(1)} - \Delta\tilde{p}^{(2)} - \frac{\partial \tilde{p}^{(2)}}{\partial \eta_{(2)}^\alpha} \Delta\eta_{(2)}^\alpha \right) \quad . \\
Dj_n &= \varepsilon_c \left(\Delta\tilde{c}^{(1)} - \Delta\tilde{c}^{(2)} - \frac{\partial \tilde{c}^{(2)}}{\partial \eta_{(2)}^\alpha} \Delta\eta_{(2)}^\alpha \right)
\end{aligned}
\tag{6.99}
$$

Given these relations, it can be shown that the directional derivatives of the various terms appearing in the integrand of δG_c are

$$
\begin{aligned}
D\left(t_n \left(\delta\mathbf{v}^{(1)} - \delta\mathbf{v}^{(2)} \right) \cdot \mathbf{g}_1^{(1)} \times \mathbf{g}_2^{(1)} \right) &= -J_\eta^{(1)} \varepsilon_n \left(\delta\mathbf{v}^{(1)} - \delta\mathbf{v}^{(2)} \right) \cdot \left(\mathbf{n}^{(1)} \otimes \mathbf{n}^{(1)} \right) \cdot \left(\Delta\mathbf{u}^{(1)} - \Delta\mathbf{u}^{(2)} \right) \\
&+ J_\eta^{(1)} t_n \frac{\partial \delta\mathbf{v}^{(2)}}{\partial \eta_{(2)}^\alpha} \cdot \left(\mathbf{n}^{(2)} \otimes \mathbf{g}_{(2)}^\alpha \right) \cdot \left(\Delta\mathbf{u}^{(1)} - \Delta\mathbf{u}^{(2)} \right) \quad , \\
&+ t_n \left(\delta\mathbf{v}^{(1)} - \delta\mathbf{v}^{(2)} \right) \cdot \left(\frac{\partial \Delta\mathbf{u}^{(1)}}{\partial \eta_{(1)}^1} \times \mathbf{g}_2^{(1)} + \mathbf{g}_1^{(1)} \times \frac{\partial \Delta\mathbf{u}^{(1)}}{\partial \eta_{(1)}^2} \right)
\end{aligned}
\tag{6.100}
$$

$$
\begin{aligned}
D\left(w_n \left(\delta\tilde{p}^{(1)} - \delta\tilde{p}^{(2)} \right) \left| \mathbf{g}_1^{(1)} \times \mathbf{g}_2^{(1)} \right| \right) &= J_\eta^{(1)} \varepsilon_p \left(\delta\tilde{p}^{(1)} - \delta\tilde{p}^{(2)} \right) \left(\Delta\tilde{p}^{(1)} - \Delta\tilde{p}^{(2)} \right) \\
&- J_\eta^{(1)} \left[\varepsilon_p \left(\delta\tilde{p}^{(1)} - \delta\tilde{p}^{(2)} \right) \frac{\partial \tilde{p}^{(1)}}{\partial \eta_{(1)}^\alpha} \mathbf{g}_{(1)}^\alpha + w_n \frac{\partial \delta\tilde{p}^{(2)}}{\partial \eta_{(2)}^\alpha} \mathbf{g}_{(2)}^\alpha \right] \cdot \left(\Delta\mathbf{u}^{(1)} - \Delta\mathbf{u}^{(2)} \right), \\
&+ w_n \left(\delta\tilde{p}^{(1)} - \delta\tilde{p}^{(2)} \right) \mathbf{n}^{(1)} \cdot \left(\frac{\partial \Delta\mathbf{u}^{(1)}}{\partial \eta_{(1)}^1} \times \mathbf{g}_2^{(1)} + \mathbf{g}_1^{(1)} \times \frac{\partial \Delta\mathbf{u}^{(1)}}{\partial \eta_{(1)}^2} \right)
\end{aligned}
\tag{6.101}
$$

$$
\begin{aligned}
D\left(j_n \left(\delta\tilde{c}^{(1)} - \delta\tilde{c}^{(2)} \right) \left| \mathbf{g}_1^{(1)} \times \mathbf{g}_2^{(1)} \right| \right) &= J_\eta^{(1)} \varepsilon_c \left(\delta\tilde{c}^{(1)} - \delta\tilde{c}^{(2)} \right) \left(\Delta\tilde{c}^{(1)} - \Delta\tilde{c}^{(2)} \right) \\
&- J_\eta^{(1)} \left[\varepsilon_c \left(\delta\tilde{c}^{(1)} - \delta\tilde{c}^{(2)} \right) \frac{\partial \tilde{c}^{(1)}}{\partial \eta_{(1)}^\alpha} \mathbf{g}_{(1)}^\alpha + j_n \frac{\partial \delta\tilde{c}^{(2)}}{\partial \eta_{(2)}^\alpha} \mathbf{g}_{(2)}^\alpha \right] \cdot \left(\Delta\mathbf{u}^{(1)} - \Delta\mathbf{u}^{(2)} \right), \\
&+ j_n \left(\delta\tilde{c}^{(1)} - \delta\tilde{c}^{(2)} \right) \mathbf{n}^{(1)} \cdot \left(\frac{\partial \Delta\mathbf{u}^{(1)}}{\partial \eta_{(1)}^1} \times \mathbf{g}_2^{(1)} + \mathbf{g}_1^{(1)} \times \frac{\partial \Delta\mathbf{u}^{(1)}}{\partial \eta_{(1)}^2} \right)
\end{aligned}
\tag{6.102}
$$

where $J_\eta^{(1)} = \left| \mathbf{g}_1^{(1)} \times \mathbf{g}_2^{(1)} \right|$.

6.5.4. Discretization

The contact integral may be discretized as

$$
\delta G_c = \sum_{e=1}^{n_e^{(1)}} \sum_{k=1}^{n_{\text{int}}^{(e)}} W_k J_\eta^{(1)} \left[t_n \left(\delta\mathbf{v}^{(1)} - \delta\mathbf{v}^{(2)} \right) \cdot \mathbf{n}^{(1)} + w_n \left(\delta\tilde{p}^{(1)} - \delta\tilde{p}^{(2)} \right) + j_n \left(\delta\tilde{c}^{(1)} - \delta\tilde{c}^{(2)} \right) \right] \tag{6.103}
$$

The variables may be interpolated over each element face according to

$$
\begin{aligned}
\delta\mathbf{v}^{(1)} &= \sum_{a=1}^{m^{(1)}} N_a^{(1)}\delta\mathbf{v}_a^{(1)}, & \delta\mathbf{v}^{(2)} &= \sum_{b=1}^{m^{(2)}} N_b^{(2)}\delta\mathbf{v}_b^{(2)} \\
\Delta\mathbf{u}^{(1)} &= \sum_{c=1}^{m^{(1)}} N_c^{(1)}\Delta\mathbf{u}_c^{(1)}, & \Delta\mathbf{u}^{(2)} &= \sum_{d=1}^{m^{(2)}} N_d^{(2)}\Delta\mathbf{u}_d^{(2)} \\
\delta\tilde{p}^{(1)} &= \sum_{a=1}^{m^{(1)}} N_a^{(1)}\delta\tilde{p}_a^{(1)}, & \delta\tilde{p}^{(2)} &= \sum_{b=1}^{m^{(2)}} N_b^{(2)}\delta\tilde{p}_b^{(2)} \\
\Delta\tilde{p}^{(1)} &= \sum_{c=1}^{m^{(1)}} N_c^{(1)}\Delta\tilde{p}_c^{(1)}, & \Delta\tilde{p}^{(2)} &= \sum_{d=1}^{m^{(2)}} N_d^{(2)}\Delta\tilde{p}_d^{(2)} \\
\delta\tilde{c}^{(1)} &= \sum_{a=1}^{m^{(1)}} N_a^{(1)}\delta\tilde{c}_a^{(1)}, & \delta\tilde{c}^{(2)} &= \sum_{b=1}^{m^{(2)}} N_b^{(2)}\delta\tilde{c}_b^{(2)} \\
\Delta\tilde{c}^{(1)} &= \sum_{c=1}^{m^{(1)}} N_c^{(1)}\Delta\tilde{c}_c^{(1)}, & \Delta\tilde{c}^{(2)} &= \sum_{d=1}^{m^{(2)}} N_d^{(2)}\Delta\tilde{c}_d^{(2)}
\end{aligned}
\quad . \tag{6.104}
$$

Then,

$$
\delta G_c = \sum_{e=1}^{n_e^{(1)}} \sum_{k=1}^{n_{\text{int}}^{(e)}} W_k J_\eta^{(1)} \left(\sum_{a=1}^{m^{(1)}} \begin{bmatrix} \delta\mathbf{v}_a^{(1)} & \delta\tilde{p}_a^{(1)} & \delta\tilde{c}_a^{(1)} \end{bmatrix} \cdot \begin{bmatrix} \mathbf{f}_a^{(1)} \\ w_a^{(1)} \\ j_a^{(1)} \end{bmatrix} + \sum_{b=1}^{m_k^{(2)}} \begin{bmatrix} \delta\mathbf{v}_{b,k}^{(1)} & \delta\tilde{p}_{b,k}^{(1)} & \delta\tilde{c}_{b,k}^{(1)} \end{bmatrix} \cdot \begin{bmatrix} \mathbf{f}_{b,k}^{(1)} \\ w_{b,k}^{(1)} \\ j_{b,k}^{(1)} \end{bmatrix} \right), \tag{6.105}
$$

where

$$
\begin{aligned}
\mathbf{f}_a^{(1)} &= N_a^{(1)} t_n \mathbf{n}^{(1)}, & \mathbf{f}_{b,k}^{(2)} &= -N_b^{(2)} t_n \mathbf{n}^{(1)} \\
w_a^{(1)} &= N_a^{(1)} w_n, & w_{b,k}^{(2)} &= -N_b^{(2)} w_n \\
j_a^{(1)} &= N_a^{(1)} j_n, & j_{b,k}^{(2)} &= -N_b^{(2)} j_n
\end{aligned}
\quad . \tag{6.106}
$$

Similarly,

$$
\begin{aligned}
-D\delta G_c = \sum_{e=1}^{n_e^{(1)}} \sum_{k=1}^{n_{\text{int}}^{(e)}} W_k J_\eta^{(1)} \\
\times \Bigg(\sum_{a=1}^{m^{(1)}} \begin{bmatrix} \delta \mathbf{v}_a^{(1)} & \delta \tilde{p}_a^{(1)} & \delta \tilde{c}_a^{(1)} \end{bmatrix} \cdot \Bigg(\sum_{c=1}^{m^{(1)}} \begin{bmatrix} \mathbf{K}_{ac}^{(1,1)} & \mathbf{0} & \mathbf{0} \\ \mathbf{g}_{ac}^{(1,1)} & g_{ac}^{(1,1)} & 0 \\ \mathbf{h}_{ac}^{(1,1)} & 0 & h_{ac}^{(1,1)} \end{bmatrix} \cdot \begin{bmatrix} \Delta \mathbf{u}_c^{(1)} \\ \Delta \tilde{p}_c^{(1)} \\ \Delta \tilde{c}_c^{(1)} \end{bmatrix} \\
+ \sum_{d=1}^{m_k^{(2)}} \begin{bmatrix} \mathbf{K}_{ad,k}^{(1,2)} & \mathbf{0} & \mathbf{0} \\ \mathbf{g}_{ad,k}^{(1,2)} & g_{ad,k}^{(1,2)} & 0 \\ \mathbf{h}_{ad,k}^{(1,2)} & 0 & h_{ad,k}^{(1,2)} \end{bmatrix} \cdot \begin{bmatrix} \Delta \mathbf{u}_d^{(2)} \\ \Delta \tilde{p}_d^{(2)} \\ \Delta \tilde{c}_d^{(2)} \end{bmatrix} \Bigg) \\
+ \sum_{b=1}^{m_k^{(2)}} \begin{bmatrix} \delta \mathbf{v}_{b,k}^{(2)} & \delta \tilde{p}_{b,k}^{(2)} & \delta \tilde{c}_{b,k}^{(2)} \end{bmatrix} \cdot \Bigg(\sum_{c=1}^{m^{(1)}} \begin{bmatrix} \mathbf{K}_{bc,k}^{(2,1)} & \mathbf{0} & \mathbf{0} \\ \mathbf{g}_{bc,k}^{(2,1)} & g_{bc,k}^{(2,1)} & 0 \\ \mathbf{h}_{bc,k}^{(2,1)} & 0 & h_{bc,k}^{(2,1)} \end{bmatrix} \cdot \begin{bmatrix} \Delta \mathbf{u}_c^{(1)} \\ \Delta \tilde{p}_c^{(1)} \\ \Delta \tilde{c}_c^{(1)} \end{bmatrix} \\
+ \sum_{d=1}^{m_k^{(2)}} \begin{bmatrix} \mathbf{K}_{bd,k}^{(2,2)} & \mathbf{0} & \mathbf{0} \\ \mathbf{g}_{bd,k}^{(2,2)} & g_{bd,k}^{(2,2)} & 0 \\ \mathbf{h}_{bd,k}^{(2,2)} & 0 & h_{bd,k}^{(2,2)} \end{bmatrix} \cdot \begin{bmatrix} \Delta \mathbf{u}_d^{(2)} \\ \Delta \tilde{p}_d^{(2)} \\ \Delta \tilde{c}_d^{(2)} \end{bmatrix} \Bigg) \Bigg) \Bigg) \qquad , \qquad (6.107)
\end{aligned}
$$

where

$$\begin{aligned}
\mathbf{K}_{ac}^{(1,1)} &= N_a^{(1)}\left(\varepsilon_n N_c^{(1)}\mathbf{N}^{(1)} + t_n \mathbf{A}_c^{(1)}\right) \\
\mathbf{K}_{ad,k}^{(1,2)} &= -\varepsilon_n N_a^{(1)} N_d^{(2)}\mathbf{N}^{(1)} \\
\mathbf{K}_{bc,k}^{(2,1)} &= -N_c^{(1)}\left(\varepsilon_n N_b^{(2)}\mathbf{N}^{(1)} + t_n \mathbf{M}_b^{(2)}\right) - t_n N_b^{(2)}\mathbf{A}_c^{(1)} \\
\mathbf{K}_{bd,k}^{(2,2)} &= N_d^{(2)}\left(\varepsilon_n N_b^{(2)}\mathbf{N}^{(1)} + t_n \mathbf{M}_b^{(2)}\right)
\end{aligned} \tag{6.108}$$

$$\begin{aligned}
\mathbf{g}_{ac}^{(1,1)} &= N_a^{(1)}\left(\varepsilon_p N_c^{(1)}\mathbf{p}^{(1)} - w_n \mathbf{A}_c^{(1)}\cdot\mathbf{n}^{(1)}\right) \\
\mathbf{g}_{ad,k}^{(1,2)} &= -\varepsilon_p N_a^{(1)} N_d^{(2)}\mathbf{p}^{(1)} \\
\mathbf{g}_{bc,k}^{(2,1)} &= N_c^{(1)}\left(-\varepsilon_p N_b^{(2)}\mathbf{p}^{(1)} + w_n \mathbf{m}_b^{(2)}\right) + w_n N_b^{(2)}\mathbf{A}_c^{(1)}\cdot\mathbf{n}^{(1)} \\
\mathbf{g}_{bd,k}^{(2,2)} &= N_d^{(2)}\left(\varepsilon_p N_b^{(2)}\mathbf{p}^{(1)} - w_n \mathbf{m}_b^{(2)}\right)
\end{aligned} \tag{6.109}$$

$$\begin{aligned}
g_{ac}^{(1,1)} &= -\varepsilon_p N_a^{(1)} N_c^{(1)} \\
g_{ad,k}^{(1,2)} &= \varepsilon_p N_a^{(1)} N_d^{(2)} \\
g_{bc,k}^{(2,1)} &= \varepsilon_p N_b^{(2)} N_c^{(1)} \\
g_{bd,k}^{(2,2)} &= -\varepsilon_p N_b^{(2)} N_d^{(2)}
\end{aligned} \tag{6.110}$$

$$\begin{aligned}
\mathbf{h}_{ac}^{(1,1)} &= N_a^{(1)}\left(\varepsilon_c N_c^{(1)}\mathbf{q}^{(1)} - j_n \mathbf{A}_c^{(1)}\cdot\mathbf{n}^{(1)}\right) \\
\mathbf{h}_{ad,k}^{(1,2)} &= -\varepsilon_c N_a^{(1)} N_d^{(2)}\mathbf{q}^{(1)} \\
\mathbf{h}_{bc,k}^{(2,1)} &= N_c^{(1)}\left(-\varepsilon_c N_b^{(2)}\mathbf{q}^{(1)} + j_n \mathbf{m}_b^{(2)}\right) + j_n N_b^{(2)}\mathbf{A}_c^{(1)}\cdot\mathbf{n}^{(1)} \\
\mathbf{h}_{bd,k}^{(2,2)} &= N_d^{(2)}\left(\varepsilon_c N_b^{(2)}\mathbf{q}^{(1)} - j_n \mathbf{m}_b^{(2)}\right)
\end{aligned} \tag{6.111}$$

$$\begin{aligned}
h_{ac}^{(1,1)} &= -\varepsilon_c N_a^{(1)} N_c^{(1)} \\
h_{ad,k}^{(1,2)} &= \varepsilon_c N_a^{(1)} N_d^{(2)} \\
h_{bc,k}^{(2,1)} &= \varepsilon_c N_b^{(2)} N_c^{(1)} \\
h_{bd,k}^{(2,2)} &= -\varepsilon_c N_b^{(2)} N_d^{(2)}
\end{aligned} \tag{6.112}$$

and

$$
\begin{aligned}
\mathbf{N}^{(1)} &= \mathbf{n}^{(1)} \otimes \mathbf{n}^{(1)} \\
\mathbf{A}_c^{(1)} &= \frac{1}{J_\eta^{(1)}} \mathcal{A} \left\{ \frac{\partial N_c^{(1)}}{\partial \eta_{(1)}^1} \mathbf{g}_2^{(1)} - \frac{\partial N_c^{(1)}}{\partial \eta_{(1)}^2} \mathbf{g}_1^{(1)} \right\} \\
\mathbf{M}_b^{(2)} &= \mathbf{n}^{(2)} \otimes \mathbf{m}_b^{(2)} \\
\mathbf{m}_b^{(2)} &= \frac{\partial N_b^{(2)}}{\partial \eta_{(2)}^\alpha} \mathbf{g}_{(2)}^\alpha \\
\mathbf{p}^{(1)} &= \frac{\partial \tilde{p}^{(1)}}{\partial \eta_{(1)}^\alpha} \mathbf{g}_{(1)}^\alpha \\
\mathbf{q}^{(1)} &= \frac{\partial \tilde{c}^{(1)}}{\partial \eta_{(1)}^\alpha} \mathbf{g}_{(1)}^\alpha
\end{aligned}
\quad . \tag{6.113}
$$

6.6. Tied Contact

In some situations it is useful to connect two non-conforming meshes together. This can be done by defining a tied contact interface. In FEBio, the tied contact works very similar to the sliding contact interface. We need to define a slave surface and a master surface, where it is assumed that the slave surface nodes will be tied to the master surface faces.

6.6.1. Gap Function

Just as in sliding contact, we need to define a gap function that measures the distance between the slave and master surface. In order to do that, we first define the projection of a slave node to the master surface.

$$\bar{\mathbf{Y}}(\mathbf{X}) = \arg \min_{\mathbf{Y} \in \Gamma^{(2)}} \|\mathbf{X} - \mathbf{Y}\| \tag{6.114}$$

This definition is similar to that of the sliding interface, except that now the projection is done in the material reference frame. This implies that the projection only needs to be calculated once, at the beginning of the analysis. We can now proceed to the definition of the gap function.

$$\mathbf{g}(\mathbf{X}) = \varphi^{(1)}(\mathbf{X}) - \varphi^{(2)}\left(\bar{\mathbf{Y}}(\mathbf{X})\right) \tag{6.115}$$

An important observation is that the gap function is now a vector quantity since the gap needs to be closed in all direction, not just the normal direction as is the case in sliding contact.

6.6.2. Tied Contact Integral

With the definition of the gap function at hand (equation (6.115)), we can define the contribution to the virtual work equation from the tied contact reaction forces.

$$W_t = \int_{\Gamma_c} \mathbf{T} \cdot \delta \mathbf{g} d\Gamma \tag{6.116}$$

Here, $\mathbf{T}$ is the reaction force that enforces the constraint $\mathbf{g}(\mathbf{X}) = 0$. Since we anticipate the use of an augmented Lagrangian formalism, we can write this reaction force as follows.

$$\mathbf{T} = \boldsymbol{\lambda} + \varepsilon \mathbf{g} \tag{6.117}$$

The vector quantity $\boldsymbol{\lambda}$ is the Lagrangian multiplier and ε is a penalty factor.

6.6.3. Linearization of the Contact Integral

Since equation (6.116) is nonlinear we need to calculate the linearization. For tied contact, this is simply given by the following equation.

$$\Delta W_t = \int_{\Gamma_c} \varepsilon \Delta \mathbf{g} \cdot \delta \mathbf{g} d\Gamma \tag{6.118}$$

Where

$$\delta \mathbf{g} = \mathbf{w}^{(1)} - \mathbf{w}^{(2)} \tag{6.119}$$

and

$$\Delta \mathbf{g} = \Delta \varphi^{(1)}(\mathbf{X}) - \Delta \varphi^{(2)}\left(\bar{\mathbf{Y}}(\mathbf{X})\right) \tag{6.120}$$

We also introduced the notation $\mathbf{w}^{(i)} = \delta \varphi^{(i)}$.

The discretization of (6.118) will lead to a contribution to the stiffness matrix. Notice that due to symmetry between $\delta \mathbf{g}$ and $\Delta \mathbf{g}$ this matrix will be symmetric.

6.6.4. Discretization

The contact integral (6.116) can be discretized as follows. First, we split the integration over all the slave surface elements.

$$W_t = \sum_{e=1}^{nel} \int_{\Gamma_c^{(e)}} \mathbf{T} \cdot \delta \mathbf{g} d\Gamma^{(e)} \tag{6.121}$$

The integration can be approximated by a quadrature rule,

$$W_t = \sum_{e=1}^{nel} \sum_{i=1}^{N_{\text{int}}^{(e)}} w^i j(\xi_i) \mathbf{T}(\xi_i) \cdot \delta \mathbf{g}(\xi_i) \tag{6.122}$$

If we use a nodally integrated elements, we have

$$\begin{aligned} \mathbf{w}^{(1)}(\xi_i) &= \mathbf{c}_i^{(1)} \\ \mathbf{w}^{(2)}(\xi_i) &= \sum_j N_j(\bar{\xi}_i) \mathbf{c}_j^{(2)} \end{aligned} \tag{6.123}$$

so that,

$$\delta\mathbf{g}\left(\xi_i\right)=\mathbf{c}_i^{(1)}-\sum_j N_j\left(\bar{\xi}_i\right)\mathbf{c}_j^{(2)} \tag{6.124}$$

We can now write the contact integral (6.121) in its final form,

$$W_t=\sum_{e=1}^{nel}\sum_{i=1}^{N_{\text{int}}^{(e)}} w^i\, j\left(\xi_i\right)\left(\mathbf{N}\left(\xi_i\right)\mathbf{T}\left(\xi_i\right)\right)\cdot\delta\mathbf{\Phi} \tag{6.125}$$

where

$$\delta\mathbf{\Phi}^T\left(\xi_i\right)=\left[\mathbf{c}_i^{(1)},\quad \mathbf{c}_1^{(2)},\quad \mathbf{c}_2^{(2)},\quad \ldots,\quad \mathbf{c}_n^{(2)}\right] \tag{6.126}$$

$$\mathbf{N}\left(\xi_i\right)=\left[\mathbf{I},\quad -\mathbf{N}_1,\quad \ldots,\quad -\mathbf{N}_n\right] \tag{6.127}$$

and

$$\mathbf{N}_i=\begin{bmatrix} N_i & 0 & 0 \\ 0 & N_i & 0 \\ 0 & 0 & N_i \end{bmatrix} \tag{6.128}$$

For the linearized tied contact integral (6.118), a similar discretization procedure leads to,

$$\Delta W_t=\sum_{e=1}^{nel}\sum_{i=1}^{N_{\text{int}}^{(e)}} w^i\, j\left(\xi_i\right)\Delta\mathbf{\Phi}\cdot\mathbf{K}_c\delta\mathbf{\Phi} \tag{6.129}$$

where

$$\mathbf{K}_c=\varepsilon\mathbf{N}^T\mathbf{N} \tag{6.130}$$

References

[1] Bonet, J., and Wood, R. D., 1997, Nonlinear continuum mechanics for finite element analysis, Cambridge University Press.
[2] Lai, W. M., Rubin, D., and Krempl, E., 2010, Introduction to continuum mechanics, Butterworth-Heinemann/Elsevier, Amsterdam ; Boston.
[3] Spencer, A. J. M., 1984, Continuum Theory of the Mechanics of Fibre-Reinforced Composites, Springer-Verlag, New York.
[4] Holzapfel, G. A., 2000, Nonlinear solid mechanics : a continuum approach for engineering, Wiley, Chichester ; New York.
[5] Weiss, J. A., Maker, B. N., and Govindjee, S., 1996, "Finite element implementation of incompressible, transversely isotropic hyperelasticity," Computer Methods in Applications of Mechanics and Engineering, 135, pp. 107-128.
[6] Horowitz, A., Sheinman, I., Lanir, Y., Perl, M., and Sideman, S., 1988, "Nonlinear Incompressilbe Finite Element for Simulating Loading of Cardiac Tissue- part I: two Dimensional Formulation for Thin Myocardial Strips," Journal of Biomechanical Engineering, Transactions of the ASME, 110(1), pp. 57-61.
[7] Humphrey, J. D., Strumpf, R. K., and Yin, F. C. P., 1990, "Determination of a constitutive relation for passive myocardium. I. A new functional form," Journal of Biomechanical Engineering, Transactions of the ASME, 112(3), pp. 333-339.
[8] Humphrey, J. D., and Yin, F. C. P., 1987, "On constitutive Relations and Finite Deformations of Passive Cardiac Tissue: I. A Pseudostrain-Energy Function," Journal of Biomechanical Engineering, Transactions of the ASME, 109(4), pp. 298-304.
[9] Bowen, R. M., 1980, "Incompressible porous media models by use of the theory of mixtures," Int J Eng Sci, 18(9), pp. 1129-1148.
[10] Mow, V. C., Kuei, S. C., Lai, W. M., and Armstrong, C. G., 1980, "Biphasic creep and stress relaxation of articular cartilage in compression: Theory and experiments," J. Biomech. Eng., 102, pp. 73-84.
[11] Truesdell, C., and Toupin, R., 1960, The classical field theories, Springer, Heidelberg.
[12] Bowen, R. M., 1976, Theory of mixtures, Academic Press, New York.
[13] Mauck, R. L., Hung, C. T., and Ateshian, G. A., 2003, "Modeling of neutral solute transport in a dynamically loaded porous permeable gel: implications for articular cartilage biosynthesis and tissue engineering," J Biomech Eng, 125(5), pp. 602-614.
[14] Ateshian, G. A., Likhitpanichkul, M., and Hung, C. T., 2006, "A mixture theory analysis for passive transport in osmotic loading of cells," J Biomech, 39(3), pp. 464-475.
[15] Albro, M. B., Chahine, N. O., Li, R., Yeager, K., Hung, C. T., and Ateshian, G. A., 2008, "Dynamic loading of deformable porous media can induce active solute transport," J Biomech, 41(15), pp. 3152-3157.
[16] Albro, M. B., Li, R., Banerjee, R. E., Hung, C. T., and Ateshian, G. A., 2010, "Validation of theoretical framework explaining active solute uptake in dynamically loaded porous media," J Biomech, 43(12), pp. 2267-2273.
[17] Tinoco Jr., I., Sauer, K., and Wang, J. C., 1995, Physical chemistry : principles and applications in biological sciences, Prentice Hall.
[18] Laurent, T. C., and Killander, J., 1963, "A Theory of Gel Filtration and its Experimental Verification," J Chromatogr, 14, pp. 317-330.

[19] Ogston, A. G., and Phelps, C. F., 1961, "The partition of solutes between buffer solutions and solutions containing hyaluronic acid," Biochem J, 78, pp. 827-833.
[20] Ateshian, G. A., 2007, "On the theory of reactive mixtures for modeling biological growth," Biomech Model Mechanobiol, 6(6), pp. 423-445.
[21] Ateshian, G. A., and Weiss, J. A., 2010, "Anisotropic hydraulic permeability under finite deformation," J Biomech Eng, 132(11), p. 111004.
[22] Eringen, A. C., and Ingram, J. D., 1965, "Continuum theory of chemically reacting media -- 1," Int J Eng Sci, 3, pp. 197 - 212.
[23] Katzir-Katchalsky, A., and Curran, P. F., 1965, Nonequilibrium thermodynamics in biophysics, Harvard University Press, Cambridge,.
[24] Sun, D. N., Gu, W. Y., Guo, X. E., Lai, W. M., and Mow, V. C., 1999, "A mixed finite element formulation of triphasic mechano-electrochemical theory for charged, hydrated biological soft tissues," Int J Numer Meth Eng, 45(10), pp. 1375-1402.
[25] Ateshian, G. A., and Ricken, T., 2010, "Multigenerational interstitial growth of biological tissues," Biomechanics and modeling in mechanobiology, 9(6), pp. 689-702.
[26] Un, K., and Spilker, R. L., 2006, "A penetration-based finite element method for hyperelastic 3D biphasic tissues in contact. Part II: finite element simulations," J Biomech Eng, 128(6), pp. 934-942.
[27] Curnier, A., Qi-Chang, H., and Zysset, P., 1994, "Conewise linear elastic materials," J Elasticity, 37(1), pp. 1-38.
[28] Ateshian, G. A., Ellis, B. J., and Weiss, J. A., 2007, "Equivalence between short-time biphasic and incompressible elastic material responses," J Biomech Eng, 129(3), pp. 405-412.
[29] Marsden, J. E., and Hughes, T. J., 1994, Mathematical Foundations of Elasticity, Dover Publications.
[30] Matthies, H., and Strang, G., 1979, "The solution of nonlinear finite element equations," Intl J Num Meth Eng, 14, pp. 1613-1626.
[31] Simo, J. C., and Taylor, R. L., 1991, "Quasi-incompressible finite elasticity in principal stretches: Continuum basis and numerical algorithms," Computer Methods in Applied Mechanics and Engineering, 85, pp. 273-310.
[32] Hughes, J. R., and Liu, W. K., 1980, "Nonlinear Finite Element Analysis of Shells: Part I. Three-dimensional Shells," Computer Methods in Applied Mechanics and Engineering, 26, pp. 331-362.
[33] Betsch, P., Gruttmann, F., and E., S., 1996, "A 4-node finite shell element for the implementation of general hyperelastic 3D-elasticity at finite strains," Comput. Methods Appl. Mech. Engrg, 130, pp. 57-79.
[34] Holmes, M. H., and Mow, V. C., 1990, "The nonlinear characteristics of soft gels and hydrated connective tissues in ultrafiltration," J Biomech, 23(11), pp. 1145-1156.
[35] Ateshian, G. A., Rajan, V., Chahine, N. O., Canal, C. E., and Hung, C. T., 2009, "Modeling the matrix of articular cartilage using a continuous fiber angular distribution predicts many observed phenomena," J Biomech Eng, 131(6), p. 061003.
[36] Azeloglu, E. U., Albro, M. B., Thimmappa, V. A., Ateshian, G. A., and Costa, K. D., 2008, "Heterogeneous transmural proteoglycan distribution provides a mechanism for regulating residual stresses in the aorta," American journal of physiology. Heart and circulatory physiology, 294(3), pp. H1197-1205.
[37] Veronda, D. R., and Westmann, R. A., 1970, "Mechanical Characterization of Skin - Finite Deformations," J. Biomechanics, Vol. 3, pp. 111-124.

[38] Arruda, E. M., and Boyce, M. C., 1993, "A Three-Dimensional Constitutive Model for the Large Stretch Behavior of Rubber Elastic Materials," J. Mech. Phys. Solids, 41(2), pp. 389-412.
[39] Puso, M. A., and Weiss, J. A., 1998, "Finite element implementation of anisotropic quasi-linear viscoelasticity using a discrete spectrum approximation," J Biomech Eng, 120(1), pp. 62-70.
[40] Quapp, K. M., and Weiss, J. A., 1998, "Material characterization of human medial collateral ligament," J Biomech Eng, 120(6), pp. 757-763.
[41] Ateshian, G. A., 2007, "Anisotropy of fibrous tissues in relation to the distribution of tensed and buckled fibers," J Biomech Eng, 129(2), pp. 240-249.
[42] Lanir, Y., 1983, "Constitutive equations for fibrous connective tissues," J Biomech, 16(1), pp. 1-12.
[43] Fung, Y. C., 1993, Biomechanics : mechanical properties of living tissues, Springer-Verlag, New York.
[44] Fung, Y. C., Fronek, K., and Patitucci, P., 1979, "Pseudoelasticity of arteries and the choice of its mathematical expression," Am J Physiol, 237(5), pp. H620-631.
[45] Ateshian, G. A., Ellis, B. J., and Weiss, J. A., 2007, "Equivalence between short-time biphasic and incompressible elastic material response," J Biomech Eng, In press.
[46] Guccione, J. M., and McCulloch, A. D., 1993, "Mechanics of active contraction in cardiac muscle: part I - constitutive relations for fiber stress that describe deactivation," J. Biomechanical Engineering, vol. 115(no. 1), pp. 72-83.
[47] Maker, B. N., 1995, "Rigid bodies for metal forming analysis with NIKE3D," University of California, Lawrence Livermore Lab Rept, UCRL-JC-119862, pp. 1-8.
[48] Laursen, T. A., 2002, Computational Contact and Impact Mechanics, Springer.
[49] Ateshian, G., Maas, S., and Weiss, J. A., 2010, "Finite element algorithm for frictionless contact of porous permeable media under finite deformation and sliding," J. Biomech. Engn., 132(6), pp. 1006-1019.